

International Consortium for Atmospheric Research on Transport and Transformation (ICARTT): North America to Europe: Overview of the 2004 summer field study

F.C. Fehsenfeld¹

J. Meagher¹

G. Ancellet²

D.D. Parrish¹

T.S. Bates³

A.A.P. Pszenny⁸

A.H. Goldstein⁴

P.B. Russell⁹

R.M. Hardesty¹

H. Schlager¹⁰

R. Honrath⁵

J. Seinfeld¹¹

K.S. Law²

M. Trainer¹

A.C. Lewis⁶

R. Talbot⁸

R. Leaitch⁷

R. Zbinden¹²

S. McKeen¹

¹ Earth System Research Laboratory, National Oceanic and Atmospheric Administration, Boulder, CO USA

² Service d'Aéronomie du Centre Nationale de la Recherche Scientifique (CNRS), Institut Pierre Simon Laplace (IPSL)/ Université Pierre et Marie Curie, Paris, France

³ Pacific Marine Environmental Laboratory, National Oceanic and Atmospheric Administration, Seattle, WA, USA

⁴ University of California, Berkeley, Department of Environmental Science, Policy and Management, Berkeley, CA USA

⁵ Michigan Technological University, Houghton, MI USA

⁶ Department of Chemistry, University of York, Heslington, York UK

⁷ Science and Technology Branch, Environment Canada, Toronto, Canada

⁸ University of New Hampshire, Institute for the Study of Earth, Oceans and Space, Durham, NH USA and Mount Washington Observatory, North Conway, NH USA

⁹ NASA Ames Research Center, Moffett Field, CA USA

¹⁰ Deutsches Zentrum für Luft- und Raumfahrt, Oberpfaffenhofen, Germany

¹¹ Departments of Environmental Science and Engineering and Chemical Engineering, California Institute of Technology, Pasadena, California, USA.

¹² Laboratoire d'Aérodynamique - Observatoire Midi-Pyrénées, UMR 5560 CNRS/Université Paul Sabatier, Toulouse, France

ABSTRACT

In the summer of 2004 several separate field programs intensively studied the photochemical, heterogeneous chemical and radiative environment of the troposphere over North America, the North Atlantic Ocean, and Western Europe. Previous studies have indicated that the transport of continental emissions, particularly from North America, influences the concentrations of trace species in the troposphere over the Atlantic and Europe. An international team of scientists, representing over 100 laboratories, collaborated under the International Consortium for Atmospheric Research on Transport and Transformation (ICARTT) umbrella to coordinate the separate field programs in order to maximize the resulting advances in our understanding of regional air quality, the transport, chemical transformation and removal of aerosols, ozone, and their precursors during intercontinental transport, and the radiation balance of the troposphere. Participants utilized nine aircraft, one research vessel, several ground-based sites in North America and the Azores, a network of aerosol-ozone lidars in Europe, satellites, balloon borne sondes, and routine commercial aircraft measurements. In this special section, the results from a major fraction of those platforms are presented. This overview is aimed at providing operational and logistical information for those platforms and summarizing the principal findings and conclusions that have been drawn from the results.

1. Introduction

Until recently research programs in global climate change and regional air quality have been conducted as separate, albeit related, activities. The investigation of intercontinental-scale transport and chemical transformation processes and radiation balance in the atmosphere have been the focus of the former, while the latter has been focused on the atmospheric science that underlies urban, regional and continental air quality. Clearly, the distinction between the research objectives of these two programs is, at least in part, simply a matter of perspective and scale. Many of the chemical and meteorological processes of interest are common to both. Also, intercontinental transport is both the starting point and the end point of regional air quality concerns since any particular region contributes outflow to and receives inflow from that transport.

In recognition of this strong linkage, a joint regional air quality and climate change study, which is described herein, was planned and carried out in the summer of 2004. The study focused on air quality in the Eastern United States, transport of North American emissions into the North Atlantic, and the influences that this transport has on regional and intercontinental air quality and climate, with a particular focus on Western Europe.

The topics addressed in the present study have a long history. There have been at least three decades of studies aimed, at least in part, at determining the causes of poor air quality outside of urban areas along the east coast of the U.S. and the transport of polluted air from North America out into the North Atlantic. Some very early studies have been followed by intensive field campaigns conducted along the eastern coast of North America and into the Western North Atlantic. Similarly, intensive field programs along the western coast of Europe and the Eastern North Atlantic have investigated the impact of polluted air flowing into Europe. To place the planning that preceded the current study into perspective, Section 2 provides a brief review of related previous research.

Several independent field studies, each focused on some aspect of climate change and air quality issues over North America, the Atlantic and Europe, were planned for the summer of 2004. Early in the planning it became evident that coordination between these studies would provide a more effective approach to addressing these issues. The International Consortium for Atmospheric Research on Transport and Transformation (ICARTT) was formed to take advantage of this synergy by planning and executing a series of coordinated experiments to study the emissions of aerosol and ozone precursors, their chemical transformations and removal during transport to and over the North Atlantic, and their impact downwind on the European continent.

The combined research conducted in the programs that make up ICARTT focused on three main areas: regional air quality, intercontinental transport, and radiation balance in the atmosphere. Although each of the programs had regionally focused goals and deployments, they shared many of the overall ICARTT goals and objectives. The aims and objectives of the individual components that compose the ICARTT program are briefly described in Section 3. The capabilities represented by the consortium allowed an unprecedented characterization of the key atmospheric processes. The scope of the study is indicated by the measurement platforms and

ground site locations that were operated during the study and are described in Section 4. This section also provides general information that can be referenced in publications that describe results obtained from the study and its interpretation.

The goal of this special journal section is to report many of the ICARTT results; Sections 5 and 6 highlight some of the particularly important findings. The NASA Intercontinental Chemical Transport Experiment - North America (INTEX-A) and the CO₂ Budget and Rectification Airborne study (COBRA) participated in ICARTT, but will publish their results elsewhere, the former in a separate special section in *J. Geophys. Res.*: INTEX-A/ICARTT.

2. Review of previous research related to ICARTT

The ICARTT studies that are described herein were planned based on the findings of many studies of regional air quality, long-range pollutant transport and atmospheric radiative forcing that have been carried out over the past three decades. These studies are briefly reviewed in this section.

2.1. Northeastern North American Continental Studies

A series of studies have been carried out in the eastern United States and Canada that focused on providing the measurements needed for the evaluation of air-quality models. During summer and fall 1988, seven surface stations constituted the North American Cooperative Network of Enhanced Measurement Sites (**NACEMS**), which focused on the production of ozone and the partitioning of reactive oxidized nitrogen species in rural regions of eastern North America [Trainer and al., 1993; Parrish, et al., 1993; Roberts, et al., 1995]. The airborne Acid Model Operational Diagnostic Evaluation Study (**AMODES**) collected daily air and precipitation chemistry data at approximately 59 sites for two years over much of the eastern United States and Canada. These data were used for the evaluation of regional scale Eulerian deposition models. [Tremmel, et al., 1993; 1994]. The North East Oxidant and Particle Study (**NARSTONE-OPS**) was carried out during the summers of 1998, 1999 and 2001 [Zhang, et al., 1998; Seaman and Michelson, 2000] to investigate meteorological and chemical processes that control the evolution of air pollution events in and around Philadelphia, PA. The results from these studies indicated that a 3-dimensional regional scale picture of the atmosphere is required to understand and predict local air pollution events.

An ongoing program of atmospheric research has been carried out at **Harvard Forest**, a rural site near Petersham, Massachusetts. This research investigates the pollution processing in the Northeast US urban/industrial corridor and the biosphere-atmosphere exchange of airborne pollutants. The results obtained from over a decade of these measurements provide a chemical climatology for all seasons over several years. Harvard Forest results particularly relevant to the ICARTT study are reported in Chin, et al. [1994]; Goldstein, et al. [1995; 1996; 1998]; Hirsch, et al. [1996]; Munger, et al. [1996; 1998] Liang, et al. [1998]; Moody, et al. [1998] and Lefer, et al. [1999].

Early measurements, begun in 1979 at Kejimikujik National Park in Canada, observed the long-range transport of plumes to central Nova Scotia from urban and industrial sources in the United

States and Canada, a distance of over 500 km from their sources [Brice, *et al.*, 1988; Beattie and Wepdale, 1989].

2.2. Western North Atlantic Studies

The long-range transport of pollution from the continents to the North Atlantic has been investigated at island sites located in the North Atlantic region. The Atmospheric-Ocean Chemistry Experiment (**AEROCE**) program conducted a systematic study of the influence of anthropogenic emissions on ozone and aerosols over the region. Long-term measurements were carried out at sites on Barbados, West Indies; Bermuda; Tenerife, Canary Islands; Mace Head, Ireland; Heimaey, Iceland and Miami, Florida [Prospero, 2001].

A great many research vessel cruises through the Atlantic Ocean included atmospheric measurements. Winkler [1988] summarized the ozone measurements from 32 of these cruises conducted in 1977 through 1986. More recently, a comprehensive investigation of the O₃ and aerosol distributions over the North Atlantic was made during a cruise of the German research vessel Polarstern in 1987 [Special section, *J. Geophys. Res.*, 95, D12, 1990].

Several NASA sponsored programs have identified transport of pollution from North America to the western North Atlantic. Airborne lidar measurements [Harriss, *et al.*, 1984] revealed persistent, highly stratified layers of aerosols extending more than 600 km into the Atlantic. In situ measurements showed that these layers correlated with elevated ozone and CO levels. Lidar and in situ measurements of ozone, CO and aerosols [Wofsy, *et al.*, 1992; Anderson, *et al.*, 1993] off the eastern coast of the U.S. identified strong correlations between these species, and concluded that anthropogenic pollution has a major impact on the budgets of these species in the near continent region. Fishman, *et al.* [1990; 1991] derived the tropospheric ozone distribution from satellite data; a striking feature is a strong, summertime maximum extending downwind from North America into the North Atlantic.

Several programs have measured the atmospheric composition of the North Atlantic region. Zeller *et al.* [1977]; Kelleher and Feder, [1978]; and Spicer [1982] found evidence for the transport of plumes along the eastern seaboard of the United States and out over 100 km or more of the North Atlantic. In the summer of 1988, the Global Change Expedition/Coordinated Air-Sea Experiment/Western Atlantic Ocean Experiment (**GCE/CASE/WATOX**) [Special section, *Global Biogeochem. Cycles*, 4., 1990] investigated atmospheric and oceanic processes, particularly transport and deposition of aerosols, affecting the biogeochemical cycles of carbon, nitrogen, sulfur, and trace metals in the North Atlantic Ocean region. The North Atlantic Regional Experiment (**NARE**) program of IGAC studied the effect of long-range transport of chemical compounds on the oxidative properties and radiation balance of the troposphere over the North Atlantic. Major field intensives were conducted by this program in the summer 1993 [two special sections JGR, 101, D22, 1996; 103, D11, 1998] early spring 1996 and late summer/early fall 1997. The interpretation of these studies has focused on the chemical evolution, removal and transport patterns of anthropogenic emissions over the North Atlantic [Cooper, *et al.*, 2001; 2002a; b; Stohl, *et al.*, 2002; Li, *et al.*, 2002].

During summer 2002, the New England Air Quality Study (**NEAQS**) deployed the research vessel *Ronald H. Brown* to study the chemical evolution of gaseous and aerosol pollution in the

New York City and Boston urban plumes over the Gulf of Maine [Bates, *et al.*, 2005]. These measurements were coordinated with intensive measurements in the AIRMAP research network and airborne measurements conducted with the DOE G-1 research aircraft.

2.3. Western Europe and Eastern North Atlantic Studies

A series of airborne studies have been carried out over the eastern North Atlantic Ocean and Western Europe to investigate the impact of long-range transport of anthropogenic emissions across the North Atlantic. The Atmospheric Chemistry Studies in the Oceanic Environment (**ACSOE**) program, which formed the European component of NARE, investigated the chemistry and transport of pollutants in North Atlantic marine air in the spring and summer 1997 through observations by the UK Met office C-130 aircraft based in the Azores [Reeves *et al* 2002]. During the Maximum Oxidation rates in the free troposphere and Testing Atmospheric Chemistry in Anticyclones (**MAXOX/TACIA**) programs in May and August 2000 detailed measurements on chemical composition were collected using the UK C-130 aircraft based in the UK during summer in the late 1990s. Reeves *et al.* [2002] estimated net photochemical O₃ production rates in pollutant plumes undergoing long-range transport. The role of frontal uplift in transporting pollutants between different regions in Europe was also investigated. The UK C-130, French Falcon-20 and DLR Falcon aircraft combined in the Atmospheric Chemistry and Transport of Ozone/European Export of Precursors and Ozone by Long-Range Transport (**ACTO/EXPORT**) experiment over North Atlantic regions and central European locations. This study investigated both the inflow of anthropogenic pollutants from North Atlantic regions [Methven *et al* 2003] and the uplift and export of European emissions from the surface [Purvis *et al* 2003]. During the Convective Transport of Trace Gases into the Middle and Upper Troposphere over Europe: Budget and Impact on Chemistry (**CONTRACE**) field experiment the German DLR Falcon intercepted pollutant plumes from North America over Europe several times in May and November 2001 [Huntrieser *et al.*, 2005].

Several ground-based studies in Europe have investigated long-range transport of pollution arriving in Europe. The influence of intercontinental transport on ozone and precursors was observed fairly regularly in free tropospheric air at mountain-top sites such as Izana (Canary Islands) [Schultz *et al.*, 1997] during the **EUROTRAC-TOR** program, at the Jungfrauoch (Switzerland) [Carpenter, *et al.*, 2001] during the 1996 and 1998 Free Tropospheric Experiments (**FREETEX**) campaigns, and Zugspitze (Germany) and Arosa (Switzerland) during the **CONTRACE** experiment [Huntrieser *et al.*, 2005]. Long-range transport events also are sometimes observed at the **Mace Head** sea-level site [Derwent and Jenkin, 1991]. This site is located on the western coast of Ireland, where extensive, continuing atmospheric measurements were initiated in 1987. Several studies in Europe have also focused on the efficient role of mountain valley circulations in the venting of boundary layer pollutants into the lower free troposphere (e.g. Wotawa and Kromp-Kolb, 2000; Prevot *et al.*, 2000).

Data from a network of **European LIDARs** combined with trajectory analysis have demonstrated long-range transport of polluted air masses from North America to Europe on several occasions (e.g. [Stohl and Trickl, 1999]). In this case rapid transport across the North Atlantic occurred due to uplift in a warm conveyor belt and transport to Europe near the jet stream.

The European community has been particularly active in the utilization of commercial aircraft for making extensive measurements in the free troposphere. The collected data are particularly concentrated over Western Europe, the North Atlantic and eastern North America. These programs include Measurements of Nitrogen Oxides and Ozone Along Air Routes (**NOXAR**) [Brunner *et al.*, 2001], Measurement of Ozone, Water Vapour, Carbon Monoxide and Nitrogen Oxides by In-service Commercial Aircraft (**MOZAIC**) [Marenco *et al.*, 1998] and Civil Aircraft for Regular Investigation of the Atmosphere Based on an Instrument Container (**CARIBIC**) [Zahn *et al.*, 2004].

2.4. Aerosol and Radiative Forcing Studies

Several field campaigns have focused on aerosol transport and transformation and the radiative forcing of those aerosols. The Atlantic Stratocumulus Transition Experiment in June 1992 studied the factors influencing the formation and dissipation of marine clouds. IGAC's Marine Aerosol and Gas Exchange (**ASTEX/MAGE**) activity conducted chemical measurements within ASTEX to investigate air-sea exchange and the formation and transformation of marine aerosols [special section JGR, 101, number D2, 1996]. The Tropospheric Aerosol Radiative Forcing Observational Experiment (**TARFOX**) in summer 1996 focused on the direct radiative impacts of aerosols, as well as the chemical, physical, and optical properties, of the aerosols carried over the western Atlantic Ocean from North America. It included coordinated measurements from four satellites (GOES-8, NOAA-14, ERS-2, LANDSAT), four aircraft (ER-2, C-130, C-131, and a modified Cessna), land sites, and ships [two special sections JGR, 104, D2, 1999; 105, D8, 2000]. The second Aerosol Characterization Experiment (**ACE-2**) contrasted the aerosol characteristics, processes and effects over the anthropogenically modified North Atlantic with those observed during ACE-1, which was conducted in the minimally polluted Southern Ocean. This summer 1997 study included 6 aircraft, one ship, and ground stations on Tenerife, Portugal and Madeira. [Special issue Tellus B, 52, 2, 2000. The shipboard **AEROSOLS99** study crossed the Atlantic Ocean from Norfolk, Virginia, to Cape Town, South Africa in winter 1999, and determined the chemical, physical, and optical properties of the marine boundary layer aerosol, [Special section of JGR, 106, D18, 2001].

3. Components of ICARTT

During the summer of 2004, ICARTT coordinated the activities of several independently planned research programs. The coordinated programs involved extensive measurements made from aircraft, a research vessel, and several ground stations located in the northeastern United States, Nova Scotia, the Azores, and Western Europe. Table 1 lists the principal measurement platforms and ground stations, the programs and agencies that supported these platforms, and the principal objectives of their measurements. The following sub-sections describe the principal goals and resources contributed by the independent programs. Appendices A and B give more experimental details of the individual platforms and sites. Figure 1 indicates the time periods over which the various platforms and sites operated.

In addition to the research that is described in this special section, the ICARTT consortium also included three other field studies that plan publication elsewhere. These are: 1) Intercontinental Chemical Transport Experiment – North America (INTEX-NA), which was NASA supported

and used the NASA DC-8 aircraft to undertake large-scale mapping of trace gases and aerosols over North America and the Atlantic Ocean; many of their results will be included in a separate INTEX-NA/ICARTT special section in JGR. 2) The 2004 CO₂ Boundary-layer Regional Atmospheric Study (COBRA) that was based out of Bangor, Maine and utilized the University of Wyoming King Air aircraft to examine regional-scale budgets and forest-atmosphere exchange of CO and CO₂. 3) The U.S. DOE-operated G1 Gulfstream aircraft collected data from locations downwind of urban areas, and sampled point sources for trace gases and aerosols. Since descriptions of their findings will not be contained in this special section, these programs will not be described further.

3.1. NEAQS-ITCT 2004 Study (NOAA)

The NOAA WP-3D and DC-3 Lidar aircraft combined with the Research Vessel *Ronald H. Brown*, the surface site at Chebogue Point, and the NOAA-DOE Cooperative Agency Radar Wind Profiler network to conduct the combined New England Air Quality Study (NEAQS) and Intercontinental Transport and Chemical Transformation (ITCT) study. The WP-3D mapped trace gases, aerosols and radiative properties over northeastern U.S., and the Lidar, deployed on a chartered DC3 aircraft, mapped the regional distribution of boundary layer ozone and aerosols over New England. *Ronald H. Brown* used both in situ and remote atmospheric sensors to examine low altitude outflow of pollution from the northeastern U.S. The Chebogue Point measurements provided continuous observations at a fixed site, allowing determination of the frequency and intensity of pollution events crossing the Canadian Maritime Provinces on their way to the North Atlantic. Chebogue Point included a very comprehensive measurement set for aerosol chemical and physical properties, along with a wide range of trace gas measurements and meteorological observations. Chebogue Point was also instrumented during NARE (July 26 – September 3, 1993), and as such provided a point of comparison for studying temporal changes in outflow of pollution from North America. A radar wind profiler network included eleven sites that provided information on regional scale trajectories and transport of air masses. The science plan that describes the research aims of NEAQS-ITCT can be found at <http://www.al.noaa.gov/csd/2004/>.

3.2. AIRMAP Network (NOAA) and CHAiOS (NSF, NOAA)

AIRMAP is a program that has been developed at the University of New Hampshire (www.airmap.unh.edu) to gain an understanding of regional air quality, meteorology, and climatic phenomena in New England. The AIRMAP network consists of five long-term measurement sites for documenting and studying persistent air pollutants such as ozone and fine particles in the region. More details of the measurements can be found at the above web site. The continuous high-resolution nature and multi-year records are strengths of the AIRMAP data set that provide a year-to-year context for the ICARTT measurements.

The Chemistry of Halogens at the Isles of Shoals (CHAiOS) study was conducted at the AIRMAP site on Appledore Island, Maine to evaluate the influence of halogen radicals on the chemical evolution of pollutant outflow from North America along the New England coast during summer. The study used an integrated analysis of field measurements and model calculations to investigate 1) the influences of halogen radicals on ozone production and destruction in polluted air along the New England east coast during summer, 2) the influence of nocturnal radical chemistry, i.e. NO₃ and N₂O₅, on halogen levels, 3) the role of halogens in the

production and chemical evolution of aerosols over the Gulf of Maine, and 4) the potential implications of the outflow on the chemistry in the MBL over the Gulf of Maine.

3.3. PICO-NARE (NOAA, NSF)

The PICO-NARE station was established to study the composition of the lower free troposphere in the central North Atlantic region, with an emphasis on the impacts of pollution outflow from the surrounding continents. The station is located on the summit caldera of Pico Mountain (2225 m asl, 38 degrees, 28.226 min north latitude, 28 degrees 24.235 min west longitude). The station is located at an elevation that allows sampling of air in the lower free troposphere [Kleissl *et al.*, 2006, this section]. Because the Azores are distant from the anthropogenic and biomass-burning sources, observations at this location are expected to be characteristic of impacts of such events over a large region. The PICO-NARE studies have as their primary objectives to: 1) determine the degree to which PICO-NARE measurements are characteristic of free tropospheric composition, by analyzing the occurrence of upslope flow events on Pico mountain; 2) use observations during frequent events of boreal biomass-burning emissions transport to determine the impact of boreal fire emissions on ozone precursors, ozone, and aerosol black carbon; 3) characterize the transport mechanisms whereby North American anthropogenic emissions are transported to the station, and to assess the importance of these lower-free troposphere transport events in the context of regional ozone impacts; and 4) determine the seasonal cycle of NMHC levels and HC/HC ratios in the North Atlantic lower free troposphere to quantify the impact of individual transport events on tropospheric composition.

3.4. ITOP (NERC, DLR)

The 2004 Intercontinental Transport of Ozone and Precursors (ITOP, c.f., <http://badc.nerc.ac.uk/data/itop/>) project involved research groups from Germany, France, and the UK. During 2004 the project made detailed observations of chemical processing occurring in air masses transported from the US to Europe at both high and low levels in the troposphere in the mid-Atlantic region. The principal components of the ITOP project in 2004 involved two aircraft (the FAAM BAE146 and the Dassault Falcon E) and the European Lidar Network. The FAAM BAE146 aircraft was based in the Azores, the approximate midpoint point in both time and space between emission studies on the US Eastern seaboard and observations of inflowing air to receptor regions in Europe. A focus of the experiment was to determine the extent to which air masses remained chemically active in the days following primary emission, and the role played by relatively stable oxidative intermediates such as PAN, organic nitrates and carbonyls in extending this activity beyond the lifetime of the initially emitted species. The impact of this chemistry, when coupled with global atmospheric transport, would be used to determine the fate of continental boundary layer pollution exported to mid and upper troposphere regions over the North Atlantic, particularly with respect to ozone production and destruction.

The Dassault Falcon E aircraft operated by the Deutsches Zentrum für Luft- und Raumfahrt (DLR) performed the ITOP measurement flights in Europe. The flight objectives included interception and measurement of urban and industrial plumes transported from Northeastern US, of forest fire plumes originating from Canada and Alaska, of European urban plumes (e.g., London, Poë valley), and of emissions from maritime shipping (e.g., in the English Channel and North Sea). The data obtained from these measurements were also used for Satellite (ENVISAT) validation, and intercomparison between the Falcon and BAE146.

Several aerosol lidar systems operated during 2004 as part of the ITOP experiment and constituted the European Lidar Network. The goal of the network was to identify atmospheric layers not influenced by the European aerosol or ozone production. The systems were capable of aerosol backscatter measurements up to at least 5 km. In addition, two systems also were able to provide ozone vertical profiles.

3.5 ICARTT Radiation-Aerosol Study (NOAA, NASA)

The twin turboprop Jetstream-31 (J31) aircraft flew missions over the Gulf of Maine during July and August 2004 in coordination with the NOAA RV *Ronald H. Brown*. Flights were generally timed to underfly the Terra and Aqua satellite overpasses. Specific science objectives of the J31 included validating satellite retrievals of aerosol optical depth (AOD) spectra and of water vapor columns, as well as measuring aerosol effects on radiative energy fluxes. The broader goal of the Radiation-Aerosol Study was to produce a refined, regional-scale understanding of anthropogenic aerosol and its direct radiative impact.

3.6. ICARTT Cloud-Aerosol Study (NSF, Environment Canada)

Two aircraft, the CIRPAS Twin Otter and NRC of Canada Convair 580 were involved in the Cloud-Aerosol study. The major scientific issues motivating the involvement of these aircraft in ICARTT centered on the relationship between cloud properties and those of the aerosols upon which the clouds are forming. Therefore, this experiment represents a continuing effort to obtain detailed, in situ field data that will aid in understanding the indirect climatic effect of aerosols. In addition, there was focus on understanding the atmospheric evolution of aerosols. Specific questions included: (1) To what extent can observed cloud drop number concentrations be predicted by theoretical aerosol-cloud activation models, given measurements of aerosol size and composition, i.e. to what extent can aerosol-cloud drop closure be achieved? What role do aerosol organic components play in determining cloud drop number concentrations? How sensitive are predicted cloud drop concentrations to the mass accommodation coefficient of water on droplets? (2) Is there evidence of liquid-phase processing of dissolved organics leading to observed organic aerosol components? (3) What processes govern the evolution of aerosols in power plant plumes as the plumes are advected from their source to the regional atmosphere? How does this evolution differ under clean versus cloudy conditions?

4. Study Coordination

Because of the scope and diverse nature of the ICARTT study, considerable coordination was required. Information concerning study planning and implementation was provided to all participants via a web site, (c.f., <http://www.al.noaa.gov/ICARTT/index.shtml>). The organization, planning and implementation of the study are given on the web site. The detailed planning was tasked to six working groups: 1) aircraft and ship coordination; 2) surface networks; 3) modeling and forecasting; 4) measurement comparison; 5) data management and 6) international coordination. These groups were charged with developing the necessary implementation required to coordinate study activities. A six-member Study Coordination Team composed of individuals representing the principal programs involved in the study was named to provide coordination among the working groups. The planning provided by these groups was presented in a series of white papers and meetings prior to the study.

During the study, participants could be informed on the progress of the study, given up-dates on operations of the various platforms and alerted to interesting finding from measurements and model predictions on the web site under the heading of “Field Operations”. Here links were provided to the participants of the study for access to: 1) the results from the measurements made at the various field sites, on the mobile platforms and realizations of satellite data; 2) model forecasts and simulations; 3) measurement intercomparison results; 4) forecast model output comparisons and forecast model comparisons with targeted field measurements; and 5) a detailed emissions map viewer that gives the location and intensity of natural and anthropogenic emission in North America.

Slightly expanded descriptions of five activities and resources that were particularly helpful in coordinating study activities will be briefly described. They are: 1) the role of model simulation and forecasting; 2) the design and implementation of the ITCT-Lagrangian-2K4 experiment; 3) the emission map viewer; 4) the measurement comparison and uncertainty determination; and 5) data management protocol.

4.1. The Role of Model Simulation and Forecasting

A large array of model studies accompanies the observations collected during the ICARTT-2004 experiment. These models include box-model analysis of in-situ photochemistry, Lagrangian transport models used in the prognosis and diagnosis of intercontinental transport, and many 3-dimensional Eulerian models spanning local to global spatial scales. The forecasts provided by these models were used extensively during the study for flight planning and event interception. In addition, they suggest interesting features of events for retrospective analysis. These simulations were often made available during the study on linked web sites that were accessible to all interested participants.

The modeling results included in this special journal section can be divided into four major components: those specific to AIRMAP and CHAiOS [*Chen et al.*, 2006; *Griffin et al.*, 2006; *Mao et al.*, 2006; this section], Lagrangian and global Eulerian models relevant to ITOP [*Stohl et al.*, 2004; *Methven et al.*, 2006; *Attie et al.*, 2006; *Cook et al.*, 2006; *Real et al.*, 2006; this section], those associated with ITCT-Lagrangian-2K4 (see section 4.3 below), and several regional-scale Eulerian air quality forecast models (AQFMs) participating in an informal model evaluation as part of ICARTT. This last component was specifically designed to take advantage of the various surface based and aircraft platforms within ICARTT to critically assess state-of-the-art forecast models for O₃ and aerosol.

Nine AQFMs from six research centers were operational in real-time during the field study covering the eastern U.S. and southeastern Canada. The research groups include two NOAA facilities (the NWS/NCEP CMAQ/Eta model and the ESRL/GSD WRF-Chem model), two groups from the Canadian Meteorological Service (the operational CHRONOS, and developmental AURAMS model groups), the University of Iowa (STEM-2K3 model), and the Baron Advanced Meteorological Service (MAQSIP-RT model). Studies that summarize the

¹ The INTEX-A/ICARTT special section in JGR contains a number of papers that focus specifically on model interpretation of the NASA DC-8 aircraft data.

2004 O₃ forecast evaluations based on the EPA AIRNOW surface O₃ monitoring network [McKeen *et al.*, 2005] and evaluations of ensemble O₃ forecast techniques [Pagowski *et al.*, 2005, Pagowski *et al.*, 2006] have already been published for this set of models. Papers covering additional O₃ forecast techniques such as bias-corrected ensemble methods [Wilczak *et al.*, 2006], Kalman filtering [Delle Monache *et al.*, 2006] and probabilistic O₃ forecasts [Pagowski and Grell, 2006] are provided in this section. ICARTT field data also play a crucial role in the O₃ forecast data assimilation study of Chai *et al.* [2006, INTEX-A/ICARTT section]. As forecasts of PM_{2.5} aerosol, much like ozone, become routinely available to the public, the need for accurate characterization of the various processes controlling PM_{2.5}, and evaluations of PM_{2.5} forecast capabilities becomes critical. Carmichael *et al.* [2006, INTEX-A/ICARTT section] utilize the various aerosol related measurements within ICARTT to evaluate PM_{2.5} formation and transformation. McKeen *et al.* [2006, this section] evaluate PM_{2.5} forecasts from seven AQFMs and their ensemble using surface-based monitoring networks and NOAA P-3 aircraft data from the ICARTT study.

4.2. The Design and Implementation of the ITCT-Lagrangian-2K4 Experiment

The goal of the ITCT-Lagrangian-2K4 Experiment is to directly observe the evolution of the aerosols, oxidants and their precursors from emission over North America, trans-Atlantic transformation and transport, and impact on aerosol and oxidant levels over Europe. In practice, two or three aircraft made multiple, sequential sampling flights into the same air mass during the time required for the intercontinental transport of that air mass. This plan required the close coordination of four aircraft deployed in North America (the NOAA WP-3D and the NASA DC-8), in the mid North Atlantic (the BAe-146) and in Europe (the DLR Falcon). In addition, data from the NOAA Ozone Lidar aircraft, the PICO-NARE surface site, MOZAIC measurements on commercial aircraft, from the European lidar network, and European surface sites were integrated into the analyses. Each of these platforms had its own regionally focused goals, but together they provided coverage during the complete transit of a polluted air mass across the North Atlantic.

The organization and realization of ITCT-Lagrangian-2K4 comprised three steps: a review of previous results, instrument comparison activities (to ensure that measurements on the disparate platforms could be accurately integrated without confounding measurement uncertainties) and flight coordination during the field deployment. The review of previous results focused on the NARE 1997 study [Stohl *et al.*, 2004], which was conducted in the same region at a similar time of year. The instrument comparison activities (described more fully in Section 4.4) were focused on six wingtip-to-wingtip flights of two aircraft that together compared measurements on all four aircraft; some of the results are reported in papers in this journal section. Flight planning was based upon trajectory forecasts by models specifically developed for the purpose [Stohl *et al.*, 2004; Methven *et al.*, 2006] and discussed in daily conference calls. Several Lagrangian opportunities were identified and aircraft successfully flown to the forecast locations of the previously sampled air masses. The results are discussed in several papers in this journal section [Methven *et al.*, 2006; Attie *et al.*, 2006; Cook *et al.*, 2006; Real *et al.*, 2006; Whalley *et al.*, 2006; Lewis *et al.*, 2006; Arnold *et al.*, 2006].

4.3. Emission Map Viewer

The analysis of the ICARTT study was facilitated by providing participants with a common emission inventory data base that could be easily accessed to help identify and quantify the impact of individual point and areas sources of natural and anthropogenic emissions. A geographic information system interface, the Emission Inventory Mapviewer (<http://map.ngdc.noaa.gov/website/al/emissions>), which was developed by NOAA (ESRL/CSD and NGDC) in support of the ICARTT study, provided this resource. This interface allows users to easily visualize emission inventories along with various geographic data and carry out analyses of these inventories. The Emission Inventory Mapviewer was built around the EPA's 1999 National Emission Inventory (NEI99) for anthropogenic sources and the EPA's Biogenic Emissions Inventory System version 3.11 (BEIS3.11) for natural sources, over a domain covering the continental US, southern Canada, and northern Mexico. NEI99 emissions of NO_x, CO, VOC, SO₂, NH₃, PM_{2.5}, and PM₁₀ from individual or groups of point sources can be viewed and downloaded. It also displays total anthropogenic emissions of these compounds on a 4-km resolution grid, and provides a convenient analysis of the partitioning between point, mobile, and area sources in any rectangular latitude-longitude region. BEIS3.11 emissions of isoprene and terpenes, the major organic components emitted by vegetation, can be visualized for standard environmental conditions. The Mapviewer can also upload and display sample aircraft flight tracks, a useful tool for planning research studies of emission sources. A complete description of the Mapviewer's data sets can be found in *Frost et al.* [2006].

4.4. Measurement Comparison and Uncertainty Determination

The goal of comparison exercises for the 2004 ICARTT campaign was to create a unified observational data set from measurements acquired from multiple aircraft, ground, and ship platforms. To achieve this goal, comparisons were planned and carried out in order to help establish data comparability between the various platforms, and to verify that different analytical approaches are mutually consistent within quantifiable uncertainties. The measurements included a wide variety of in situ and remotely sensed gas-phase chemical species, aerosol chemical and physical data, radiative effects, and meteorological parameters. These data were acquired using a variety of techniques, each with specific instrumental accuracy and precision. Quantifying data uncertainty established an objective basis upon which subsequent scientific interpretations are founded.

The effort required coordination between the multiple participating organizations of ICARTT, and primarily involved side-by-side measurement opportunities between combinations of aircraft, ship, and ground stations located in and between North America and Europe. In particular, comparison opportunities linked the platforms participating in the ITCT-Lagrangian-2K4 described in Section 4.2. Additional comparisons of these data sets to satellite retrievals and model output are ongoing and the analyses involve the entire 2004 data set. The protocol for acquiring, evaluating, and disseminating the results of side-by-side data comparison activities for all participating platforms exclusive of satellite and model data can be found at <http://www.al.noaa.gov/ICARTT/>

4.5. Data Management Protocol

The ICARTT study involved a large number of measurement platforms that yielded a large volume of data. Each of the several laboratories involved in the study had its own procedures for handling data, so it was necessary to identify a common procedure prior to the study. This

facilitated data transfer both during the study and, more importantly, after the campaign was completed. All of the principals in the study agreed upon a data transfer and archiving standard modeled after the NASA Ames format, which was chosen because it satisfied the identified data handling issues, and is easily handled by most computer-based data manipulation programs. The specifications for the Ames file exchange format can be found at:

<http://cloud1.arc.nasa.gov/solve/archiv/archive.tutorial.html>. Each group designated a data manager who was responsible for ensuring that all data from that group were available on an accessible server in the common format. These separate data servers are operated and maintained by each group, and can be accessed either via the web or ftp. Collectively, these servers constitute a distributed data repository, so no central data collection and distribution server exists.

5. Meteorological and Precursor Context of ICARTT

The meteorology that prevails during a field campaign generally exerts a profound effect upon the resulting data set, and thus that data set must be interpreted within that meteorological context. Meteorology strongly affects transport patterns and stagnation conditions as well as important parameters such as radiation intensity and ambient temperature. It also affects the precursor emissions, both local (e.g. biogenic and anthropogenic hydrocarbons) and more remote (e.g. boreal forest fire emissions.)

Figure 2 puts the 2004 ozone and CO distributions of the ICARTT region into a larger spatial and temporal context. It presents the 2004 ozone and CO vertical profiles measured by the MOZAIC program over the eastern U.S. and over Germany, and compares those measurements with an average of all MOZAIC measurements from previous years. Compared to the longer-term averages, in 2004 ozone concentrations in the free troposphere were 5 to 10 ppbv higher over the eastern U.S. and about 5 ppbv higher over Germany. In contrast, CO was approximately 10 ppbv lower over the eastern U.S. and about 20 ppbv lower over Germany. During ICARTT a great deal of attention was focused on the large boreal forest fires (5.8 million hectares [*Petzold et al.*, 2006, this section]) in Alaska and northwest Canada, which would be expected to raise the 2004 ambient CO to above normal concentrations. However, 2002 and 2003 were years of even larger scale fires in Siberia (7.5 and 14.5 million hectares, respectively) [*Mollicone et al.*, 2006], which likely account for the higher CO concentrations throughout the mid-latitude northern hemisphere in those years. It is notable that even though 2004 was characterized by few ozone extremes over the northeastern U.S. (see next paragraph), the average ozone profiles are not particularly low; Figure 2 shows that the 2004 ozone concentrations were higher than the preceding ten year average, even in the continental boundary layer, at least as sampled by the MOZAIC aircraft.

White et al. [2006, this section] have evaluated the meteorology that impacted the New England area during ICARTT. This part of the study region is particularly important because it is the “tail pipe” of North America in the sense that many of the polluted air masses leaving North America pass through this region. Thus, the source for long-range transport into the North Atlantic and across to Europe may be sampled in this region. *White et al.* [2006, this section] contrast the July-August 2004 ICARTT period with the July-August 2002 period during which the NEAQS 2002 study was conducted in the same region. They show that these two years

1 represent extremes for the 1996-2005 decade, both in meteorological conditions and in observed
2 ozone levels. July-August 2004 accounted for the minimum number of ozone exceedences in the
3 New England, while 2002 had the maximum. Both studies were conducted under meteorological
4 extremes by some measures: 2002 was much warmer and drier than normal and 2004 was
5 appreciably cooler and wetter than normal. *White et al.* [2006, this section] attribute the ozone
6 extremes to these meteorological extremes. In contrast, southwesterly flow (which is most
7 closely associated with high pollution events) was actually more prevalent in 2004 than in 2002,
8 and frequency of cold front passage (which is associated with disruption of pollution
9 accumulation) was similar in the two years.

11 **6. Overview of Results**

13 **6.1. Air Quality: Instruments, Measurements and Observational Based Analyses**

14 *Instruments:*

15 The 2004 ICARRT study represented the first deployment of several significant newly
16 developed instruments. For the first time the NOAA WP-3D aircraft carried a cavity ring-down
17 spectroscopy (CARDS) system for simultaneous measurement of NO₃ and N₂O₅ with 1-s
18 temporal resolution [*Dubé et al.*, 2006], a chemical ionization mass spectrometer (CIMS)
19 instrument for the measurement of NH₃, also with 1-s resolution [*Nowak et al.*, this section], a
20 pulsed quantum cascade laser spectrometer for formaldehyde and formic acid [*Herndon et al.*,
21 this section], a Particle-into-Liquid Sampler (PILS) coupled to a Total Organic Carbon (TOC)
22 analyzer for 3-s integrated measurements of water-soluble organic carbon (WSOC) ambient
23 aerosol [*Sullivan et al.*, this section], and a visible-ultraviolet spectroradiometer system for the
24 measurement of the photolysis rate of NO₃ [*Stark et al.*, this section]. The Ronald H. Brown
25 Research Vessel carried a newly developed CARDS system for the measurement of aerosol
26 extinction and a CARDS system for the measurement of NO₂ as well as NO₃ and N₂O₅ [*Osthoff*
27 *et al.*, this section], and multi-sensor wind profiling system that combined a radar wind profiler,
28 a high-resolution doppler LIDAR, and GPS rawinsondes [*Wolfe et al.*, this section]. The wind
29 profiler, system provided continuous hourly wind profiles at 60- and 100-m vertical resolutions
30 to 3-5 km height. A Thermal desorption Aerosol GC/MS-FID (TAG) instrument deployed at the
31 Chebogue Point site reports the first ever hourly in-situ measurements of speciated organic
32 aerosol composition [*Williams et al.*, this section]. At the very remote PICO-NARE site *Helmig*
33 *et al.* [2006, this section] deployed a completely automated and remotely controlled gas
34 chromatograph for the measurement of C₂-C₆ NMHC. The system used minimal power,
35 prepared all consumable gases and blank air at the site, and required no cryogenes.

36
37 *Pikelnaya et al.* [2006, this section] deployed a Multi-Axis Differential Optical Absorption
38 Spectroscopy (MAX-DOAS) instrument at a surface site in the Gulf of Maine to make trace gas
39 measurements simultaneously with long path DOAS measurements. The comparison shows that
40 MAX-DOAS accurately measures trace gases that are well mixed within the boundary layer.
41 The successful identification by MAX-DOAS of an elevated layer at 1-2 km altitude that was
42 rich in aerosol and formaldehyde illustrates the potential for aerosol remote sensing and for
43 obtaining information on the vertical distribution of pollutants in and above the boundary layer.
44 However, horizontal inhomogeneities in trace gas concentrations within the spatial range of the
45 MAX-DOAS viewing geometry make the derivation of trace gas profiles difficult if not
46 impossible without additional measurements.

1
2 *Continental aerosol characterization:*

3 Multiphase chemistry along the New England coast was investigated at Appledore Island, which
4 receives processed continental air masses during southwesterly and westerly flow. *Fischer et al.*
5 [2006, this section] investigated the behavior of nitric acid/nitrate in relation to air mass transport
6 history and local meteorology. Although median total nitrate ($\text{HNO}_3 + \text{NO}_3^-$) concentrations
7 were higher under westerly flow, higher median dry-deposition rates of total nitrate were
8 associated with southwesterly flow. *Smith et al.* [2006, this section] performed a parallel
9 analysis of the ammonia system. Under cleaner northwest flow, total NH_x ($\text{NH}_3 + \text{NH}_4^+$)
10 concentrations were relatively low (median = 50.0 nmol m^{-3}) and partitioned roughly equally
11 between phases; under the more polluted westerly flow, total NH_3 concentrations were
12 substantially higher (median = 171 nmol m^{-3}) but dominated by particulate NH_4^+ .

13
14 *Role of nitrate radicals and N_2O_5 :*

15 *Brown et al.* [2006a,b] made the first airborne measurements of NO_3 and N_2O_5 from the NOAA
16 WP-3D aircraft. The nocturnal concentrations of NO_3 are much larger aloft than at the surface,
17 and therefore far more effective at oxidizing reactive VOC, consistent with previous suggestions
18 from models and lower resolution determinations by remote sensing techniques. They also
19 performed the first direct measurements of the reaction of N_2O_5 with aerosol particles. Its rate
20 showed surprising variability that depended strongly on aerosol composition, particularly sulfate
21 content. The correlation with aerosol composition provides evidence for a link between aerosol
22 and ozone that is larger than previously recognized. Nitrogen oxide emissions catalyze the
23 photochemical production of ozone during the day, but react to form nitric acid and remove
24 ozone at night. Quantification of the nocturnal loss processes has identified the factors that
25 influence this balance, including emissions timing, aerosol, nocturnal VOC reactions and the
26 stability of and mixing within the nighttime atmosphere. The results have implications for the
27 quantification of regional-scale ozone production and suggest a stronger interaction between
28 anthropogenic sulfur and nitrogen oxide emissions than previously recognized.

29
30 Simultaneous, in-situ measurements of atmospheric dimethyl sulfide (DMS) and NO_3 from the
31 NOAA research vessel *Ronald H. Brown* off the New England Coast during the summer of 2002
32 show a clear anticorrelation between these compounds during the night. Comparison between
33 model and observed diurnal profiles of DMS and NO_3 shows that between 65 and 90% of the
34 DMS oxidation was due to NO_3 , depending on the NO_3 mixing ratios. The results have
35 implications for the yield of sulfate aerosol from marine DMS emissions in areas affected by
36 anthropogenic NO_x pollution. The area over which DMS oxidation by NO_3 is at least as strong
37 as by OH can extend as far as 3000 km over the ocean surface [*Stark et al.*, this section].

38
39 NO_3 and N_2O_5 are normally considered only in the context of nighttime atmospheric chemistry.
40 Although their importance during the day is usually small, it is not always negligible. *Brown et al.*
41 [2005] present daylight observations of both compounds from the NOAA WP-3D aircraft.
42 The observations imply that the loss of ozone through photolysis of NO_3 to $\text{NO} + \text{O}_2$, oxidation
43 of biogenic VOC, and conversion of NO_x to HNO_3 via N_2O_5 hydrolysis can be significant. For
44 example, NO_3 oxidation of α -pinene in the presence of NO_x was predicted to contribute up to
45 40% of the total daytime oxidation rate, and hydrolysis of N_2O_5 increases the daytime
46 conversion rate of NO_x to HNO_3 by several percent, with a maximum of 13%, relative to OH+

1 NO₂. *Osthoff et al.* [2006, this section] measured N₂O₅ from the NOAA research vessel *Ronald*
2 *H. Brown*. They demonstrate that NO₃ is an important daytime oxidant for DMS, terpenes, and
3 some anthropogenic NMHC in the polluted marine boundary layer. In foggy or hazy conditions,
4 heterogeneous loss of N₂O₅ may be a significant NO_x sink compared to OH + NO₂.

5 6 *Role of halogen radicals:*

7 The CHAiOS study, conducted at Appledore Island, Maine, focused on the role of halogen
8 radicals in tropospheric chemistry. *Zhou et al.* [2006, this section] report bromoform (CHBr₃)
9 and dibromomethane (CH₂Br₂) measurements, and discuss their implications for the sources of
10 these species. *Keene et al.* [2006, this section] found that production from sea salt was the
11 primary source for inorganic Cl and Br species in the atmosphere even though sea-salt mass
12 averaged 4 to 8 times lower than that typically observed over the open North Atlantic Ocean.
13 Acid displacement of sea-salt Cl⁻ by HNO₃ sustained high HCl mixing ratios (often >2 ppbv)
14 during daytime, and resulted in highly acidic sea-salt aerosol. Cl* (an instrumentally defined
15 quantity that includes HOCl and Cl₂) ranged from <20 to 421 pptv Cl but was less than the
16 detection limit during most sampling intervals. Br radical chemistry was relatively unimportant.
17 *Pszenny et al.* [2006, this section] estimated chlorine atom concentrations of 2.2 to 5.6 x 10⁴ cm⁻³
18 based upon variability-lifetime relationships for selected nonmethane hydrocarbons.

19 20 **6.2. Air Quality: Meteorological and Modeling Studies**

21 *Marine boundary layer characterization:*

22 A shallow (≈50 m), stable boundary layer is ubiquitous over the cool waters of the Gulf of Maine
23 in summer. This layer affects pollutant transport throughout the region by isolating overlying
24 flow from the surface. In particular, emissions from the urban corridor of the northeastern
25 United States can be efficiently transported long distances [*Neuman et al.*, 2006, this section].
26 Transport as far as Europe in the lower troposphere has been observed. *Angevine et al.* [2006,
27 this section] find that the temperature profile of the lowest 1-2 km of the atmosphere over the
28 Gulf of Maine is remarkably similar regardless of transport time over water or the time of day
29 when the flow left the land, provided only that the flow is offshore. The (roughly) constant
30 water temperature and the (roughly) constant temperature of the free troposphere over the
31 continent force this similarity. Air leaving the coast at night already has a stable profile, whereas
32 air leaving the coast at midday or afternoon has a deep mixed layer. In the latter case, the stable
33 layer formation over the water occurs within 10 km and a half hour after leaving the coast.
34 Turbulent kinetic energy advected from the land over the water, is the identified source of the
35 turbulence required to produce the observed cooling. *Fairall et al.* [2006, this section] find that
36 the stable boundary layer significantly suppresses the transfer coefficients for momentum,
37 sensible heat, and latent heat between the ocean and the atmosphere. Their estimate for the mean
38 ozone deposition velocity is 0.44 mms⁻¹, which corresponds to a boundary removal time scale of
39 about one day. Such a short lifetime of ozone in the marine boundary layer significantly
40 complicates the interpretation of surface ozone measurements in this marine environment.

41 42 *Trajectory calculations:*

43 [*White, et al.*, 2006, this section] present a trajectory tool that uses the radar wind profiler
44 network observations to calculate forward or backward particle trajectories. The algorithm
45 interpolates the wind observations to determine hourly trajectory positions. Surface observations

1 from buoy and coastal station networks were assembled to enhance coverage over the Gulf of
2 Maine. The continuous profiler observations allows the trajectory tool to capture changes in
3 transport associated with mesoscale and synoptic weather events that occur between the twice-
4 daily operational balloon soundings, thereby providing a more accurate depiction of the
5 horizontal transport over the Gulf of Maine.

6
7 *Model prediction of cloud liquid water content:*

8 *Zhang et al.* [2006, this section] used measured liquid water contents (LWC) in a variety of
9 clouds to compare with values predicted from the Canadian meteorological forecast model at two
10 horizontal resolutions (15 and 2.5 km). A point-by-point comparison along flight tracks shows
11 that the model-observation correlation for LWC is poor for most of the flights due to the
12 mismatch in timing and positioning of the clouds between the model simulations and
13 observations. Comparison of the statistical properties of modeled and observed clouds over
14 flight domains shows that the model predicted the vertical distribution of LWC well. However,
15 the in-cloud LWC values were over-predicted by the model at both resolutions by 23%-99%.
16 The over prediction of LWC will impact on the chemical processing by clouds, reinforcing the
17 question of how best to parameterize sub-grid scale cloud processing.

18
19 *Effect of reductions in NO_x Emissions from power plants*

20 *Frost et al.* [2006] studied recent decreases in NO_x emissions from eastern US power plants and
21 the resulting effects on regional ozone. Using the EPA 1999 National Emission Inventory as a
22 reference emission data set, NO_x and sulfur dioxide emission rates at selected power plants were
23 updated to their summer 2003 levels using Continuous Emission Monitoring System (CEMS)
24 measurements. The validity of the CEMS data was established by comparison to observations
25 made on the NOAA WP-3 aircraft. Summertime NO_x emission rates decreased by
26 approximately 50% between 1999 and 2003 at the subset of power plants studied. Simulations
27 with the WRF-Chem regional chemical forecast model indicated NO_x emission reductions
28 resulted in important changes in regional ozone concentrations. Effects in individual plant
29 plumes varied depending on the plant's NO_x emission strength, the proximity of other NO_x
30 sources, and the availability of VOC and sunlight. This study provides insight into the ozone
31 changes that can be anticipated as power plant NO_x emission reductions continue to be
32 implemented throughout the US.

33
34 *Ozone and PM_{2.5} model forecasts:*

35 Three papers in this section deal specifically with improved methods for forecasting surface
36 ozone based on model ensemble techniques. Ensemble techniques have been commonly, and
37 successfully used in meteorological forecasts to improve real-time forecasts of precipitation,
38 tornado danger, hurricane tracks, and other weather-related phenomena important to the public.
39 For air-quality applications ensemble techniques are a newer development, due primarily to their
40 relatively high computational demand, and limited number of air-quality forecast models
41 available to populate an ensemble. As part of the model validation component of the ICARTT
42 program, the hourly observations collected at 358 surface ozone monitors throughout the
43 northeast U.S. and southern Canada (administered by the U.S. EPA AIRNow program) have
44 been compared with the real-time forecasts from eight models operational during the 2004 field
45 campaign, and two simple ensembles created from these seven models [*McKeen et al.*, 2005].
46 That study showed a persistent positive bias in all models, and confirmed the improvements

1 afforded by the bias-corrected ensemble forecast compared to any single forecast. *Pagowski et*
2 *al.* [2005] and *Pagowski et al.* [2006] have further utilized the ICARTT/NEAQS-2K4 surface O₃
3 forecast analysis by proposing two corrected ensemble techniques applicable to real-time
4 operational forecasts. The three ensemble-based O₃ forecast papers within this section use the
5 same ICARTT/NEAQS-2K4 model and observed surface O₃ data-set to present additional
6 techniques and analysis methods related to O₃ forecast improvements from an operational
7 perspective.

8
9 One of the first ever real-time ensemble ozone forecasts, as well as the first real-time bias
10 corrected forecast, was made available during the ICARTT study period
11 [<http://www.etl.noaa.gov/programs/2004/neaqs/verification/>]. *Wilczak et al.* [2006, this section]
12 retrospectively analyze the effects of different bias correction strategies on the performance of
13 the ensemble O₃ forecast, concluding that bias correction based on only the previous one or two
14 day's statistics is necessary to account for significant forecast improvement. The bias corrected
15 ensemble results are further analyzed using techniques and measures that are traditionally
16 applied to meteorological ensemble and probability forecasts such as rank histograms, attributes
17 diagrams, ROC (Relative Operating Characteristic) curves, and spread-skill relationships. The
18 analysis found that the temporal correlation of spatially averaged comparisons exhibit much
19 higher correlations than the correlation of time-series comparisons averaged spatially. This
20 suggests that model and ensemble forecasts would benefit more from improved representations
21 of local meteorology and emissions as opposed to improvements in the representation of larger,
22 continental-scale processes.

23
24 Kalman filter techniques have found widespread acceptance within the meteorological
25 community, and are used in data-assimilation applications to improve forecast initial conditions,
26 as well as bias-correction during post-processing of short-term forecasts. The use of Kalman
27 filters for air quality applications is a more recent development. *Delle Monache et al.* [2006]
28 first outlined and applied Kalman filtering to a five day O₃ episode for five surface O₃ stations in
29 western Canada during August of 2004. *Delle Monache et al.* [2006, this section] utilize the
30 longer forecast period (56 days) and the 358 stations within the ICARTT/NEAQS-2K4 model
31 verification data set to explore key parameters and strategies for Kalman filter design of discrete
32 model, ensemble, and probabilistic forecasts. A useful concept in their analysis is the
33 decomposition of model O₃ forecast errors into systematic and random components. Similar to
34 the case of simple bias-correction methods, the combination of Kalman filtering, which reduce
35 systematic forecast errors, and ensembles, which reduce random forecast errors, are shown to
36 provide the best possible forecasts.

37
38 *Pagowski and Grell* [2006, this section] further examine probabilistic O₃ forecasts based on the
39 surface O₃ forecast and observed data-sets collected during ICARTT/NEAQS-2K4. Analysis of
40 probabilistic forecast skill based on Brier scores for different thresholds of O₃ exceedance are
41 used to illustrate the improvements by using the dynamic linear regression technique of
42 *Pagowski et al.* [2006] to correct biases in the individual models. Similar to the findings of
43 *Wilczak et al.* [2006, this section] reliability diagrams show the need for bias removal within the
44 model forecasts in order for probabilistic forecasts to be useful. The economic value of a
45 particular forecast as a function of a cost/loss ratio, a useful analysis concept recently adapted to
46 meteorological forecasts, is also applied to the set of uncorrected model O₃ forecasts, corrected

1 and uncorrected ensemble forecasts, and corrected and uncorrected probabilistic forecasts. This
2 analysis demonstrates the marked improvement afforded by ensemble and probabilistic forecasts
3 compared to any single deterministic model, and the benefits of probabilistic forecasts over
4 ensemble forecasts. Consistent with the Kalman filter correction results of *Delle Monache et al.*
5 [2006, this section] the probabilistic forecast corrected by dynamic linear regression appears to
6 be an improvement over the uncorrected probabilistic forecast for O₃ exceedance thresholds less
7 than 70 ppbv, or for a limited range of cost/loss ratios for higher O₃ thresholds. Both studies
8 attribute this behavior to the low number of high O₃ events during 2004 combined with the linear
9 nature of the correction algorithms.

10
11 Compared to ozone, real-time forecasts of PM_{2.5} are a more recent development. *McKeen et al.*
12 [2006, this section] evaluate the PM_{2.5} forecasts from six models (and their ensembles) that
13 were part of the ICARTT model evaluation project. The evaluation is based on comparisons
14 with three observational platforms: the U.S. EPA AIRNow surface PM_{2.5} network, composition
15 and aerosol size distribution measurements from the NOAA WP-3 aircraft, and composition
16 from the U.S. EPA administered STN (Speciated Trends Network) monitors. From the AIRNow
17 comparisons the PM_{2.5} forecasts in general show lower bias errors, significant forecast skill, and
18 similar correlations relative to ozone under equivalent mid-day averaging conditions. Similar to
19 the case of ozone, the ensembles generated by averaging all of the PM_{2.5} forecasts (both
20 arithmetic and geometric means) yield significantly improved forecasts compared to any single
21 model. A comparison of model and observed diurnal variations for urban and suburban
22 AIRNow sites illustrates the sensitivity of PM_{2.5} forecasts to PBL (planetary boundary layer)
23 parameterizations, particularly under stable conditions. Comparisons of aerosol composition
24 with the WP-3 aircraft data clearly illustrate the under-prediction of organic carbon for all
25 models within the PBL, which illustrates a serious deficiency in the current understanding of
26 aerosol mass formation. Biases in aerosol sulfate and SO₄/SO₂ ratios are distinctively different
27 between models that include oxidation of SO₂ by clouds (high biases) and those models that
28 ignore sulfate production in clouds. Aerosol ammonium biases and aerosol/gas-phase
29 partitioning of NH₄/NH₃ directly correlate with sulfate biases.

30 31 *Regional Air Quality Model Studies:*

32 *Tang et al.* [2006, this section] studied the sensitivity of a regional air quality model to various
33 lateral and top boundary conditions derived from global models. The simulations were shown to
34 be sensitive to the boundary conditions from the, especially for relatively long-lived species; for
35 example, differences in the mean CO concentrations from 3 different boundary conditions were
36 as large as 50 ppbv. *Griffin et al.* [2006, this section] investigated the photochemical generation
37 of CO on the regional scale in two areas of the United States. No more than 10% of CO comes
38 from VOC oxidation. The dominant hydrocarbons are biogenic (principally isoprene) in
39 northeast US, and anthropogenic hydrocarbons in the western US, where the maximum
40 contribution is 1% which can approach 45 ppbv.

41 42 **6.3. Aerosol Formation, Composition, and Chemical Processing**

43 44 *Tropospheric aerosol characterization:*

45 *Murphy et al.* [2006, this section] report the composition of single particles measured by the
46 Particle Analysis by Laser Mass Spectrometry (PALMS) instrument. The measurements from

1 the ICARTT campaign are placed in the context of those from a number of airborne and ground-
2 based campaigns. In the regions studied, 30% to over 80% of the aerosol mass in the free
3 troposphere was carbonaceous material. Although there were variations in their amounts, over
4 90% of accumulation mode particles away from local sources were internal mixtures of sulfates
5 and carbonaceous material. Within this internal mixing, there was variation in the pattern of
6 organic peaks in the spectra, especially in peaks related to organic acids. Particles with a
7 biomass-burning signature were a significant fraction of accumulation mode particles even far
8 from fires. The accumulation mode near the ocean surface off the coasts of New England and
9 California had significant numbers of organic-sulfate particles whereas at Cape Grim, Tasmania,
10 the organic-sulfate particles were apparently all smaller than 160 nm. Three kinds of nitrate
11 were evident: on mineral particles, on sulfate-organic particles when the sulfate was fully
12 neutralized, and at temperatures below about 198 K. Most mineral particles showed evidence of
13 the uptake of nitrates and chlorine.

14
15 *Ziemba et al.* [2006a, this section] describe the bulk aerosol inorganic chemical composition in
16 northern New England, particularly in relation to aerosol acidity. They find that the aerosol is
17 dominated by sulfate and ammonium yielding weakly acidic aerosols, while nitrate plays a small
18 role. The average sulfate and ammonium aerosol concentration was highest during the summer
19 coinciding with the highest median acidity. Nitrate concentrations were highest in the winter.

20 21 *Aerosol nucleation:*

22 Nanoparticle growth events were observed 48 times in particle size distributions measured at
23 Appledore Island during ICARTT/CHAIOS in July and August of 2004 [*Russell et al.*, 2006, this
24 section]. Eighteen of the events occurred during the morning when plentiful α - and β -pinene
25 and ozone made production of condensable products of photochemical oxidation probable.
26 Nanoparticle growth continued over several hours, and growth rates varied from 3 to 13 nm h⁻¹.
27 Apparent nanoparticle yields were estimated to range from less than 0.03% to almost 1%
28 assuming α - and β -pinenes were the particle source. These yields are up to two orders of
29 magnitude greater than predictions from extrapolated laboratory parameterizations and provide a
30 more accurate assessment of SOA formation for global models.

31
32 *Ziemba et al.* [2006b, this section] present observations of frequent aerosol nucleation events in
33 northern New England. These events are photochemically driven, most common in winter and
34 spring, and may be associated with a variety of mechanisms including oxidation products of
35 biogenic compounds, ternary homogeneous nucleation involving SO₂, and iodine chemistry from
36 marine sources.

37 38 *Marine aerosol evolution:*

39 Measurements in the marine boundary layer over the Gulf of Maine from the R/V *Ronald H.*
40 *Brown* were used to study the evolution of aerosols as they were transported away from the
41 continental source regions. As distance from the source region increased, the aerosol measured
42 in the marine boundary layer became more acidic, had a lower particulate organic matter (POM)
43 mass fraction, and the POM became more oxidized. A factor analysis performed on a combined
44 data set of aerosol and gas phase parameters showed that the POM measured during the
45 experiment was predominantly of secondary anthropogenic origin [*Quinn et al.*, 2006, this
46 section]. The relative humidity dependence of light extinction reflected the change in aerosol

1 composition being lower for the near-source aerosol and higher for the more processed aerosol
2 [*Quinn et al.*, 2006, this section; *Wei et al.*, 2006, this section]. The aerosol light absorption to
3 extinction ratio also changed with distance from the sources. The increase in the single
4 scattering albedo with increasing distance from the continent was attributed to condensation of
5 non-absorbing mass and mixing with other air masses [*Sierau et al.*, 2006, this section].
6

7 *Allan et al.* [2006, this section] and *Williams et al.* [2006, this section] characterized aerosols at
8 Chebogue Point on the southern tip of Nova Scotia, approximately 500 km downwind of the
9 New York-Boston urban corridor. The fine particulate matter was principally secondary in
10 nature. The fine aerosols within plumes from the eastern U.S. were mainly composed of acidic
11 sulfate and highly oxidized organics, while those from more northerly regions were mainly
12 organic and less oxidized. The fine particulate mass burden was much higher in both cases
13 compared to the marine sector, while the particle number concentrations were largely
14 independent of the terrestrial sector. The differences in composition were manifested in the
15 hygroscopic properties and volatility of the particles; particles observed during eastern U.S.
16 influence were larger with a much higher inorganic content, the latter of which was manifested
17 in the hygroscopic properties and volatility of the particles. A combination of these changing
18 properties also lead to higher light scattering and particle activation potentials being measured in
19 the U.S. sector [*Allan et al.*, this section].
20

21 Both anthropogenic and biogenic sources affected gas and particle organics at Chebogue Point.
22 Anthropogenic and oxygenated volatile organic compounds accounted for the bulk of the gas-
23 phase organic carbon under most conditions; however, biogenic compounds were important in
24 terms of chemical reactivity [*Millet et al.*, 2006, this section; *Holzinger et al.*, 2006, this section].
25 A suite of related oxygenated VOCs (including acetic acid, formaldehyde, acetaldehyde, formic
26 acid and hydroxyacetone) were detected and shown to be related to chemical species in aerosols.
27 The compounds match the oxidation products of isoprene observed in smog chamber studies,
28 and appear to be formed in parallel with biogenic secondary organic aerosol [*Holzinger et al.*,
29 2006, this section]. Organic aerosol mass was highest during U.S. pollution events, but made up
30 the largest fraction (up to 83%) of the total aerosol during biogenic oxidation events arriving
31 from Maine and Canada [*Williams et al.*, 2006, this section; *Allan et al.*, 2006, this section;
32 *Millet et al.*, 2006, this section]. In addition to anthropogenic northeastern U.S. sources, hourly
33 measurements of particulate organic marker compounds identified several other source types,
34 including particles formed from isoprene oxidation, particles formed from local terpene
35 oxidation, locally produced aerosol containing large alkanes, and locally produced aerosol
36 apparently originating from marine or dairy processing sources [*Williams et al.*, 2006, this
37 section].
38

39 *Continental aerosol evolution:*

40 The CIRPAS Twin Otter measured aerosol size distributions during cross wind transects of the
41 Conesville power plant plume [*Fountoukis et al.*, 2006, this section]. Ultrafine particles, just
42 above the observation threshold at 8 km downwind, grew appreciably at each subsequent
43 transect farther downwind under clear sky conditions. Under cloudy conditions, the same
44 growth phenomenon was observed. Hygroscopic growth analysis indicates that the aging
45 process tended to decrease the hygroscopicity of the plume aerosol: larger particles farther away
46 from the plant exhibited smaller water uptake than the fine particles observed closer to the plant.

1 This may be the result of the partitioning of ambient volatile organic compounds or their
2 oxidation products into the particle phase.

3
4 The particle-into-liquid sampler (PILS) on the CIRPAS Twin Otter quantified the chemical
5 composition of the water-soluble aerosol components. The highest total mass loadings were
6 measured downwind of the Conesville Power Plant, a coal-burning power generation facility. In
7 general, sulfate dominated the sub-micron particulate ionic mass. Ammonium was the next
8 largest contributor to the ionic mass, with its level highly correlated with that of sulfate. Nitrate
9 concentrations were usually below $1 \mu\text{g}/\text{m}^3$, dropping to their lowest levels under acidic
10 conditions downwind of power plants. PILS data provide clear evidence for aqueous-phase
11 production of oxalic acid [*Sorooshian et al.*, 2006, this section]. The highest mass loadings for
12 oxalate were measured for total aerosol and droplet residual samples in clouds influenced by
13 power plant plumes. A chemical cloud parcel model [*Ervens et al.*, 2004], initialized with
14 measured aerosol size distributions, gas-phase concentrations, and meteorological conditions,
15 predicted the same relative magnitudes of oxalic acid and SO_4^{2-} production as those observed.
16 Agreement between measurements and predictions for the growth of glyoxylate, malonate,
17 pyruvate, and glutarate provides evidence for aqueous-phase processing of dissolved organic
18 gases as contributing to aerosol organic constituents.

19
20 *Hayden et al.* [2006, this section] use observations of gas-phase nitrate, size-distributed
21 particulate nitrate, cloud water nitrate and size-distributed cloud droplet residual nitrate to study
22 changes in the partitioning of nitrate from pre-cloud to post-cloud as a function of particle size.
23 Little nitrate was measured in the aerosol below cloud, whereas the nitrate levels in the bulk
24 cloud-water were comparable to those of sulfate; most of the nitrate entered the cloud water as
25 HNO_3 . Nitrate in the dry residuals of the cloud droplets was intermediate between the below-
26 cloud and cloud-water nitrate. The mode of the mean size distribution of the residual nitrate is
27 smaller than that of sulfate. Simulations with an aerosol-cloud parcel model indicate that the
28 smaller nitrate residuals are a result of the control of the transfer of HNO_3 to cloud droplets by
29 gas-phase mass transfer, whereas most of the initial sulfate in the cloud water is due to
30 nucleation scavenging. Thus, the clouds are capable of venting gas-phase nitrate from the
31 boundary layer and partitioning some of it to particles smaller than where the main mass of the
32 sulfate is found.

33
34 *Leithead et al.* [2006, this section] examine the airborne measurements of seven carbonyl species
35 (HCHO, acetaldehyde, acetone, valeraldehyde, benzaldehyde, propionaldehyde, and
36 butanaldehyde) in cloud-water together with concurrent gas phase measurements of HCHO
37 measurements. The total in-cloud HCHO (liquid plus interstitial aqueous-phase) was generally
38 similar to below cloud gas-phase HCHO. The cloud-water HCHO was in equilibrium with the
39 interstitial gas-phase HCHO in two of five cases and significantly lower in two of five cases.
40 The deviations are attributed to liquid phase processes such as adduct formation or oxidation.
41 The predicted equilibrium gas phase concentrations for the other six carbonyls, based on the
42 cloud water concentrations, were unreasonably high (order of magnitude) compared with
43 typically observed gas-phase levels. If the Henry's Law constants for these species are valid
44 under these conditions, then surface adsorption and reactions, including polymerization, may
45 contribute to the relatively high aqueous-phase levels.

1 *Aerosol organic carbon characterization:*

2 The NOAA WP-3D aircraft investigated water-soluble organic carbon (WSOC) sources
3 [Sullivan *et al.*, 2006, this section] over the northeastern U.S. and Canada. Two main sources
4 were identified: biomass burning emissions from fires in the Alaska/Yukon region and emissions
5 emanating from urban centers. Biomass burning WSOC was correlated with carbon monoxide
6 (CO) and acetonitrile ($r^2 > 0.88$). These plumes were intercepted in layers at altitudes between 3
7 and 4 km and contained the highest fine particle volume and WSOC concentrations of the
8 mission. Apart from the biomass burning influence, the highest concentrations were at low
9 altitudes in distinct plumes of enhanced particle concentrations from urban centers, whereas
10 generally the lowest WSOC concentrations were recorded in rural air masses. WSOC and CO
11 were highly correlated ($r^2 > 0.78$) in the urban plumes. The ratio of the enhancement in WSOC
12 relative to that of CO enhancement was found to be low in plumes that had been in transit for a
13 short time, and increased with plume age to a maximum after approximately one day. The
14 results suggest WSOC in fine particles is produced from compounds co-emitted with CO and
15 that these species are rapidly converted to organic particulate matter within ~1 day.

16
17 *Heald et al.* [2006, this section] examined the NOAA WP-3D aircraft measurements of WSOC
18 aerosol with the GEOS-Chem global chemical transport model to test our understanding of the
19 sources of organic carbon (OC) aerosol in the free troposphere (FT). Outside of the boreal fire
20 plumes, observed WSOC aerosol concentrations averaged $0.9 \pm 0.9 \mu\text{gCm}^{-3}$ in the free
21 troposphere. The corresponding model value is $0.7 \pm 0.6 \mu\text{gCm}^{-3}$, including 42% from biomass
22 burning, 36% from biogenic secondary organic aerosol (SOA), and 22% from anthropogenic
23 emissions. Previous OC aerosol observations over the NW Pacific in spring 2001 (ACE-Asia)
24 averaged $3.3 \pm 2.8 \mu\text{gCm}^{-3}$ in the FT, compared to a model value of $0.3 \pm 0.3 \mu\text{gCm}^{-3}$. WSOC
25 aerosol concentrations in the boundary layer (BL) during ITCT-2K4 are consistent with OC
26 aerosol observed at the IMPROVE surface network. The model is low in the boundary layer by
27 30%, which we attribute to secondary formation at a rate comparable to primary anthropogenic
28 emission. Observed WSOC aerosol concentrations decrease by a factor of 2 from the BL to the
29 FT, as compared to a factor of 10 decrease for sulfur oxides, indicating that most of the
30 WSOC aerosol in the FT originates *in situ*.

31
32 *Gilardoni et al.* [2006, this section] collected submicron atmospheric aerosol samples on four
33 platforms: Chebogue Point, Appledore Island, the CIRPAS Twin Otter, and the NOAA R/V
34 Ronald Brown. Alkanes, alkene plus aromatic, organic sulfur, carbonyl and hydroxyl functional
35 groups were measured by calibrated Fourier Transform Infrared (FTIR) spectroscopy. Samples
36 show high contributions of C-H groups from alkanes, alkenes and aromatic compounds. The
37 functional group composition shows significant differences across the ICARTT region, with
38 each site showing characteristic fractions of unsaturated and oxygenated carbon. Organic
39 particles collected during the Twin Otter flights over Ohio show a lower carbonyl concentration
40 relative to alkane concentration than samples collected at the coastal locations, suggesting that
41 fresh emissions are predominant in those samples. Retroplume analysis for Appledore Island
42 and Chebogue Point samples suggested that air masses that reached these locations from Canada
43 were characterized by higher carbonyl relative to alkane groups compared to the air masses from
44 U.S. sources. Organic sulfur compounds were often observed, with higher concentrations
45 associated with high sulfate, high carbonyl, and high relative humidity.

46

6.4. Aerosols as CCN

Three cloud condensation nucleus (CCN) closure experiments were carried out using data sets collected during ICARTT. The data sets were collected in very different environments; from the CIRPAS Twin Otter aircraft in the mid-Western U.S. [Fountoukis *et al.*, 2006, this section], from the UNH-AIRMAP Thompson Farm site (an inland rural location receiving continental air masses) [Medina *et al.*, 2006, this section; Sotiropoulou *et al.*, 2006] and from Chebogue Point, Nova Scotia (a marine rural site receiving well aged air masses) [Ervens *et al.*, 2006, this section]. Each of the three experiments found excellent agreement between measured and modeled CCN concentrations, and each concluded that organic carbon does not contribute substantial amounts of solute to affect CCN activation.

A principal goal of the CIRPAS Twin Otter mission in ICARTT was to elucidate aerosol-cloud drop relationships in the eastern U.S. region. A unique feature of the dataset is the sampling of highly polluted clouds within the vicinity of power plant plumes. Twenty-seven cumuliform and stratiform clouds were sampled [Fountoukis *et al.*, 2006]. The dataset was used to assess cloud droplet closure using (1) a detailed adiabatic cloud parcel model, and (2) a state-of-the-art cloud droplet activation parameterization. Excellent closure between predicted and observed cloud droplet concentrations was achieved (on average to within 10%) for both parcel model and parameterization. The uncertainty in predicted cloud droplet concentration was mostly sensitive to updraft velocity. Optimal closure is obtained for a value of the water vapor mass accommodation coefficient of 0.06, but its value can range between 0.03 and 1.0. The sensitivity of cloud droplet prediction to the value of the accommodation coefficient, organic solubility, and surface tension depression suggests that aerosol organics in the ICARTT region do not contribute substantial amounts of solute, compared to sulfate.

Medina *et al.* [2006, this section] obtained measurements CCN, aerosol size distribution and chemical composition at the rural Thompson Farm site. CCN concentrations predicted from "simple" Köhler theory were compared with CCN measurements from 0.2%, to 0.6% supersaturation. Including size-dependent chemical composition yielded excellent closure (average error $17.4 \pm 27.2\%$). The closure was worse during periods of changing wind direction, suggesting that introduction of aerosol mixing state would further improve closure. Knowledge of the soluble salt fraction is sufficient for description of CCN activity, suggesting that the organic aerosol component had little effect on CCN activity during this study.

Sotiropoulou *et al.* [2006] used the Medina *et al.* [2006, this section] treatment, coupled with the Fountoukis and Nenes [2005] activation parameterization, to evaluate the importance of CCN predictions for indirect effect assessments. They concluded that if size-resolved chemical composition and accurate representation of size distribution is considered, the CCN prediction error is roughly 20%, and droplet number uncertainty being half of that. As a followup, Sotiropoulou *et al.* [2006, in review] introduced the CCN uncertainty analysis within the GISS II' global climate model for an online assessment of CCN prediction error; simulations suggest that application of Köhler theory introduces between 10% and 20% (global annual average) uncertainty in aerosol indirect forcing. CCN prediction errors could introduce a 50% uncertainty in predictions of autoconversion rates, especially over anthropogenically perturbed regions of the globe. Thus, even if CCN prediction errors are not likely a significant source of uncertainty for

1 assessments of the “first” (albedo) indirect effect, they could be important for assessments of the
2 “second” (lifetime) indirect effect.

3
4 *Nenes and Medina* [2006, in preparation], using a novel measurement technique, known as
5 “Scanning Mobility CCN Analysis” (SMCA), obtained high-resolution size-resolved CCN
6 measurements at Thompson Farm during ICARTT. SMCA provides insight into the chemical
7 composition of the aerosol, as well as detailed information on the CCN mixing state and size-
8 resolved droplet growth kinetics. Introducing the mixing state into the CCN closure further
9 improved predictions of CCN (average error: 4%), while the CCN activity could be reproduced
10 with a mixture of sulfate and an “insoluble” organic. The close agreement between inferred
11 sulfate and measurements with the AMS suggest that the organic does not contribute substantial
12 amounts of solute, and most of the soluble fraction is from the sulfate present in the aerosol.
13 Finally, droplet growth kinetics could be influenced by the presence of organics.

14
15 *Ervens et al.* [2006, this section] predicted the number concentration of CCN from measurements
16 of aerosol size distribution, composition, and hygroscopic growth, and compared to measured
17 CCN. It is shown that CCN can be predicted quite reliably using measured size distributions, a
18 simple soluble/insoluble aerosol model, and either the diameter growth factor $g(RH)$ or the light
19 scattering growth factor $f(RH)$. The organic aerosol at Chebogue Point, which was mostly
20 oxygenated, was effectively completely insoluble from the point of view of hygroscopicity and
21 activation. This supports the notion that concentrated, oxygenated organic aerosol is effectively
22 insoluble under subsaturated conditions.

23
24 *Garrett et al.* [2006, this section] provide a measurement technique for assessing the extent to
25 which concentrations of CCN and HNO_3 are scavenged by precipitation, distinct from the
26 separate sinks of dilution, dry deposition, and chemical transformation. The technique does not
27 require detailed knowledge of the aerosols, clouds and precipitation involved, only
28 measurements of HNO_3 and CO in clear air. This technique may provide a method for
29 evaluating parameterizations of chemical and aerosol sinks parameterized in transport models.

30 31 **6.5. Aerosol Radiative Effects**

32 During ICARTT the Jetstream 31 aircraft flew over the Gulf of Maine to characterize aerosol,
33 water vapor, cloud, and ocean surface radiative properties and effects in flights that sampled
34 polluted and clean air masses in coordination with measurements by other ICARTT platforms,
35 including several satellites. *Redemann, et al.*, [2006, This section] report J31 measurements of
36 aerosol effects on radiative energy fluxes. They measured net (downwelling minus upwelling)
37 spectral irradiance as a function of aerosol optical depth (AOD), which gives the instantaneous
38 spectral aerosol radiative forcing efficiency, E_i . Numerical integration over a given spectral
39 range yields the instantaneous broadband aerosol radiative forcing efficiency. Within 10 case
40 studies suitable for analysis they found a high variability in the derived aerosol forcing
41 efficiencies for the visible wavelength range (350–700 nm), with a mean of $-79.6 \pm 21.8 \text{ W m}^{-2}$
42 (mean \pm std). An analytical conversion of the instantaneous forcing efficiencies to 24h-average
43 values yielded $-45.8 \pm 13.1 \text{ W m}^{-2}$.

44
45 *Avey et al.* [2006, this section] characterize the “indirect effect” of pollution aerosol on clouds
46 and climate using combined satellite retrievals of clouds and aerosols. Anthropogenic CO is used

1 as a pollution tracer. Aircraft data near land indicate that measured CO perturbations correspond
2 to smaller measured values of cloud droplet effective radii, r_e , and higher droplet number
3 concentrations. Satellite data show, to a high degree of statistical significance, that mean values
4 of retrieved r_e are smaller under modeled polluted conditions. However, there is no apparent
5 trend in the sensitivity with distance downwind from the source region, suggesting stability in
6 the sensitivity of marine clouds to continental pollution.

7 8 **6.6. Long Range Transport: North American Outflow**

9 During ICART a surface site was operated at Chebogue Point on the southern tip of Nova Scotia
10 to sample surface outflow from the eastern seaboard of North America. This is the same site that
11 was operated in the summer of 1993 during the NARE study. 3-D chemical transport model
12 results show that Chebogue Point is well situated to sample surface-layer pollution outflow from
13 the United States. However, 70% of the export takes place above 3 km, so that aircraft and
14 satellite observations are also needed to fully characterize North American outflow. The overall
15 distributions of ozone and CO in air arriving at Chebogue Point were very similar in 1993 and
16 2004. Using a chemical factor indicative of U.S. pollution, it was shown that the criteria
17 pollutants CO, ozone, and submicron aerosol mass are enhanced by 30-300% during U.S.
18 outflow events [*Millet et al.*, this section]. Measured particulate matter within plumes from the
19 eastern U.S. was principally secondary in nature, mainly composed of acidic sulfate and highly
20 oxidized organics [*Allan et al.*, this section; *Williams et al.*, this section].

21
22 The NOAA WP-3 aircraft extensively studied plumes of North American emissions over the
23 Western north Atlantic. *Neumann et al.* [2006, this section] characterize urban emissions, and
24 plume transport and transformation processes in aged plumes located up to 1000 km downwind
25 from the east coast of North America. Emission outflow was observed primarily below 1.5 km
26 altitude in well-defined layers that were decoupled from the marine boundary layer. In aged
27 plumes located over the North Atlantic Ocean, the nitric acid (HNO_3) mixing ratios were large
28 (up to 50 ppbv) and HNO_3 accounted for the majority of reactive nitrogen. Plume CO and
29 reactive nitrogen enhancement ratios were nearly equivalent in fresh and aged plumes, which
30 indicated efficient transport of HNO_3 . Without substantial HNO_3 loss, the ratio of HNO_3 to NO_x
31 was between 13 and 42 in most highly aged plumes and sometimes exceeded calculated
32 photochemical steady state values, which indicate the contribution of nighttime reactions in the
33 conversion of NO_x to HNO_3 . Photolysis and OH oxidation of over 10 ppbv HNO_3 that was in
34 the troposphere for days resulted in reformation of hundreds of pptv of NO_x , which is sufficient
35 to maintain photochemical ozone production. The efficient transport of HNO_3 carried both
36 HNO_3 and NO_x far from their sources, extended their atmospheric lifetimes, and increased their
37 photochemical influence.

38
39 *Parrish et al.* [2006, this section] describe a model for investigating the combined influences of
40 photochemical processing and air mass mixing on the evolution of non-methane hydrocarbon
41 (NMHC) ratios. The model-measurement comparisons indicate that the interaction of mixing
42 and photochemical processing prevent a simple interpretation of “photochemical age”, but that
43 the average age of any particular NMHC can be well defined, and can be approximated by a
44 properly chosen and interpreted NMHC ratio. The relationships of NMHC concentration ratios
45 not only yield useful measures of photochemical processing in the troposphere, but also provide
46 useful test of the treatment of mixing and chemical processing in chemical transport models.

1
2 *Lagrangian balloon systems:*

3 During the ICARTT campaign, altitude-controlled balloons were used extensively to track urban
4 pollution plumes. Nine balloons flew a total of 670 flight hours, measuring the quasi-Lagrangian
5 evolution of the winds, temperature, and ozone downwind of major pollution source regions and
6 helping mission scientists to find the emission plumes in real time. Two types of balloons were
7 flown: NOAA's SMART balloons [Mao *et al.*, 2006, this section], released from the eastern tip
8 of Long Island in New York, measured meteorological parameters and ozone over the Gulf of
9 Maine and North Atlantic with one flight reaching Europe. Smaller Controlled Meteorological
10 (CMET) balloons [Riddle *et al.*, 2006, this section] were able to be vehicle launched from
11 multiple locations in order to target specific plumes. Flights ranging from 12 to 120 hours in
12 duration measured the quasi-Lagrangian evolution of the low-level winds, temperature, and, in
13 one case, ozone and relative humidity, downwind of major source regions. Riddle *et al.* [2006,
14 this section] use the balloon data to show that ECMWF wind fields are significantly more
15 accurate than those of GFS for low-level outflow during ICARTT. For trajectory durations
16 between 2 and 12 hours, mean trajectory errors are found to be approximately 25% of the flight
17 distance for ECMWF-based trajectories. Anomalously large model errors observed during two
18 flights were found to be the result of a low-level coastal jet and synoptic-scale divergence.

19
20
21 **6.7. Long Range Transport: Mid-Atlantic Environment**

22 The PICO-NARE site, which has been established at a 2.2 km elevation mountain top site in the
23 Azores, has provided an unprecedented site for measurements in the free troposphere in the most
24 remote part of the central North Atlantic Ocean. The year round data are elucidating seasonal
25 cycles of tropospheric chemistry in this region with good statistics from relatively long-term
26 measurements.

27
28 *Boreal fire impact:*

29 Emissions from the 2004 North American boreal fires frequently reached the PICO-NARE
30 station during summer 2004, significantly increasing levels of nitrogen oxides, carbon monoxide
31 and black carbon, and increasing ozone as well in most cases [Val Martin *et al.*, this section]. A
32 large fraction of the originally emitted nitrogen oxides and black carbon is present in the plumes
33 at arrival in the Azores. The magnitude of the impacts and the distance of the Azores from the
34 fires implies large-scale impacts of boreal fires on lower tropospheric NO_x, ozone, and black
35 carbon, and is consistent with multi-year analyses of correlations between upwind boreal fires
36 and increased ozone at the station [Lapina *et al.*, 2006].

37
38 *Low-level anthropogenic pollution outflow:*

39 Owen *et al.* [2006, this section] analyze low-level transport events that bring North American
40 anthropogenic emissions to the PICO-NARE station. Low-level transport during summer 2003
41 resulted in frequent CO enhancements at the station. Although exported and transported at low
42 altitudes, these events were observed at 2.2 km, well above the marine boundary layer, and were
43 characterized by significant enhancements in ozone as well. These ozone enhancements may
44 reflect the efficient transport of nitric acid in plumes above the marine boundary layer [Neuman
45 *et al.*, 2006, this section]. Owen *et al.* [2006, this section] suggest that transport, in the lower
46 free troposphere above the marine boundary layer, may provide an effective mechanism for

1 long-range impacts of anthropogenic emissions on lower tropospheric ozone in distant
2 downwind regions.

3
4 *Helmig et al.* [2006, this section] utilize one year of continuous measurements of non-methane
5 hydrocarbons (NMHC) at the PICO-NARE station to investigate seasonal oxidation chemistry.
6 Substantially enhanced NMHC levels during the summer of 2004 were attributed to the impact
7 of long-range transport of biomass burning plumes. Interpretations of NMHC ratios as a relative
8 scale for photochemical processing indicate that in spring enhanced ozone levels were observed
9 in air that had relatively 'fresh' photochemical signatures and ozone at lower levels was
10 observed in more processed air. This relationship indicates that the lower troposphere over the
11 central North Atlantic is a region characterized by net ozone destruction in spring.

12 13 *PICO-NARE station future:*

14 Research documented in this section has contributed to the continuation of active measurements
15 at the PICO-NARE station, which was originally installed as a temporary research station but is
16 now the focus of development of a permanent Portuguese observatory. *Kleissl et al.* [this
17 section] determined that measurements there are usually characteristic of the free troposphere,
18 even during summer (when buoyant upslope flow affects the station much less frequently than it
19 does many other mountaintop observatories). This is the result of the latitude, small size, and
20 topography of Pico Mountain. The station is valuable for the observation of highly aged but
21 detectable plumes of anthropogenic [*Owen et al.*, this section] and boreal biomass-burning [*Val*
22 *Martin et al.*, this section] plumes, and provides a platform for year-round observations
23 characteristic of regional background levels, as demonstrated for NMHCs by *Helmig et al.* [this
24 section].

25 26 **6.8. Long Range Transport: Lagrangian Related Studies**

27 A combination of air mass trajectory analyses and independent chemical signatures was used to
28 establish the occurrence of events where chemical processing could be studied in a Lagrangian
29 framework. The ITCT-Lagrangian-2K4 study conducted as part of ICARTT provided evidence
30 that this type of experiment has for the first time been successfully achieved in the free
31 troposphere on intercontinental scales. Analysis of identified Lagrangian events on the North
32 America to Europe intercontinental scale indicated for the most part a small tendency for net
33 ozone production with a concurrent loss of CO [*Methven et al.*, 2006, this section].

34
35 A major feature of the ICARTT study period was the strength and importance of low-level
36 (below 700 hPa) transport of continental emissions at altitudes just above the marine boundary
37 layer [*Lewis et al.*, 2006, this section]. This transport is in addition to the expected transport
38 pathways in the mid and upper troposphere. The observations were in particular contrast to
39 previous aircraft studies made in 1996, also based in the Azores. A consequence was the
40 elevation in NO available in the lower troposphere in mid Atlantic (both from direct transport
41 and *via* decomposition of sequestered forms), with notable impacts on calculated ozone
42 production efficiency in this region.

43
44 The evolution of non-methane hydrocarbons (NMHC) between the interceptions in the
45 Lagrangian events identified by *Methven et al.* [2006, this section] was exploited by *Arnold et al.*
46 [2006, this section] to estimate the mean OH concentrations and dilution rates acting over the

1 time intervals between observations. These are the first estimates of time-mean OH
2 concentrations following individual air masses over several days, which are well constrained by
3 observations up and downwind. An Alaskan fire plume with high NMHC concentrations gave
4 the best estimates of $[\text{OH}] = 1.7 \times 10^6 \text{ cm}^{-3}$ due to a distinct hydrocarbon fingerprint, and large
5 concentrations.

6
7 The interception of biomass burning plumes several thousand kilometers downwind of NOAA
8 WP-3D and NASA DC-8 observations indicate that mixing was often very limited between the
9 stretching filaments and the background. Tracers such as CO reached concentrations as high as
10 600 ppbv in biomass burning plumes intercepted in the mid-Atlantic, similar values to those seen
11 much closer to source, and that within these air masses there remained a significant distribution
12 of reactive chemicals, notably the elevation of the unsaturated hydrocarbon ethene [Lewis *et al.*,
13 2006, this section]. However, when the filaments reached frontal boundaries, mixing produced
14 more pronounced effects [Real *et al.*, 2006, this section]

15
16 *Real et al.* [2006, this section] analyze in detail one case of long-range transport of a biomass
17 burning plume from Alaska to Europe. This plume was sampled several times in the free
18 troposphere over North America, the North Atlantic and Europe by three different aircraft. The
19 measurements showed enhanced values of CO, VOCs and NO_y , primarily in the form of PAN
20 and the measured ozone increased by 17 ppbv over the 5 days of transport from North America
21 to Europe. They used a photochemical trajectory model initialized with upwind data to examine
22 the chemical evolution of the plume. The high aerosol loading in the plume was found to reduce
23 photolysis rates by about 20%, which led to a decrease of 18% in ozone production and 28% in
24 ozone destruction over five days. The large ozone increases were attributed primarily to PAN
25 decomposition during descent of the plume towards Europe. The predicted ozone changes are
26 very dependent on temperature changes during transport, and also, on water vapor levels in the
27 lower troposphere which can lead to ozone destruction. Inclusion of mixing of the plume with
28 adjacent air masses was found to be important for the model simulations to agree well with
29 observed changes in CO and ozone. The simulated evolution of the O_3/CO correlations in the
30 plume agreed well with observations, where the slopes changed from negative to positive over
31 the five days of transport. This change can be attributed largely to photochemistry. The possible
32 impact of this biomass burning plume on ozone levels in the European boundary layer is also
33 examined by running the model for a further five days, and comparing with data collected at
34 surface sites.

35
36 Mid-Atlantic interceptions of the biomass burning plumes reinforced the importance of the
37 height at which the emissions were injected. Peroxyacetylnitrate was the major nitrogen carrier
38 species, and the chemistry and processing state within plumes was tied closely to the rates of its
39 decomposition. Emissions initially lofted to above 6km, were neutral in ozone and appeared
40 chemically inactive; the presence of reactive hydrocarbons such as ethene at concentrations as
41 high as 2 ppbv some 3 days from emissions suggests that chemical processing within plume was
42 not efficient. At lower altitudes PAN decomposition was clearly occurring with concurrent
43 production of ozone from this source [Whalley *et al.*, 2006, this section].

44
45 *Attie et al.* [2006, this section] and *Cook et al.* [2006, this section] use the ICARTT aircraft
46 observations to evaluate the treatment of biomass burning emissions by two different global

1 models, and in turn use the models to evaluate the hemisphere-wide effect of the Alaskan forest
2 fire emissions. Interestingly, the comprehensive dataset allowed the separate evaluation of the
3 model representations of emissions, transport and chemical processes. *Cook et al.* [2006, this
4 section] conclude that the increased O₃ over the northern hemisphere in the model simulations
5 reached a peak in July 2004 in the range 2.0 to 6.2 Tg.

6 7 **6.9. Long Range Transport: Impact in Inflow Regions**

8 The final destination of a significant fraction of the emissions that have been transported over
9 long distances is transport over downwind continental regions, where they can be entrained into
10 the continental boundary layer and affect those regions' air quality. The ICARTT program in
11 general and the ITCT-Lagrangian-2K4 study in particular were designed to evaluate the impact
12 of North American emissions on Europe; however, the impact of intense Alaskan and Canadian
13 forest fires on aerosol, CO, ozone and other species were also noted at distant locations in North
14 America.

15
16 *Petzold et al.* [2006, this section] use the data collected during ICARTT study and combine it
17 with data from two ground sites in Central Europe (Hohenpeissenberg Observatory: 989 m a.s.l.,
18 47°48'N, 11°0'E; Jungfraujoch Observatory: 3580 m a.s.l., 46°33' N, 7°59'E) in order to
19 investigate the influence of the forest fire smoke layers from Alaskan and Canadian forest fires
20 on the aerosol properties in the free troposphere and the continental boundary layer of Central
21 Europe. They find that the black carbon to CO enhancement ratios in the transported plumes
22 were still at the emission ratios, indicating very efficient transport of black carbon on
23 intercontinental scales. The black carbon in such layers exceeded the European free troposphere
24 background concentration by about two orders of magnitude. A strong accumulation mode, a
25 nearly depleted nucleation mode, and an entirely internal mixture characterized the forest fire
26 aerosol.

27
28 *Ravetta et al.* [2006, this section] operated two ground-based ozone lidars at Observatoire de
29 Haute Provence (OHP) for eleven days during ICARTT. They measured ozone vertical profiles
30 and scattering ratio from the boundary layer up to the tropopause. They linked ozone rich layers
31 within the free troposphere to long range transport of pollutants. These layers were thin (< 1 km)
32 and exhibited ozone mixing ratios 50% larger than background values. The origin of these
33 layers is discussed by combining cluster of particles analysis and upstream airborne in situ
34 measurements of the chemical composition of these air masses. These layers had their origin in
35 North America where they are uplifted either by forest fires or by warm conveyor belts in the
36 vicinity of frontal regions. The polluted layers remained coherent during transport over the
37 Atlantic Ocean. As seen at OHP, these ozone layers occupied a significant amount of the
38 Western Mediterranean lower free troposphere (between 3 and 5 km above sea level) and could
39 have contributed to the summer enhancement of background ozone level when mixing with the
40 European boundary layer.

41
42 *Duck et al.* [2006, this section] report aerosol lidar observations at Chebogue Point, Nova Scotia,
43 which indicate transport of a biomass burning emission plume from Alaskan forest fires to the
44 site on July 11-13, 2004. The plume had been transported in the free troposphere, and was
45 brought to the surface by synoptic-scale meteorology in the middle of the period. A comparison
46 of vertical profiles of measured aerosol backscatter ratios and the simulated biomass burning CO

1 showed remarkable agreement. Smoke aerosols were first detected in the free troposphere up to
2 8 km altitude, and did not appear to have undergone significant removal processes during the 8-
3 10 day trip. The smoke particles were strongly absorbing despite their age, and characterized by
4 high levels of black carbon (BC) and organic matter (OM). The BC/OM fraction was shown to
5 be a robust indicator of forest fire emissions, and was significantly greater than what is typically
6 observed for fresh smoke.

7
8 The NOAA WP-3 aircraft observed aged biomass burning plumes that had originated in Alaska
9 and northwest Canada and were intercepted over the New England area [*de Gouw et al.* 2006].
10 The removal of aromatic VOCs was slow, implying that the average OH concentrations were
11 low during the transport. These low concentrations were due to the low humidity and high
12 concentrations of carbon monoxide and other pollutants in the plumes. In contrast with previous
13 work, no strong secondary production of acetone, methanol and acetic acid were inferred from
14 the measurements. A clear case of removal of submicron particle volume and acetic acid due to
15 precipitation scavenging was observed. *Warneke et al.* [2006, this section] conducted a source
16 apportionment study of CO downwind of the Boston-New York City urban complex, and find
17 that as much as 30% of the measured CO enhancement is attributed to the forest fires in Alaska
18 and Canada transported into the region.

19 20 **7. Conclusions**

21
22 The ICARTT measurements comprise a remarkably rich data set for investigating
23 regional air quality, the transport, chemical transformation and removal of aerosols, O₃, and their
24 precursors during intercontinental transport, and the radiation balance of the troposphere. The
25 results presented in this special section of JGR represent only the initial analysis; the data set is
26 available to the atmospheric chemistry community for further analysis in the coming years.

27 28 **Appendix A: Mobile Platform Instrument Payloads and Deployment Details**

29
30 The **NOAA WP-3D Orion aircraft** was instrumented to study aerosol composition and gas-
31 phase chemical transformations. The aircraft operated from the PBL up to 6.4 km and had
32 sufficient range to reach from the central-northeastern U.S. to the maritime Canadian Provinces,
33 and well out into the North Atlantic while stationed at the Pease Tradeport in New Hampshire.
34 Table A1 summarizes the characteristics of the WP-3D instrumentation, and Table A2 and
35 Figure A1 summarize the ICARTT flights.

36
37 The **NOAA airborne ozone/aerosol differential absorption lidar (DIAL)** [*Alvarez et al.*,
38 1998] was deployed on a chartered DC-3 aircraft, also stationed at the Pease Tradeport. The
39 nadir-looking lidar measured ozone profiles in the boundary layer with high spatial resolution
40 (90 m vertical, 600 m horizontal) with a precision that varied between 5 and 15 ppbv, depending
41 on the total atmospheric extinction. The lidar also provided aerosol backscatter profiles with a
42 vertical resolution of 15 m. In addition, an analyzer measured ozone at flight levels, an infrared
43 radiometer observed surface skin temperature variations, and there were dropsonde capabilities.
44 The DC-3 flew a total of 98 flight hours during ICARTT, in flights ranging between about 5 and
45 8 hours duration. The aircraft generally flew at 3 km ASL where lidar observations were

1 obtained from 2.2 km ASL to just above the surface. Figure A2 illustrates the DC-3 flight
2 tracks.

3
4 The **NOAA Research Vessel *Ronald H. Brown*** conducted two 19 day cruises out of
5 Portsmouth, New Hampshire from July 5 to 23, 2004 and July 26 to August 13, 2004. The ship
6 was instrumented to measure an extensive set of in-situ gas and aerosol parameters as well as
7 many remotely sensed parameters (Table A3). Radiosondes (2-8 times per day) and ozonesondes
8 (daily) also were launched from the ship. The cruise tracks in the Gulf of Maine are shown in
9 figure A3.

10
11 ITOP provided the first science mission for the new **FAAM BAE146 research aircraft**,
12 instrumented primarily for gas phase measurements, but with a limited capacity for concurrent
13 aerosol observations. The aircraft operated within the altitude range from 50ft over the sea
14 surface to 9 km, and spatially between 20°- 40°W and 33°- 47°N. Operations were based in
15 Horta Airport, on Faial Island one of the Azores archipelago. Table A4 summarizes the
16 characteristics of the BAE146 instrumentation, and Table A5 and Figure A4 summarize the
17 ITOP flights

18
19 The **DLR Falcon** performed the ITOP measurement flights in Europe. The missions were
20 performed from 2 July to 3 August 2004 from the DLR airport in Oberpfaffenhofen near Munich
21 and the airport in Creil near Paris. The aircraft has a maximum flight altitude of 41000 feet
22 when fully instrumented including wing pods. The minimum flight altitude is 100 and 300 m
23 over the ocean and over land, respectively. Maximum range and endurance is 3000 km and 4
24 hours. The measurement speed varies between 100 and 180 m s⁻¹ depending on flight altitude.
25 Table A6 compiles the instrumentation used for ITOP. The instruments were provided and
26 operated by DLR-Institute for Atmospheric Physics in Oberpfaffenhofen, the Max-Planck-
27 Institutes for Chemistry and Nuclear Physics in Mainz and Heidelberg, respectively, and the
28 Institute for Atmospheric Environmental Research (IFU) of the Research Center in Karlsruhe.
29 Table A7 gives an overview of all Falcon measurement flights during ITOP including flight
30 objectives. Missions were conducted on 11 different days, some of them including fuel stops (in
31 Cranfield, UK, San Sebastian, Spain and Shannon, Ireland).

32
33 The **NASA Jetstream-31 aircraft** carried two instruments that measure how aerosols, clouds,
34 water vapor, and the ocean surface affect solar radiation. The NASA Ames Airborne Tracking
35 Sunphotometer (AATS) measured how aerosols and water vapor attenuate the direct beam from
36 the Sun. The Solar Spectral Flux Radiometer (SSFR) measured solar energy from all directions
37 (Sun, open sky, clouds, and land and water surfaces) with sensors looking both above and below
38 the aircraft. Both AATS and SSFR cover a wide range of wavelengths, from the ultraviolet,
39 through the visible, and into the near infrared. Together AATS and SSFR provide measurements
40 test many aspects of the absorption, scattering, and reflection of radiation by aerosols, clouds,
41 and the earth's surface. Table A8 summarizes the characteristics of the J31 instrumentation and
42 Figure A5 summarizes the J31 flights in ICARTT.

43
44 During August 2-21, 2004, the **CIRPAS Twin Otter aircraft** was based at Hopkins
45 International Airport in Cleveland, Ohio. The payload consisted of a wide array of
46 instrumentation for aerosol cloud physical and chemical characterization, employing both on-

1 line and off-line techniques (Table A9). The general focus of the mission was on characterizing
2 aerosol and cloud droplets, from within the boundary layer up to the free troposphere. A variety
3 of air mass types was sampled during this study, including plumes from coal-fired power plants
4 (Conesville and Detroit Monroe plants) both in clear sky and under cloudy conditions, cloud
5 systems over Ohio and Lake Erie, urban outflow from Detroit and Cleveland, and clear air
6 masses on various transit legs. Table A10 lists the research flights during ICARTT, and Figure
7 A6 shows the individual flight tracks. Six of the 12 flights were also flown in coordination
8 with the MSC Convair aircraft, which enabled complementary aerosol and gas-phase
9 measurements.

10
11 The **MSC Convair 580** also was based at Hopkins International Airport in Cleveland, Ohio for
12 ICARTT from July 21 to August 18, 2004. The Convair carried instrumentation to measure or
13 collect trace gases (O₃, CO, SO₂, NO, NO₂, HCHO, H₂O₂, HNO₃ and some VOCs), aerosol
14 particles and cloud droplets. Both the physical size distributions and the chemistry of the aerosol
15 particles were measured using a DMA, an APS, a PCASP, a FSSP300, a PILS and an AMS. An
16 Alquist three-wavelength integrating nephelometer and a PSAP were used to measure the
17 scattering and absorption properties of the particles. Cloud liquid water content was measured
18 with a PMS King probe and a Nezorov probe. Cloud microphysics were measured with two
19 PMS FSSP 100 probes, a PMS 2D Grey scale and a PMS 2DP. Light scattering by cloud
20 droplets was measured with a Gerber CIN probe. The chemistry of the cloud droplets was
21 measured in two ways: sampling the residuals from a CVI into the AMS, and collecting bulk
22 samples of the cloudwater using slotted rod collectors. A total of 23 flights were conducted with
23 the Convair. After August 1, six flights were made in unison with the CIRPAS Twin Otter.
24 Table A11 lists the project flights during ICARTT, and Figure A7 shows a compilation of the
25 individual flight tracks.

26
27 During the ICARTT campaign, **altitude-controlled balloons** were used to track urban pollution
28 plumes. Nine balloons flew a total of 670 flight hours, measuring the evolution of the winds,
29 temperature, and ozone downwind of major pollution source regions and helping to track the
30 plumes in real time. Two types of balloons were flown: NOAA's SMART balloons measured
31 meteorological parameters, sea surface temperatures, and ozone over the Gulf of Maine and
32 North Atlantic with one flight reaching Europe. Smaller Controlled Meteorological (CMET)
33 balloons measured primarily winds and temperatures, but were able to be vehicle launched from
34 multiple locations in order to target specific plumes. Version 4.1 of the Smart Balloon was
35 employed for the ICARTT flight series (S. Businger et al., Scientific insights from four
36 generations of Lagrangian Smart Balloons in atmospheric research, submitted to *Bull. Amer.*
37 *Meteoro. Soc.*, , 2006). Previous versions of the balloon and its deployment in field campaigns
38 have been described by *Johnson et al.* [2000] and *Businger et al.*, [1999]. The balloons were
39 released from the town of Orient on the promontory tip of the northern peninsula of Long Island,
40 New York. Four balloons were released with flight durations over the North Atlantic ranging
41 from 2 to 12.3 days and travel distances of 1,030 to 6,780 km. Five CMET balloons tracked
42 urban air pollution plumes over New England and the Gulf of Maine, Eastern Canada, and the
43 Atlantic Ocean. They were vehicle launched into emerging urban plumes from New York and
44 Boston. Flights ranging from 12 to 120 hours in duration measured the quasi-Lagrangian
45 evolution of the low-level winds, temperature, and, in one case, ozone and relative humidity,
46 downwind of major source regions.

Appendix B: Surface Site Instrumentation and Other Details

The **Chebogue Point site** (43.75°N , 66.12°W) was instrumented to study outflow of air pollution from North America with a focus on aerosol composition and ozone photochemistry. Chebogue Point is located at the southwest tip of Nova Scotia (Fig. B1), 9 km south-southwest of Yarmouth, 130 km southeast of the Maine coastline, 430 km northeast from Boston, MA, and 730 km northeast from New York, NY. Measurements included a broad array of trace gas, aerosol, radiation, and meteorological measurements (Table B1). Most of the sampling inlets were mounted on a 10 m scaffolding tower, and instruments were housed in climate-controlled laboratories at the base of the tower. The site operated continuously from July 1 through August 15, 2004.

The **radar wind profiler network** comprised ten land-based and one shipboard 915-MHz Doppler radar wind profilers [Carter, *et al.*, 1995] that measured winds in the planetary boundary layer (see Fig. B1 and Table B2). Typical vertical coverage was from 120 m to ~4000 m above the surface, depending on atmospheric conditions. Radio acoustic sounding systems (RASS) were operated in conjunction with most of the wind profilers to measure temperature profiles up to ~1500. The vertical resolutions of both the wind and temperature measurements were either 60 m or 100 m. The wind profiler data were quality controlled after the data collection period using the continuity technique developed by [Weber, *et al.*, 1993]. Operation of the wind profiler on the R/V Ronald H. Brown was hindered by sea clutter (i.e., side-lobe reflections from the ocean surface), which often prevented wind retrievals in approximately the lowest 500 m above the surface. A Doppler lidar on the Ronald H. Brown measured winds below clouds with up to 5 m resolution using the velocity-azimuth display (VAD) technique [Browning and Wexler, 1968]. After the study, the lidar wind profiles were merged with wind profiler data to take advantage of the unique measurement capabilities of each instrument [Wolfe, *et al.*, 2006, this section].

Figure B2 gives the locations of the **AIRMAP Network** sites and the **CHAIOS** study at the Appledore Island AIRMAP site. Table B3 summarizes the CHAIOS measurements.

Atmospheric composition measurements at the **PICO-NARE station** are designed to study ozone photochemistry plus aerosol absorption. Measurements began in July 2001, with CO, ozone, and black carbon. Nitrogen oxides instrumentation was added in 2002, with nearly continuous observations from spring 2004 through August 2005, and NMHC measurements began in summer 2004 and were nearly continuous fall 2004 through summer 2005. The measurement techniques are summarized in Table B4. Standard meteorological observations are also made. During the summer 2004 ICARTT period, additional meteorological stations were added along the mountainside to study upslope flow, as described by Kleissl *et al.* [2006, this section].

Eight systems contributed to the **European Lidar Network** during the ITOP/ICARTT experiment. Figure B3 gives a map of this network and Table B5 gives a measurement timetable. All systems measured aerosol backscatter profiles. The Observatoire de Haute

1 Provence (OHP) and Athens systems had a UV-DIAL measurement capability and were able to
2 provide ozone vertical profiles (respectively up to 12 km and 4 km). The joint measurements of
3 ozone and aerosol backscatter profiles together with meteorological model simulations make
4 possible the separation between export of European pollution above the PBL and layers related
5 to long range transport.

6
7 **Acknowledgements.** The Climate Change and Air Quality Programs of the National Oceanic
8 and Atmospheric Administration (NOAA) supported the WP-3D, O₃ Lidar aircraft and Ronald
9 H. Brown R/V measurements. The ITCT Lagrangian 2K4 campaign was conducted under the
10 framework of the IGAC (International Global Atmospheric Chemistry) Project
11 (<http://www.igac.noaa.gov/>). The J31 measurements were supported by NOAA's Atmospheric
12 Composition and Climate Program and by NASA's Programs in Radiation Science, Suborbital
13 Science, and Tropospheric Chemistry. J31 analyses were supported by NASA's Earth Observing
14 System Inter-Disciplinary Science (EOS-IDS) Program. The ITOP project was funded by the
15 United Kingdom Natural Environment Research Council through its Upper Troposphere - Lower
16 Stratosphere (UTLS) research programme. Additional support research staff came from the U.K.
17 National Centre for Atmospheric Science and the NERC Facility for Airborne Atmospheric
18 Measurements. The PICO-NARE study was supported by the NOAA Climate Program and the
19 NSF Atmospheric Chemistry program. The MOZAIC program is supported by the European
20 Commission (EVK2-CT1999-00015), Airbus and the airlines (Lufthansa, Air France, Austrian
21 and former Sabena who have been carrying the MOZAIC instrumentation free of charge since
22 1994). The CHAios project was funded principally by the NSF Atmospheric Chemistry
23 Program with additional support provided by NOAA through the AIRMAP program.

24 25 **References:**

- 26 Ahlquist, N. and R.C. Charlson, (1967) A new instrument for evaluating the visual quality of air, *APCA Journal*, 17,
27 467-469.
- 28 Aliche, B., U. Platt and J. Stutz, Impact of nitrous acid photolysis on the total hydroxyl radical budget during the
29 Limitation of Oxidant Production/Pianura Padana Produzione di Ozono study in Milan, *J. Geophys. Res.*, 107,
30 doi:10.1029/2000JD000075, 2002.
- 31 Alvarez, R.J., et al, (1998), Comparisons of airborne lidar measurements of ozone with airborne in situ
32 measurements during the 1995 Southern Oxidants Study, *J. Geophys. Res.*, 103, 31,155-31,171.
- 33 Anderson, B. E., et al. (1993), The impact of U.S. continental outflow on ozone and aerosol distributions over the
34 North Atlantic, *J. Geophys. Res.*, 98, 23,477-23,489.
- 35 Arnott, W.P., H. Moosmuller, C.F. Rogers, T.F. Jin, and R. Bruch, Photoacoustic spectrometer for measuring light
36 absorption by aerosol: instrument description, *Atmos. Environ.*, 33, 17, 2845-2852, 1999.
- 37 Arnott, W.P., J.W. Walker, I. Moosmuller, R.A. Elleman, H.H. Jonsson, G. Buzorius, W.C. Conant, R.C. Flagan,
38 and J.H. Seinfeld, Photoacoustic insight for aerosol light absorption aloft from meteorological aircraft and
39 comparison with particle soot absorption photometer measurements: DOE Southern Great Plains climate
40 research facility and the coastal stratocumulus imposed perturbation experiments, *J. Geophys. Res.*, 111,
41 D05502, doi:10.1029/2005JD005964, 2006.
- 42 Bahreini, R., et al. (2003), Aircraft-based aerosol size and composition measurements during ACE-Asia using an
43 Aerodyne aerosol mass spectrometer, *J. Geophys. Res.*, 108, 8645, doi:8610.1029/2002JD003226.
- 44 Bates, T.S., P.K. Quinn, D.J. Coffman, J.E. Johnson, T.L. Miller, D.S. Covert, A. Wiedensohler, S. Leinert, A.
45 Nowak and C. Neusüß (2001), Regional Physical and Chemical Properties of the Marine Boundary Layer
46 Aerosol across the Atlantic during Aerosols99: An overview, *J. Geophys. Res.*, 106, 20,767-20,782.
- 47 Bates, T.S., P.K. Quinn, D.S. Covert, D.J. Coffman, J.E. Johnson, and A. Wiedensohler (2000). Aerosol physical
48 properties and processes in the lower marine boundary layer: A comparison of shipboard sub-micron data from
49 ACE 1 and ACE 2. *Tellus*, 52, 258-272.

1 Bates, T.S., P.K. Quinn, D.J. Coffman, J.E. Johnson, and A.M. Middlebrook (2005), Dominance of organic aerosols
2 in the marine boundary layer over the Gulf of Maine during NEAQS 2002 and their role in aerosol light
3 scattering. *J. Geophys. Res.*, 110, D18, D18202, doi:10.1029/2005JD005797.

4 Baumgardner, D., H. Jonsson, W. Dawson, D. O'Connor, and R. Newton, The cloud, aerosol and precipitation
5 spectrometer: a new instrument for cloud investigations, *Atmos. Res.*, 59, 251-264, 2001.

6 Baumgardner, D., G. Kok, and G. Raga, Warming of the Arctic lower stratosphere by light absorbing particles,
7 *Geophys. Res. Lett.*, 31, 6, 2004.

8 Baynard, T., E.R. Lovejoy, A. Pettersson, S.S., Brown, D. Lack, H. Osthoff, P. Massoli, S. Ciciora, B. Dube, and
9 A.R. Ravishankara (2006), Design considerations and application of cavity ring-down aerosol extinction
10 spectroscopy, in preparation.

11 Beattie, B. L., and D. M. Wepdale (1989), Meteorological characteristics of large acidic deposition events at
12 Kejimikujik, Nova Scotia, *Water, Air, and Soil Pollution*, 46, 45-59.

13 Bohn, B., A. Kraus, M. Müller, and A. Hofzumahaus (2004), Measurement of atmospheric $O_3 \rightarrow O(^1D)$ photolysis
14 frequencies using filterradiometry, *J. Geophys. Res.*, 109, D10S90, doi:10.1029/2003JD004319.

15 Bond, T.C., T.L. Anderson, and D. Campbell, (1999) Calibration and intercomparison of filter-based measurements
16 of visible light absorption by aerosols, *Aerosol Sci. Technol.*, 30, 582-600.

17 Brice, K. A., et al. (1988), Long-term measurements of atmospheric peroxyacetylnitrate (PAN) at rural sites in
18 Ontario and Nova Scotia; seasonal variations and long-range transport, *Tellus*, 40B, 408-425.

19 Brock, C. A., et al. (2000), Ultrafine particle size distributions measured in aircraft exhaust plumes, *J. Geophys.*
20 *Res.*, 105, 26,555-26,567.

21 Brock, C. A., et al. (2003), Particle growth in urban and industrial plumes in Texas, *J. Geophys. Res.*, 108, 4111,
22 doi:4110.1029/2002JD002746.

23 Brough, N., et al, (2003), Intercomparison of aircraft instruments on board the C-130 and Falcon 20 over southern
24 Germany during EXPORT 2000, *Atmospheric Chemistry and Physics*, 3, 2127-2138.

25 Brown, S. S., et al., (2006a) Variability in Nocturnal Nitrogen Oxide Processing and Its Role in Regional Air
26 Quality, *Science*, 311, pp. 67 - 70 doi: 10.1126/science.1120120

27 Brown, S. S., et al. (2006b), Nocturnal odd-oxygen budget and its implications for ozone loss in the lower
28 troposphere, *Geophys. Res. Lett.*, 33, L08801, doi:10.1029/2006GL025900.

29 Brown, S. S., et al. (2005), Aircraft observations of daytime NO_3 and N_2O_5 and their implications for tropospheric
30 chemistry, *Journal of Photochemistry and Photobiology A: Chemistry*, 176, 270-278

31 Browning, K. A., and R. Wexler (1968), The determination of kinematic properties of a wind field using Doppler
32 radar, *J. Appl. Meteor.*, 7, 105-113.

33 Brunner, D., J. Staehelin, D. Jeker, H. Wernli, and U. Schumann, Nitrogen oxides and ozone in the tropopause
34 region of the Northern Hemisphere Measurements from commercial aircraft in 1995/96 and 1997, *J. Geophys.*
35 *Res.*, 106, 27,673-27,699, 2001.

36 Burtscher, H., U. Baltensperger, N. Bukowiecki, P. Cohn, C. Hüglin, M. Mohr, U. Matter, S. Nyeki, V. Schmatloch,
37 N. Streit, and E. Weingartner (2001), Separation of volatile and non-volatile aerosol fractions by
38 thermodesorption: instrumental development and applications, *J. Aerosol. Sci.*, 32, 427-442.

39 Businger, S., R. Johnson, J. Katzfey, S. Siems, and Q. Wang (1999), Smart tetroons for lagrangian air mass tracking
40 during ACE-1. *J. Geophys. Res.*, 104, 11,709-11,722.

41 Buzorius, G., Cut-off sizes and time constants of the CPC TSI 3010 operating at 1-3 lpm flow rates, *Aerosol Sci.*
42 *Technol.*, 35, 1, 577-585, 2001.

43 Buzorius, G., C. S. McNaughton, A. D. Clarke, D. S. Covert, B. Blomquist, K. Nielsen, and F. J. Brechtel, (2004)
44 Secondary aerosol formation in continental outflow conditions during ACE-Asia. *J. Geophys. Res.*, 109,
45 D24203, doi:10.1029/2004JD004749.

46 Cárdenas, L.M., Brassington, D.J., Allan, B.J., Coe, H., Alicke, B., Platt, U., Wilson, K.M., Plane, J.M.C., and
47 Penkett, S.A., (2000), Intercomparison of Formaldehyde Measurements In Clean and Polluted Atmospheres.
48 *Journal of Atmospheric Chemistry*, 37, 53-80.

49 Carpenter, L.J., T.J. Green, G.P. Mills, S. Bauguitte, S.A. Penkett, P. Zanis, E. Schuepbach, N. Schmidbauer, P.S.
50 Monks, C. Zellweger, Oxidised Nitrogen and Ozone Production Efficiencies in the Springtime Free
51 Troposphere over the Alps. *J. Geophys. Res.* 105(D11), 14,547-14,559, 2000.

52 Carrico, C.M., P. Kus, M.J. Rood, P.K. Quinn and T.S. Bates (2003). Mixtures of pollution, dust, seasalt and
53 volcanic aerosol during ACE-Asia: Light scattering properties as a function of relative humidity. *J. Geophys.*
54 *Res.*, 108(D23), 8650, doi:10.1029/2003JD003405.

1 Carter, D. A., et al. (1995), Developments in UHF lower tropospheric wind profiling technology at NOAA's
2 Aeronomy Laboratory, *Radio Sci.*, **30**, 997-1001.

3 Cerni, T.A., Determination of the Size and Concentration of Cloud Drops with an FSSP, *J. Climate Appl. Meteorol.*,
4 **22**, 8, 1346-1355, 1983.

5 Chin, M., et al. (1994), Relationship of ozone and carbon monoxide over North America, *J. Geophys. Res.*, **99**,
6 14,565-14,573.

7 Cimini, D., J.A. Shaw, E.R. Westwater, Y. Han, V. Irisov, V. Leuski, and J.H. Churnside (2003), Air temperature
8 profile and air/sea temperature difference measurements by infrared and microwave scanning radiometers,
9 *Radio Sci.*, **38**(3), 8045, doi:10.1029/2002RS002632.

10 Clark, A., A thermo-optical technique for in situ analysis of size-resolved aerosol physicochemistry, *Atmos. Environ.*
11 **25A**, 635-644, 1991.

12 Comstock, K.K., C.S. Bretherton, and S.E. Yuter (2005), Mesoscale variability and drizzle in Southeast Pacific
13 stratocumulus. *J. Atmos. Sci.*, **62**, 3792-3807

14 Cooper, O. R., et al. (2002a), Trace gas composition of mid-latitude cyclones over the western North Atlantic
15 Ocean: A seasonal comparison of O₃ and CO, *J. Geophys. Res.*, **107**, 4057, doi:10.1029/2001JD000902.

16 Cooper, O. R., et al. (2002b), Trace gas composition of mid-latitude cyclones over the western North Atlantic
17 Ocean: A conceptual model, *J. Geophys. Res.*, **107**, 4056, doi:10.1029/2001JD000901.

18 Cooper, O. R., et al. (2001), Trace gas signatures of the airstreams within North Atlantic cyclones: Case studies
19 from the North Atlantic Regional Experiment (NARE '97) aircraft intensive, *J. Geophys. Res.*, **106**, 5437-5456.

20 Cross, E. S., J. G. Slowik, P. Davidovits, J. D. Allan, T. B. Onasch, J. T. Jayne, D. K. Lewis, M. Canagranata, and
21 D. R. Worsnop: Aerosol Particle Density Determination using Light Scattering in Conjunction with Mass
22 Spectrometry, *Aerosol Sci. Tech.*, in preparation.

23 Cubison, M. J., H. Coe, and M. Gysel (2005), A modified hygroscopic tandem DMA and a data retrieval method
24 based on optimal estimation, *J. Aerosol. Sci.*, **36**, 846-865.

25 Day, D. A., P. J. Wooldridge, M. B. Dillon, J. A. Thornton, and R. C. Cohen (2002), A thermal dissociation laser-
26 induced fluorescence instrument for in situ detection of NO₂, peroxy nitrates, alkyl nitrates, and HNO₃, *J.*
27 *Geophys. Res.*, **107**(D6), 4046, doi:10.1029/2001JD000779.

28 de Gouw, J. A., et al. (2003), Sensitivity and specificity of atmospheric trace gas detection by proton-transfer-
29 reaction mass spectrometry, *International Journal of Mass Spectrometry and Ion Processes*, **223-224**, 365-382.

30 de Gouw, J. A., et al. (2006), Volatile organic compounds composition of merged and aged forest fire plumes from
31 Alaska and western Canada, *J. Geophys. Res.*, **111**, D10303, doi:10.1029/2005JD006175.

32 Delene, D.J. and J. A. Ogren, (2002) Variability of aerosol optical properties at four North American surface
33 monitoring sites, *J. Atmos. Sci.*, **59**, 1135-1150.

34 Delle Monache, L., X. Deng, Y. Zhou, and R. Stull, Ozone ensemble forecasts. Part II: a Kalman-filter predictor
35 bias correction, *J. Geophys. Res.*, **111**, D05308, doi:10.1029/2005JD006311, 2006.

36 Derwent, R.G. and Jenkin, M.E., Hrocarbons and the long range transport of ozone and PAN across Europe.
37 *Atmospheric Environment* **25A**, 1661-1678, 1991.

38 Dibb, J. E., E. Scheuer, S. I. Whitlow, M. Vozella, E. Williams, and B. Lerner (2004), Ship-based nitric acid
39 measurements in the Gulf of Maine during New England Air Quality Study 2002, *Journal of Geophysical*
40 *Research* **109**, D20303, doi:10.1029/2004JD004843.

41 Dubé, W. P., S. S. Brown, H. D. Osthoff, M. R. Nunley, S. J. Ciciora, M. W. Paris, R. J. McLaughlin, and A. R.
42 Ravishankara (2006), Aircraft instrument for simultaneous, in-situ measurements of NO₃ and N₂O₅ via cavity
43 ring-down spectroscopy, *Rev. Sci. Instr.*, **77**, 034101.

44 Eisele, F. L., and D. J. Tanner (1993), Measurement of the gas phase concentration of H₂SO₄ and methane sulfonic
45 acid and estimates of H₂SO₄ production and loss in the atmosphere, *J. Geophys. Res.*, **98**, 9001-9010.

46 Ervens, B., G. Feingold, G. J. Frost, and S. M. Kreidenweis (2004), A modeling study of aqueous production of
47 dicarboxylic acids: 1. Chemical pathways and speciated organic mass production, *J. Geophys. Res.*, **109**,
48 D15205, doi:10.1029/2003JD004387.

49 Fairall, C.W., A.B. White, J.B. Edson, and J.E. Hare (1997), Integrated shipboard measurements of the marine
50 boundary layer. *J. Atmos. Oceanic Tech.*, **14**, 338-359.

51 Fairall, C.W., E.F. Bradley, J.E. Hare, A.A. Grachev, and J.B. Edson (2003), Bulk parameterization of air-sea
52 fluxes: Updates and verification for the COARE algorithm. *J. Clim.*, **16**, 571-591.

53 Feldpausch, P., et al., Measurements of ultrafine aerosol size distribution by a combination of diffusion screen
54 separators and condensation particle counters, *J. Aerosol. Sci.*, **36**, 1353-1372, 2005.

55 Fialho, P., A. D. A. Hansen, and R. E. Honrath (2005) Absorption coefficients by aerosols in remote areas: a new

1 approach to decouple dust and black carbon absorption coefficients using seven-wavelength Aethalometer data,
2 , *J. Aerosol Sci.*, 36, 267-282.

3 Fischer, H., et al., Synoptic tracer gradients in the upper troposphere over central Canada during the Stratosphere-
4 Troposphere Experiment by aircraft measurements 1998 summer campaign, *J. Geophys. Res.*, 107, 4064, doi:
5 10.1020/200JD000312, 2002.

6 Fishman, J., et al. (1991), Identification of widespread pollution in the Southern Hemisphere deduced from satellite
7 analyses, *Science*, 252, 1693-1696.

8 Fishman, J., et al. (1990), Distribution of tropospheric ozone determined from satellite data, *J. Geophys. Res.*, 95,
9 3599-3617.

10 Fountoukis, C., and A. Nenes (2005), Continued development of a cloud droplet formation parameterization for
11 global climate models, *J. Geophys. Res.*, 110, D11212, doi:10.1029/2004JD005591.

12 Frisch, A.S., B.E. Martner, J.S. Gibson (1989), Measurement of the vertical flux of turbulent kinetic energy with a
13 single Doppler radar. *Bound.-Layer Meteorol.*, 49, 331 – 337.

14 Frost G. J., et al. (2006), Effects of changing power plant NO_x emissions on ozone in the eastern United States:
15 Proof of concept, *J. Geophys. Res.*, 111, D12306, doi:10.1029/2005JD006354.

16 Gerber, H., B.G. Arends, and A.S. Ackerman, New microphysics sensor for aircraft use, *Atmos. Res.*, 31, 4, 235-
17 252, 1994.

18 Gerbig, C.D., et al., Fast response resonance fluorescence CO measurements aboard the C130: instrument
19 characterization and measurements made during North Atlantic Regional Experiment 1993, *J. Geophys. Res.*,
20 101, 29229-29238, 1996.

21 Gerbig, C., et al. (1999), An improved fast-response VUV resonance fluorescence CO instrument, *J. Geophys. Res.*,
22 104, 1699-1704.

23 Goldan, P.D., W.C. Kuster, E. Williams, P.C. Murphy, F.C. Fehsenfeld, J. Meagher (2004), Nonmethane
24 hydrocarbon and oxy hydrocarbon measurements during the 2002 New England Air Quality Study, *J.*
25 *Geophys. Res.*, 109, D21309, doi:10.1029/2003JD004455.

26 Goldstein, A. H., et al. (1996), Emissions of ethene, propene, and 1-butene by a midlatitude forest, *J. Geophys. Res.*,
27 101, 9149-9157.

28 Goldstein, A. H., et al. (1998), Seasonal course of isoprene emissions from a midlatitude deciduous forest, *J.*
29 *Geophys. Res.*, 103, 31,045-31,056.

30 Goldstein, A. H., et al. (1995), Seasonal variations of nonmethane hydrocarbons in rural New England: Constraints
31 on OH concentrations in northern midlatitudes, *J. Geophys. Res.*, 100, 21,023-21,033.

32 Goldstein, A.H., D.B. Millet, M. McKay, L. Jaegle, L. Horowitz, O. Cooper, R. Hudman, D.J. Jacob, S. Oltmans, A.
33 Clark, Impact of Asian Emissions on Observations at Trinidad Head, California, during ITCT 2K2, *Journal of*
34 *Geophysical Research*, Vol. 109, No. D23, D23S17, 10.1029/2003JD004406, 2004.

35 Green, T. J., et al. (2006), An Improved Dual Channel PERCA Instrument For Atmospheric Measurements Of
36 Peroxy Radicals, *Journal of Environmental Monitoring*.

37 Grund, C. J., R.M. Banta, J.L. George, J.N. Howell, M.J. Post, R.A. Richter, and A.M. Weickmann (2001), High-
38 resolution doppler lidar for boundary layer and cloud research, *J. Atmos. Oceanic Technol.*, 18, 376-393.

39 Harriss, R. C., et al. (1984), Atmospheric transport of pollutants from North America to the North Atlantic Ocean,
40 *Nature*, 308, 722-724.

41 Hering, S. V., Stolzenburg, M.R., Quant R. R., Oberreit D. R., Keady P. B., A laminar-flow, water-based
42 condensation particle counter (WCPC), *Aerosol Science and Technology*, in 659-672 (2005).

43 Hirsch, A. I., et al. (1996), Seasonal variation of the ozone production efficiency per unit NO_x at Harvard Forest,
44 Massachusetts, *J. Geophys. Res.*, 101, 12,659-12,666.

45 Holloway, J. S., et al. (2000), Airborne intercomparison of vacuum ultraviolet fluorescence and tunable diode laser
46 absorption measurements of tropospheric carbon monoxide, *J. Geophys. Res.*, 105, 24,251-24,261.

47 Honrath, R. E., R. C. Owen, M. Val Marti'n, J. S. Reid, K. Lapina, P. Fialho, M. P. Dziobak, J. Kleissl, and D. L.
48 Westphal (2004), Regional and hemispheric impacts of anthropogenic and biomass burning emissions on
49 summertime CO and O₃ in the North Atlantic lower free troposphere, *J. Geophys. Res.*, 109, D24310,
50 doi:10.1029/2004JD005147.

51 Hopkins, J.R., et al. (2003), A two column method for long-term monitoring of non-methane hydrocarbons
52 (NMHC) and oxygenated volatile organic compounds, *J. Environ. Monitr.*, 5, 8-13.

53 Huffman, J. A., J. T. Jayne, D. R. Worsnop, P. J. Ziemann, and J. L. Jimenez: A stepping thermal denuder-AMS
54 system for composition-resolved aerosol volatility measurements, *Aerosol Sci. Tech.*, in preparation, 2006.

- 1 Huntrieser, H. et al., Intercontinental air pollution transport from North America to Europe : Experimental evidence
2 from airborne measurements and surface observations, *J. Geophys. Res.*, 110, D01305, doi:
3 1029/2004JD005045, 2005.
- 4 Jayne, J.T., D.C. Leard, X.F. Zhang, P. Davidovits, K.A. Smith, C.E. Kolb, and D.R. Worsnop, (2000),
5 Development of an aerosol mass spectrometer for size and composition analysis of submicron particles, *Aerosol*
6 *Science and Technology*, 33 (1-2), 49-70.
- 7 Jimenez, R., et al. (2005), Atmospheric trace gas measurements using a dual quantum-cascade laser mid-infrared
8 absorption spectrometer, *SPIE Proceedings*, 5738, 318.
- 9 [Johnson, R., S. Businger, and A. Baerman \(2000\), Lagrangian air mass tracking with smart balloons during ACE-2,](#)
10 [Tellus B, 52, 321-334.](#)
- 11 Junkerman, W., et al. (1989), A Photoelectric Detector for the Measurement of Photolysis Frequencies of Ozone
12 and other Atmospheric Molecules, *Journal of Atmospheric Chemistry*, 8, 203-227.
- 13 Kellerhals, M., Beauchamp, S., Belzer, W., Blanchard, P., Froude, F., Harvey, B., McDonald, K., Pilote, M.,
14 Poissant, L., Puckett, K., Schroeder, B., Steffen, A., Tordon, R (2003): Temporal and spatial variability of total
15 gaseous mercury in Canada: results from the Canadian Atmospheric Mercury Measurement Network
16 (CAMNet). *Atmospheric Environment*, 37, 1003-1011
- 17 Kelleher, T. J., and W. A. Feder (1978), Phytotoxic concentrations of ozone on Nantucket Island: Long range
18 transport from the Middle Atlantic States over the open ocean confirmed by bioassay with ozone-sensitive
19 tobacco plants, *Environmental Pollution*, 17, 187-194.
- 20 Kollias, P., B.A. Albrecht, R. Lhermitte, and A. Savtchenko (2001), Radar observations of updrafts, downdrafts,
21 and turbulence in fair-weather cumuli. *J. Atmos. Sci.*, 58, 1750-1766.
- 22 Lapina, K., R. E. Honrath, R. C. Owen, M. Val Martín, and G. Pfister (2006), Evidence of significant large-scale
23 impacts of boreal fires on ozone levels in the midlatitude Northern Hemisphere free troposphere, *Geophys. Res.*
24 *Lett.*, 33, L10815, doi:10.1029/2006GL025878.
- 25 Law, D.C., S.A. Mclaughlin, M.J. Post, B.L. Weber, D.C. Welsh, D.E. Wolfe, and D.A. Merritt (2002), An
26 electronically stabilized phased array system for shipborne atmospheric wind profiling, *J. Atmos. Oceanic*
27 *Technol.*, 19, 924-933.
- 28 Lefer, B. L., et al. (1999), Nitric acid and ammonia at a rural northeastern U.S. site, *J. Geophys. Res.*, 104, 1645-
29 1661.
- 30 Li, Q., et al. (2002), Transatlantic transport of pollution and its effects on surface ozone in Europe and North
31 America, *J. Geophys. Res.*, 107(D13), 4166, doi:10.1029/2001JD001422.
- 32 Liang, J., et al. (1998), Seasonal budgets of reactive nitrogen species and ozone over the United States, and export
33 fluxes to the global atmosphere, *J. Geophys. Res.*, 103, 13,435-413,450.
- 34 Marengo Alain, Thouret Valérie, Nédélec Philippe, Smit Herman, Helten Manfred, Kley Dieter, Karcher Fernand,
35 Simon Pascal, Law Kathy, Pyle John, Poschmann Georg, Von Wrede Rainer, Hume Chris, and Cook Tim,
36 Measurement of ozone and water vapor by Airbus in-service aircraft: The MOZAIC airborne program, An
37 overview, *J. Geophys. Res.*, 103, 25,631-25,642, 1998.
- 38 Maria, S.F., L.M. Russell, B.J. Turpin, and R.J. Porcja, FTIR measurements of functional groups and organic mass
39 in aerosol samples over the Caribbean, *Atmos. Environ.*, 36, 33, 5185-5196, 2002.
- 40 Maria, S.F. and L.M. Russell (2005), Organic and inorganic aerosol below-cloud scavenging by suburban New
41 Jersey precipitation, *Environ. Sci. Technol.*, 39, 4793-4800 doi:10.1021/es0491679.
- 42 McKeen, S., et al. (2005), Assessment of an ensemble of seven real-time ozone forecasts over eastern North
43 America during the summer of 2004, *J. Geophys. Res.*, 110, D21307, doi:10.1029/2005JD005858.
- 44 Mertes, S., F. Schroder, and A. Wiedensohler, The Particle-Detection Efficiency Curve of the Tsi-3010 CPC as a
45 Function of the Temperature Difference between Saturator and Condenser, *Aerosol Sci. Technol.*, 23, 2, 257-
46 261, 1995.
- 47 Methven, J., S. R. Arnold, F. M. O'Connor, H. Barjat, K. Dewey, J. Kent, and N. Brough (2003), Estimating
48 photochemically produced ozone throughout a domain using flight data and a Lagrangian model, *J. Geophys.*
49 *Res.*, 108(D9), 4271, doi:10.1029/2002JD002955.
- 50 Millet, D.B., N.M. Donahue, S.N. Pandis, A. Polidori, C.O. Stanier, B.J. Turpin, and A.H. Goldstein (2005),
51 Atmospheric volatile organic compound measurements during the Pittsburgh Air Quality Study: Results,
52 interpretation and quantification of primary and secondary contributions, 110, D07S07,
53 doi:10.1029/2004JD004601.
- 54 Mollicone, D., H. Eva, and F. Achard (2006), Human role in Russian wild fires, *Nature*, 440, 436-437,
55 doi:10.1038/440436a.

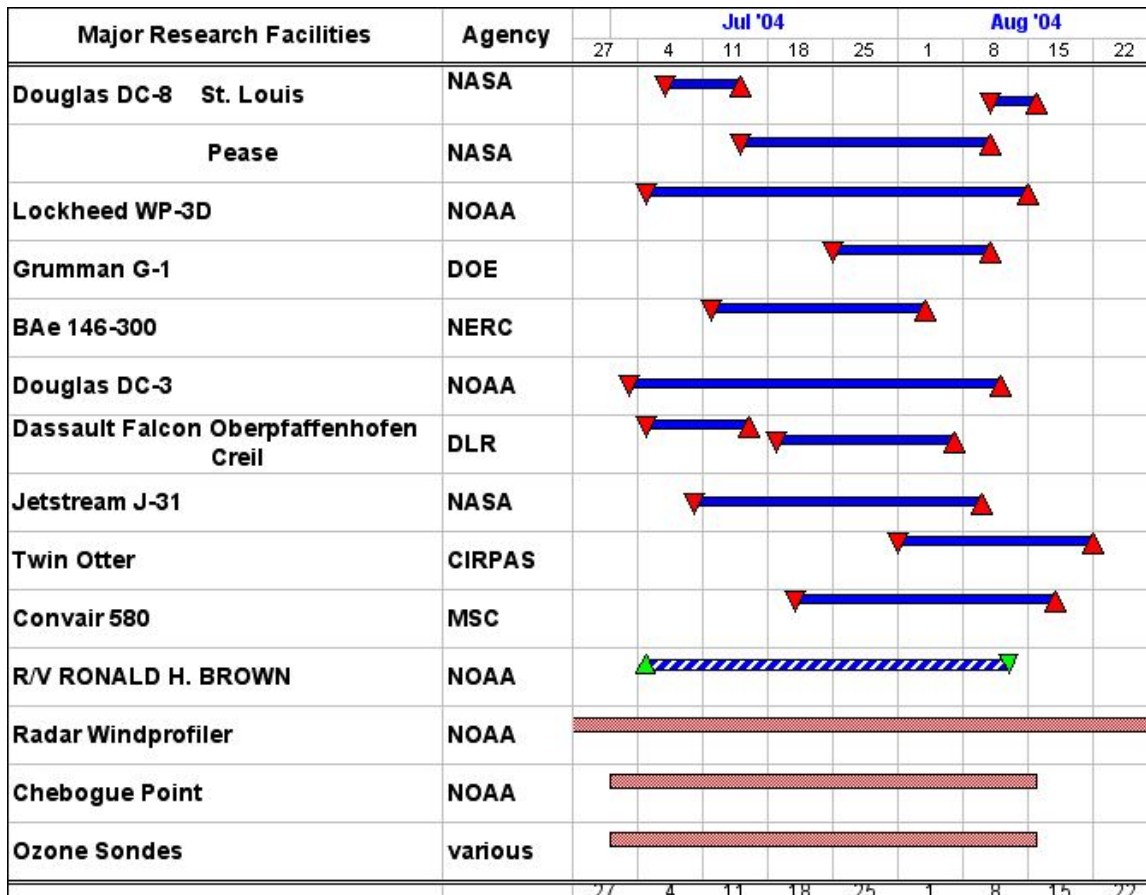
- 1 Monks, P. S., et al. (1998), Fundamental ozone photochemistry in the remote marine boundary layer: The SOAPEX
2 experiment, measurement and theory, *Atmospheric Environment*, 32, 3647-3664.
- 3 Moody, J. L., et al. (1998), Harvard Forest regional-scale air mass composition by PATH (Patterns in atmospheric
4 transport history), *J. Geophys. Res.*, 103, 13,181-113,194.
- 5 Munger, J. W., et al. (1998), Regional budgets for nitrogen oxides from continental sources: Variations of rates for
6 oxidation and deposition with season and distance from source regions, *J. Geophys. Res.*, 103, 8355-8368.
- 7 Munger, J. W., et al. (1996), Atmospheric deposition of reactive nitrogen oxides and ozone in a temperate
8 deciduous forest and a sub-arctic taiga woodland, *J. Geophys. Res.*, 101, 12,639-12,657.
- 9 Neuman, J. A., et al. (2002), Fast-response airborne in situ measurement of HNO₃ during the Texas Air Quality
10 Study, *J. Geophys. Res.*, 107, 4436, doi:4410.1029/2001JD001437.
- 11 Noone, K.J., J.A. Ogren, J. Heintzenberg, R.J. Charlson, and D.S. Covert, Design and Calibration of a Counterflow
12 Virtual Impactor for Sampling of Atmospheric Fog and Cloud Droplets, *Aerosol Sci. Technol.*, 8, 3, 235-244,
13 1988.
- 14 Orsini, D. A., et al. (2003), Refinements to the particle-into-liquid sampler (PILS) for ground and airborne
15 measurements of water-soluble aerosol composition, *Atmos. Environ.*, 37, 1243-1259.
- 16 Osthoff, H.D., S.S. Brown, T.B. Ryerson, T.J. Fortin, B.M. Lerner, E.J. Williams, A. Pettersson, T. Baynard, W.P.
17 Dubé, S.J. Ciciora, and A.R. Ravishankara (2006), Measurement of atmospheric NO₂ by pulsed cavity ring-
18 down spectroscopy, *J. Geophys. Res.*, 111, D12305, doi:10.1029/2005JD006942.
- 19 Pagowski, M., G.A. Grell, S.A. McKeen, D. Dévényi, J.M. Wilczak, V. Bouchet, W. Gong, J. McHenry, S.
20 Peckham, J. McQueen, R. Moffet, and Y. Tang, A simple method to improve ensemble-based ozone forecasts,
21 *Geophys. Res. Lett.*, 32, L07814, doi:10.1029/2004GL022305, 2005.
- 22 Pagowski, M., et al., Application of dynamic linear regression to improve skill of ensemble-based deterministic
23 ozone forecasts, *Atmos. Environ.*, 40, 3,240-3,250, doi:10.1016/j.atmosenv.2006.02.006, 2006.
- 24 Parrish, D. D., et al. (1993), The total reactive oxidized nitrogen levels and the partitioning between the individual
25 species at six rural sites in eastern North America, *J. Geophys. Res.*, 98, 2927-2939.
- 26 [Penkett, S.A.](#), [Bandy, B.J.](#), [Reeves, C.E.](#), [McKenna, D.](#), and [Hignett, P.](#), (1995), Measurements of peroxides in the
27 atmosphere and their relevance to the understanding of global tropospheric chemistry, *Faraday Discussions*,
28 100, 155-174.
- 29 Petzold, A., et al., Vertical variability of aerosol properties observed at a continental site during LACE 98, *J.*
30 *Geophys. Res.*, 107, 8128, doi: 10.1029/2001JD001043, 2002.
- 31 Prévôt, A. S. H., J. Dommen, M. Baumle, and M. Furger, 2000: Diurnal variations of volatile organic compounds
32 and local circulation systems in an Alpine valley. *Atmos. Environ.*, 34, 1413-1423.
- 33 Prospero, J. M. (2001), The Atmosphere-Ocean Chemistry Experiment (AEROCE): Background and major
34 accomplishments, *IGACTivities Newsletter*, 24, 3-5.
- 35 Pszenny, A.A.P., J. Moldanová, W.C. Keene, R. Sander, J.R. Maben, M. Martinez, P.J. Crutzen, D. Perner, and R.G. Prinn,
36 Inorganic halogens and aerosol pH in the Hawaiian marine boundary layer, *Atmos. Chem. Phys.*, 4, 147-168, 2004.
- 37 Purvis, R.M., Lewis, A.C., Carney, R.A., et al., (2003), Rapid Uplift Of Non-methane Hydrocarbons In A Cold
38 Front Over Central Europe. *J. Geophys. Res.* 108, doi:10/1029/2002JD002521.
- 39 Quinn, P.K., T.S. Bates, T.L. Miller, D.J. Coffman, J.E. Johnson, J. M. Harris, J.A. Ogren, G. Forbes, T.L.
40 Anderson, D.S. Covert, and M.J. Rood, Surface Submicron Aerosol Chemical Composition: What Fraction is
41 Not Sulfate? *J. Geophys. Res.*, 105, 6785 – 6806, 2000.
- 42 Quinn, P.K. and T.S. Bates (2005), Regional aerosol properties: Comparisons from ACE 1, ACE 2, Aerosols99,
43 INDOEX, ACE Asia, TARFOX, and NEAQS, *J. Geophys. Res.*, 110, D14, doi:10.1029/2004JD004755.
- 44 Rahn, K.A., R.D. Borys, and R.A. Duce, Tropospheric halogen gases: Inorganic and organic components, *Science*,
45 192, 549-550, 1976.
- 46 Rappenglueck et al., Quasi-continuous measurements of Non Methane Hydrocarbons (NMHC) in the greater
47 Athens Area during MEDCAPHOT-TRACE, *Atm. Environment*, 32, 2103-2121, 1998.
- 48 Redemann, J., et al. (2006), Airborne measurements of spectral direct aerosol radiative forcing in INTEX/ITCT, *J.*
49 *Geophys. Res.*, in press, doi:10.1029/2005JD006812.
- 50 Reeves, C. E., et al. (2002), Potential for photochemical ozone formation in the troposphere over the North Atlantic
51 as derived from aircraft observations during ACSOE, *J. Geophys. Res.*, 107(D23), 4707,
52 doi:10.1029/2002JD002415.
- 53 Rissman, T.A., T.M. VanReken, J. Wang, R. Gasparini, D.R. Collins, H.H. Jonsson, F.J. Brechtel, R.C. Flagan, and
54 J.H. Seinfeld, Characterization of ambient aerosol from measurements of cloud condensation nuclei during the

1
2 2003 Atmospheric Radiation Measurement Aerosol Intensive Observational Period at the Southern Great Plains
3 site in Oklahoma, *J. Geophys. Res.*, 111, D05511, doi:10.1029/2004JD005695, 2006.
4 Roberts, J. M., et al. (1995), Relationships between PAN and ozone at sites in eastern North America, *J. Geophys.*
5 *Res.*, 100, 22,821-22,830.
6 Roberts, J. M., et al. (2004), Measurement of peroxy-carboxylic nitric anhydrides (PANs) during the ITCT 2K2
7 aircraft intensive experiment, *J. Geophys. Res.*, 109, D23S21, doi:10.1029/2004JD004960.
8 Roberts, G., and A. Nenes, A Continuous-Flow Streamwise Thermal-Gradient CCN Chamber for Atmospheric
9 Measurements, *Aeros. Sci. Technol.* 39, 3, 206-221, 2005
10 Rood, M.J., M.A. Shaw, T.V. Larson, and D.S. Covert (1989), Ubiquitous Nature of Ambient Metastable Aerosol,
11 *Nature*, 337, 537-539.
12 Ryerson, T. B., et al. (1998), Emissions lifetimes and ozone formation in power plant plumes, *J. Geophys. Res.*,
13 103, 22,569-22,583.
14 Ryerson, T. B., et al. (1999), Design and initial characterization of an inlet for gas-phase NO_y measurements from
15 aircraft, *J. Geophys. Res.*, 104, 5483-5492.
16 Sabine, C.L., R. Wanninkhof, R.M. Key, C. Goyet, and F.J. Millero (2000): Seasonal CO₂ fluxes in the tropical and
17 subtropical Indian Ocean. *Mar. Chem.*, 72, 33–53.
18 Schaufliker, S. M., et al. (1999), Distributions of brominated organic compounds in the troposphere and lower
19 stratosphere, *J. Geophys. Res.*, 104, 21,513-21,535.
20 Schlager, H., et al., In situ observations of air traffic emission signatures in the North Atlantic flight corridor, *J.*
21 *Geophys. Res.*, 102, 10,739-10,750, 1997.
22 Schöder, F.P. and J. Stroem, Aircraft measurements of sub-micrometer aerosol particles (> 7 nm) in the midlatitude
23 free troposphere and tropopause region, *Atmos. Res.*, 44, 333-356, 1997.
24 Schultz, M., R. Schmitt, K. Thomas, and A. Volz-Thomas, Photochemical box modeling of long-range transport
25 from North America to Tenerife during NARE 1993, *J. Geophys. Res.*, 103, 13,477-13,488, 1997.
26 Schumann, U., et al., Estimate of diffusion parameters of aircraft exhaust plumes near the tropopause from nitric
27 oxide and turbulence measurements, *J. Geophys. Res.*, 100, 14,147-14,162, 1995.
28 Seaman, N. L., and S. A. Michelson (2000), Mesoscale meteorological structure of a high-ozone episode during the
29 1995 NARSTO-Northeast Study, *J. Appl. Met.*, 39, 384-398.
30 Shetter, R. E., et al., (2003) Photolysis frequency of NO₂: Measurement and modeling during the International
31 Photolysis Frequency Measurement and Modeling Intercomparison (IPMMI), *J. Geophys. Res.*, 108 (D16),
32 8544, doi:10.1029/2002JD002932.
33 Sinclair, D and G.S. Hoopes (1975) A continuous flow nucleus counter, *J. Aerosol Sci.*, 6, 1-7.
34 Sinreich R., U. Frieß, T. Wagner and U. Platt (2005), Multi axis differential optical absorption spectroscopy
35 (MAXDOAS) of gas and aerosol distributions, *Faraday Discuss.*, 130, 153-164, DOI: 10.1039/B419274P.
36 Sive, B. C., Y. Zhou, D. Troop, Y. Wang, W.C. Little, O.W. Wingenter, R.S. Russo, R.K. Varner and R. Talbot,
37 Development of a cryogen-free concentration system for measurements of volatile organic compounds, *Anal. Chem.*,
38 7(21), 6989–6998, doi:10.1021/ac0506231, 2005.
39 Slusher, D. L., et al. (2004), A thermal dissociation–chemical ionization mass spectrometry (TD-CIMS) technique
40 for the simultaneous measurement of peroxyacyl nitrates and dinitrogen pentoxide, *J. Geophys. Res.*, 109,
41 D19315, doi:10.1029/2004JD004670.
42 Sorooshian, A., F.J. Brechtel, Y. Ma, R.J. Weber, A. Corless, R.C. Flagan, and J.H. Seinfeld, Modeling and
43 Characterization of a Particle-into-Liquid Sampler (PILS), *Aerosol Sci. Technol.*, 2006.
44 Sotiropoulou, R.E.P, Medina, J., Nenes A., (2006) CCN predictions: is theory sufficient for assessments of the
45 indirect effect?, *Geoph.Res.Lett.*, 33, L05816, doi:10.1029/2005GL025148
46 Spicer, C. W. (1982), Nitrogen oxide reactions in the urban plume of Boston, *Science*, 215, 1095-1097.
47 Spichtinger, N., M. Wenig, P. James, T. Wagner, U. Platt, and A. Stohl, Satellite detection of a continental-scale
48 plume of nitrogen oxides from boreal forest fires. *Geophys. Res. Lett.* 28, 4579-4582, 2001.
49 Stohl, A., and T. Trickl, A textbook example of long-range transport: Simultaneous observation of ozone maxima of
50 stratospheric and North American origin in the free troposphere over Europe. *J. Geophys. Res.* 104, 30,445-
51 30,462, 1999.
52 Stohl, A., et al. (2002), Export of NO_y from the North American boundary layer during 1996 and 1997 North
53 Atlantic Regional Experiments, *J. Geophys. Res.*, 107, 4131, doi:10.1029/2001JD000519.
54 Stohl, A., et al. (2004), Forecasting for a Lagrangian aircraft campaign, *Atmos. Chem. Phys.*, 4, 1113–1124.
55 Stolzenburg, M. R. and MuMurry, P. H., (1991), An Ultrafine Condensation Particle Counter, *Aerosol Science and*
Technology, 14, 48-65.

- 1 Stutz, J., R. Ackermann, J. D. Fast, and L. Barrie, Atmospheric reactive chlorine and bromine at the Great Salt
2 Lake, Utah, *Geophys Res Lett*, 29, 1380, 2002.
- 3 Talbot, R., H. Mao, and B. Sive, Diurnal characteristics of surface level O₃ and other important trace gases in New
4 England, *J. Geophys. Res.*, 110, D09307, doi:10.1029/2004JD005449, 2005.
- 5 Tanner D., D. Helmig, J. Hueber and P. Goldan (2006) Gas chromatography system for the automated, unattended,
6 and cryogen-free monitoring of C₂ to C₆ non-methane hydrocarbons in the remote troposphere. *J. Chrom.*,
7 1111, 76-88. 777
- 8 Thompson, A.M., B.G. Doddridge, J.C. Witte, R.D. Hudson, W.T. Luke, J.E. Johnson, B.J. Johnson, S.J. Oltmans,
9 and R. Weller (2000), Shipboard and satellite views of a tropical Atlantic tropospheric ozone maximum and
10 wave-one in January-February 1999, *Geophys. Res. Lett.*, 27, 3317-3320.
- 11 Thomson, D. S., et al. (2000), Particle analysis by laser mass spectrometry WB-57 instrument overview\, *Aerosol*
12 *Sci. Technol.*, 33, 153-169.
- 13 Trainer, M. et al. (1993), Correlation of ozone with NO_y in photochemically aged air, *J. Geophys. Res.*, 98, 2917-
14 2925.
- 15 Tremmel, H. G., et al. (1994), Distribution of organic hydroperoxides during aircraft measurements over the
16 northeastern United States, *J. Geophys. Res.*, 99, 5295-5307.
- 17 Tremmel, H. G., et al. (1993), On the distribution of hydrogen peroxide in the lower troposphere over the
18 northeastern United States during late summer 1988, *J. Geophys. Res.*, 98, 1083-Stolzenburg, M. R. and
19 MuMurry, P. H., (1991), An Ultrafine Condensation Particle Counter, *Aerosol Science and Technology*, 14, 48
20 - 65.
- 21 Volz-Thomas, A., et al. (1996), Airborne Measurements of the Photolysis of NO₂, *Journal of Geophysical*
22 *Research*, 101, 18,613-18,627.
- 23 Wang, J., R.C. Flagan, and J.H. Seinfeld, A differential mobility analyzer (DMA) system for submicron aerosol
24 measurements at ambient relative humidity, *Aerosol Sci. Technol.*, 37, 1, 46-52, 2003.
- 25 Wang, S.C., and R.C. Flagan, Scanning Electrical Mobility Spectrometer, *Aerosol Sci. Technol.*, 13, 2, 230-240,
26 1990.
- 27 Warneke, C., J. A. De Gouw, E. R. Lovejoy, P. C. Murphy, W. C. Kuster, and R. Fall (2005), Online volatile
28 organic compound measurements using a newly developed proton-transfer ion-trap mass spectrometry
29 instrument during New England Air Quality Study - Intercontinental Transport and Chemical Transformation
30 2004: Performance, intercomparison, and compound identification, *Environ. Sci. Technol.*, 39, 5390-5397,
31 DOI: 10.1021/es050602.
- 32 Weber, B. L., et al. (1993), Quality controls for profiler measurements of winds and RASS temperatures, *J. Atmos.*
33 *Ocean. Technol.*, 10, 452-464.
- 34 Weber, R. J., et al. (2001), A particle-in-liquid collector for rapid measurement of aerosol chemical composition,
35 *Aerosol Science and Technology*, 35, 718-727.
- 36 Whittlestone, S. and W. Zahorowski (1998), Baseline radon detectors for shipboard use: Development and
37 deployment in the First Aerosol Characterization Experiment (ACE1), *J. Geophys. Res.*, 103, 16,743-16,751.
- 38 Wienhold, F., et al., Tristar – A tracer in situ TDLAS for atmospheric research, *Appl. Phys.*, B, 67, 411, 1998.
- 39 Williams, B.J., A.H. Goldstein, N.M. Kreisberg, S.V. Hering, An In-Situ Instrument for Speciated Organic
40 Composition of Atmospheric Aerosols: Thermal Desorption Aerosol GC/MS-FID (TAG). (2006) *Aerosol Sci.*
41 *Technol.*, In Press.
- 42 Williams, E.J., K. Baumann, J.M. Roberts, S.B. Bertman, R.B. Norton, F.C. Fehsenfeld, S.R. Springston, L.J.
43 Nunnermacker, L. Newman, K. Olszyna, J. Meagher, B. Hartsell, E. Edgerton, J.R. Pearson, and M.O. Rodgers
44 (1998), Intercomparison of ground-based NO_y measurement techniques, *J. Geophys. Res.*, 103, 22,261–22,280.
- 45 Williams, E.J., F.C. Fehsenfeld, B.T. Jobson, W.C. Kuster, P.D. Goldan, J. Stutz, and W.A. McClenny (2006),
46 Comparison of ultraviolet absorbance, chemiluminescence, and DOAS instruments for ambient ozone
47 monitoring, *Environ. Sci. Technol.*, in press.
- 48 Williams, P. I., M. W. Gallagher, T. W. Choularton, H. Coe, K. N. Bower, and G. McFiggans (2000), Aerosol
49 development and interaction in an urban plume, *Aerosol Sci. Technol.*, 32, 120-126.
- 50 Wilson, J. C., et al. (2004), Function and performance of a low turbulence inlet for sampling super-micron particles
51 from aircraft platforms, *Aerosol Science and Technology*, in press.
- 52 Winkler, P. (1988), Surface Ozone over the Atlantic Ocean, *Journal of Atmospheric Chemistry*, 7, 73-91.
- 53 Wofsy, S. C., et al. (1992), Atmospheric Chemistry in the Arctic and Subarctic: Influence of natural fires, industrial
54 emissions, and stratospheric inputs, *J. Geophys. Res.*, 97, 16,731-16,746.
- 55 Worton, D., (2006), Ph.D. Thesis, University of East Anglia, Norwich, U.K.

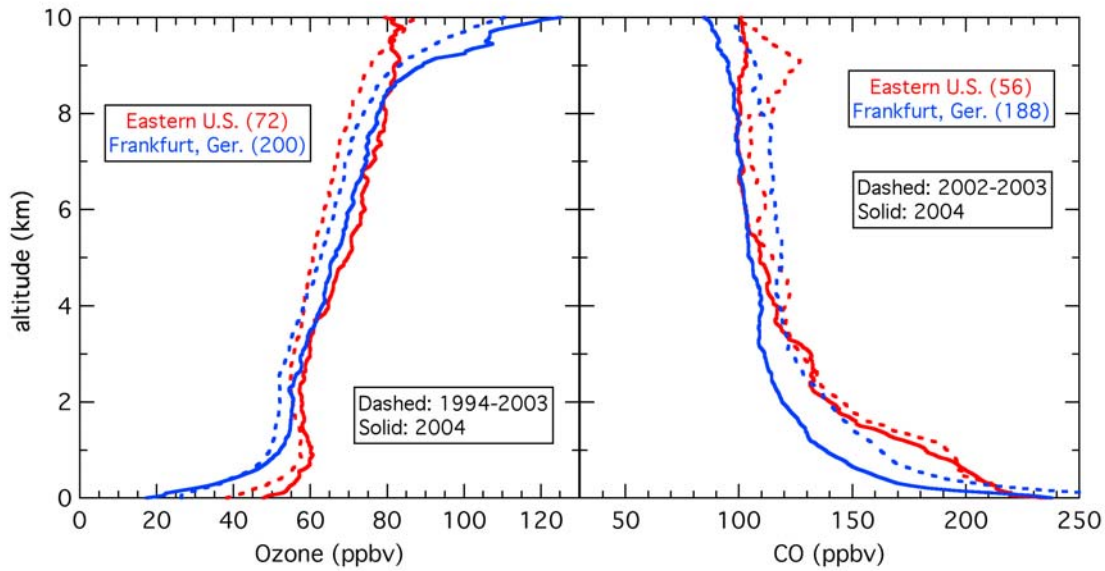
1 Wotawa G. and H. Kromp-Kolb (2000), The research project VOTALP – general objectives and main results,
 2 Atmos. Environ. 34, 1319-1322.
 3 Zahn, A., C.A.M. Brenninkmeijer, P.F.J. van Velthoven: Passenger aircraft project CARIBIC 1997-2002, Part I: the
 4 extratropical chemical tropopause, *Atmos. Chem. Phys. Discuss.* 4, 1091-1117, 2004
 5 Zeller, K. F., et al. (1977), Mesoscale analysis of ozone measurements in the Boston Environs, *J. Geophys. Res.*, 82,
 6 5879-5888.
 7 Zhang, J., et al. (1998), Meteorological processes and ozone exceedances in the northeastern United States during
 8 the 12-16 July 1995 episode, *J. Appl. Met.*, 37, 776-789.
 9 Zhao, Y., J. N. Howell, R. M. Hardesty (1993), Transportable lidar for the measurement of ozone concentration and
 10 aerosol profiles in the lower troposphere. AWMA/SPIE International Symposium on Optical Sensing for
 11 Environmental Monitoring, October 11-14, 1993, Atlanta, Georgia, pp.310-320
 12 Zhou, Y., R. K. Varner, R. S. Russo, O. W. Wingenter, K. B. Haase, R. Talbot, and B. C. Sive, Coastal water source
 13 of short-lived halocarbons in New England, *J. Geophys. Res.*, 110, D21302, doi:10.1029/2004JD005603, 2005.
 14 Ziereis, H., et al., Distributions of NO, NO_x, and NO_y in the upper troposphere and lower stratosphere between 28°
 15 and 61°N during POLINAT 2, *J. Geophys. Res.*, 105, 3653-3664, 2000.
 16 Zuidema, Paquita, C. W. Fairall, E. Westwater, and D. Hazen (2005), Ship-based liquid water path estimates in
 17 marine stratus. *J. Geophys., Res.*, 110, Art. No. D20206.
 18
 19
 20
 21
 22
 23
 24

25 Figures



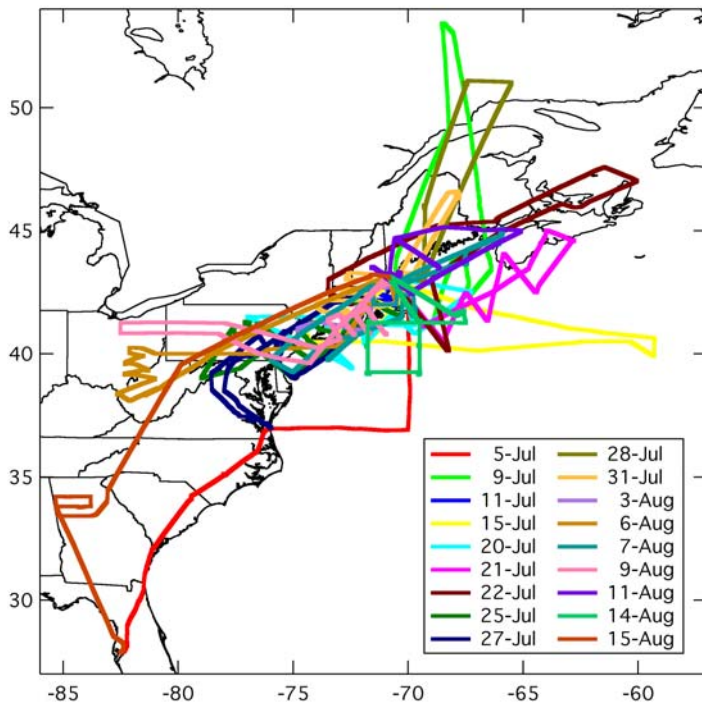
1
2
3

Figure 1. Dates of deployment of the major ICARTT platforms and surface sites.

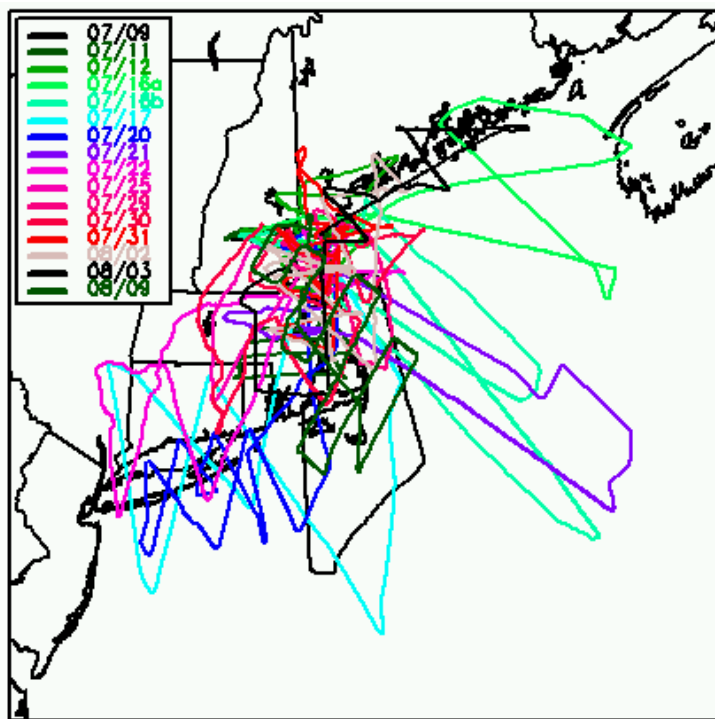


1
 2 **Figure 2.** Average altitude profiles of ozone and CO for July-August measured by the MOZAIC
 3 program. Solid lines indicate 2004 data and dashed lines the average of all earlier years of
 4 measurements (1994-2003 for ozone and 2002-2003 for CO). Eastern U.S. represents the
 5 average from all flights into New York City, Boston, and Washington D.C. The numbers in
 6 parentheses give the number of vertical profiles averaged in each curve for 2004.

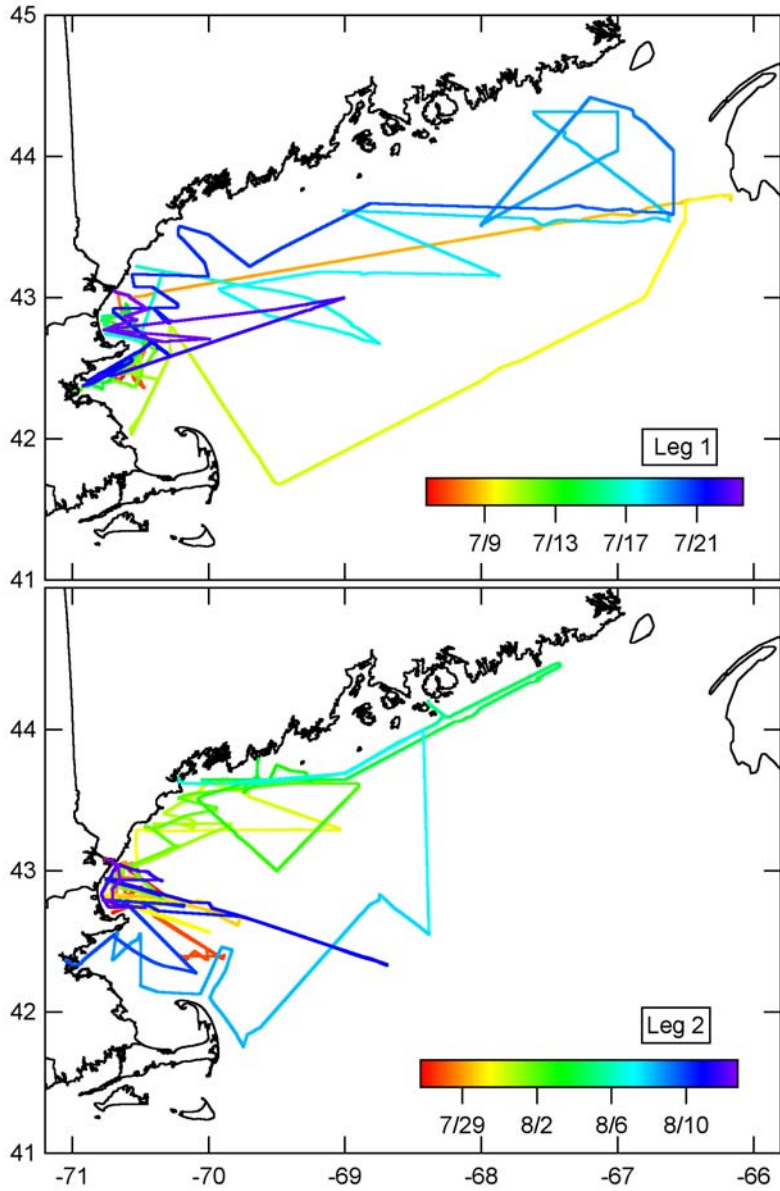
7
 8



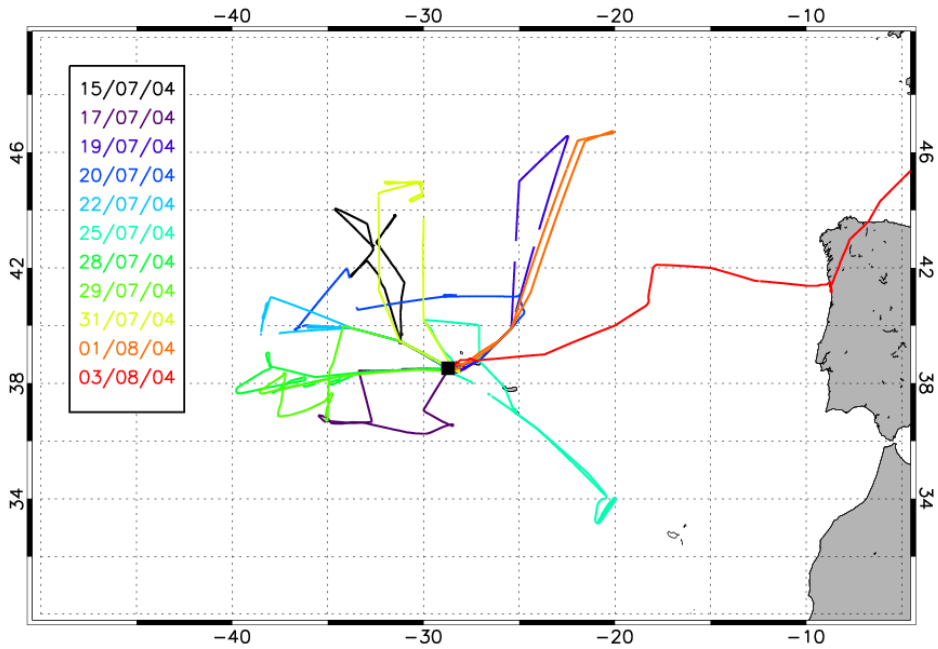
9
 10 **Figure A1.** Flight tracks of NOAA WP-3D aircraft during ICARTT.



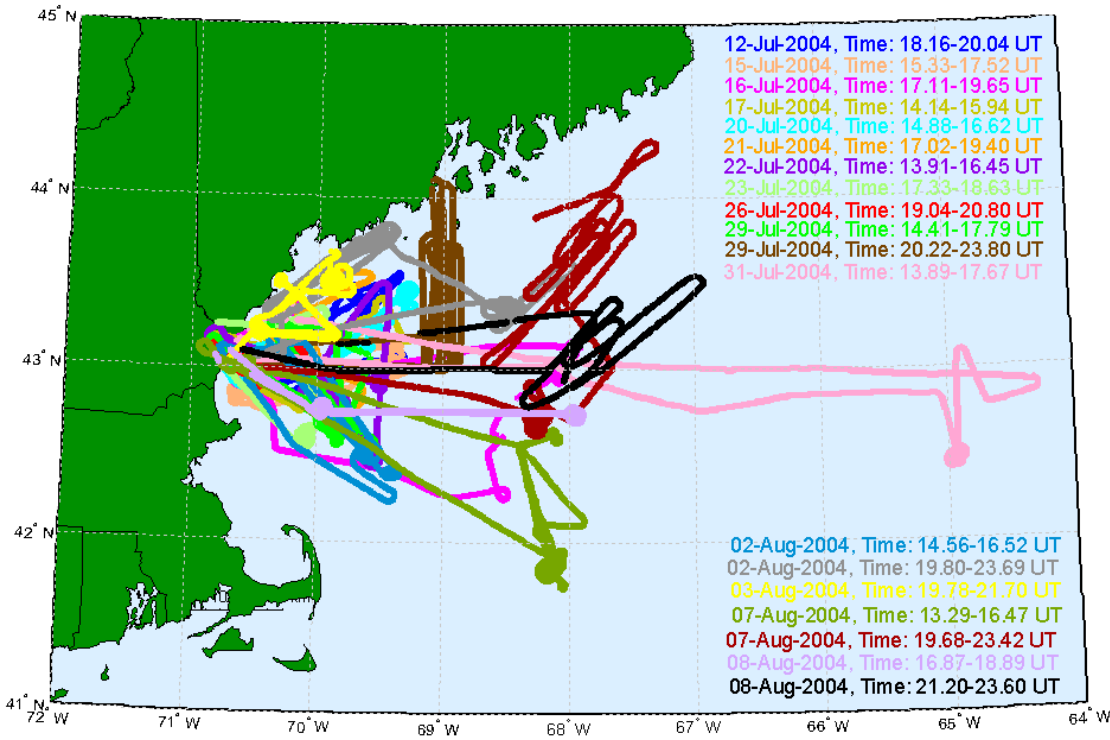
1
 2 **Figure A2.** Flight tracks of NOAA DC-3 lidar aircraft during ICARTT.
 3



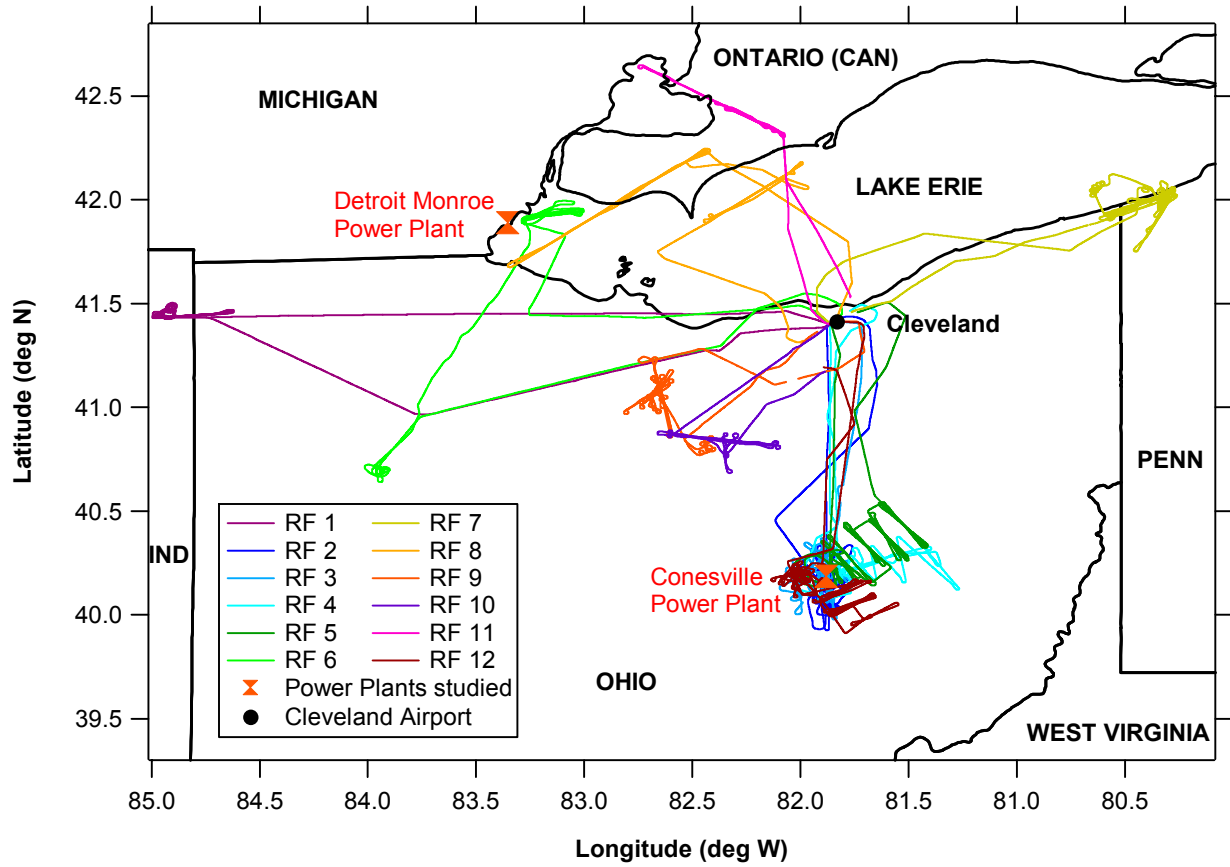
1
 2 **Figure A3.** Cruise tracks NOAA R/V *Ronald H. Brown* during ICARTT.
 3



1
2 **Figure A4.** Map indicating FAAM BAE146 Aircraft flights during ICARTT.

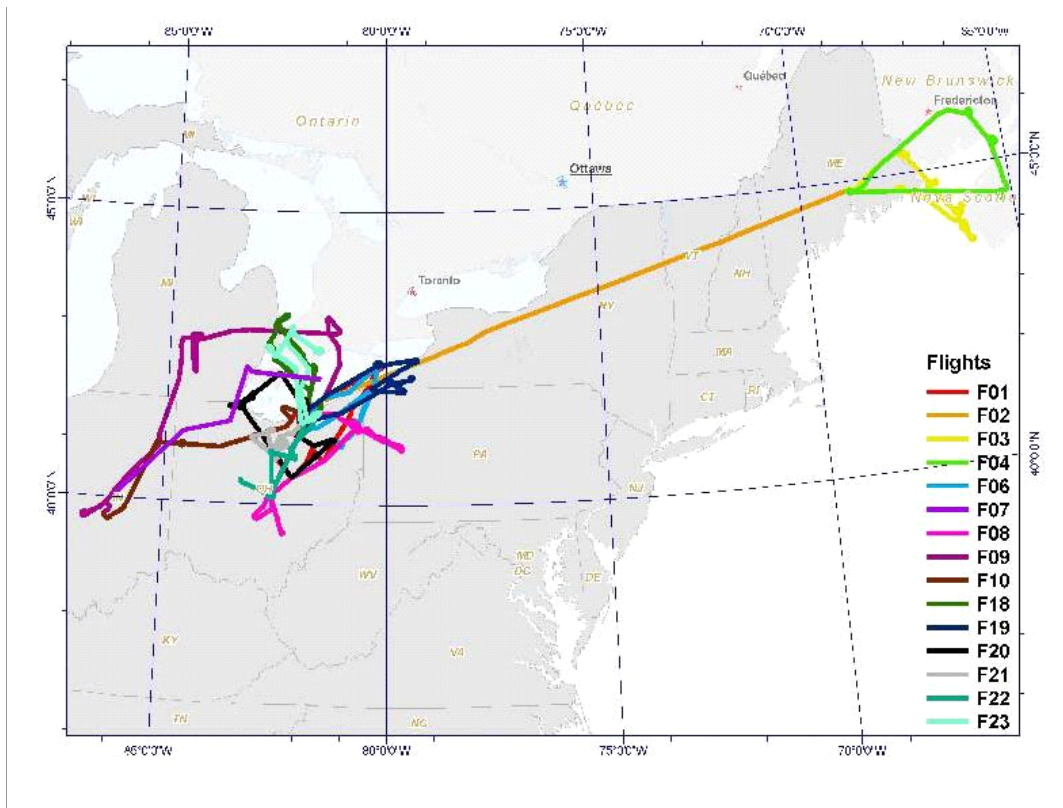


3
4 **Figure A5.** Map indicating J31 aircraft flights during ICARTT.
5



1
2
3
4

Figure A6. Flight tracks of the CIRPAS Twin Otter during ICARTT



1
2
3
4

Figure A7. Flight tracks of the Canadian Convair 580 during ICARTT

1
2
3
4
5
6
7
8
9
10
11
12
13
14
15
16
17
18
19
20
21
22
23
24

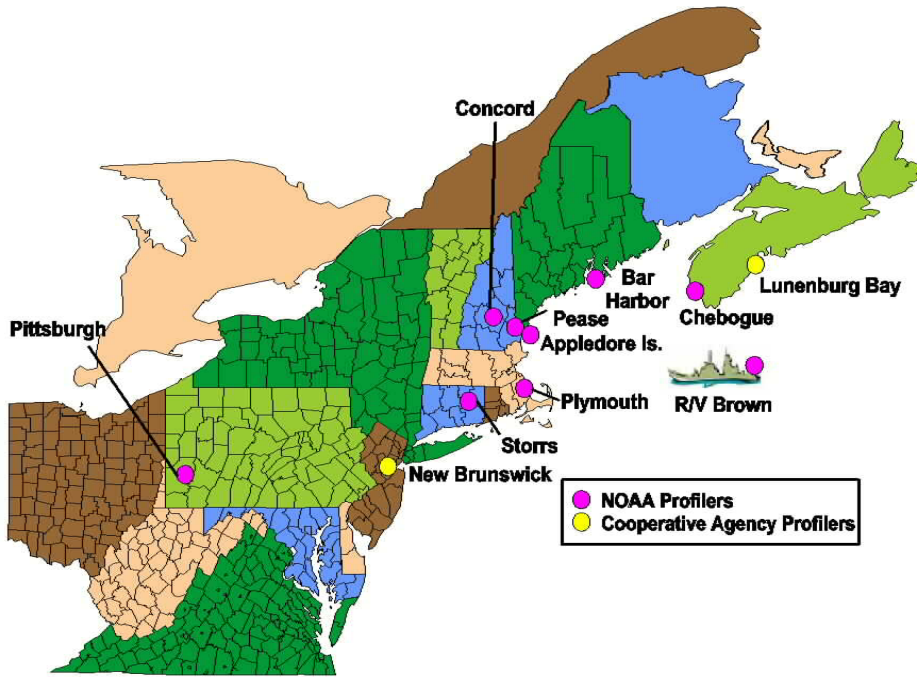


Figure B1. Map of observing sites in the ICARTT wind profiler network.

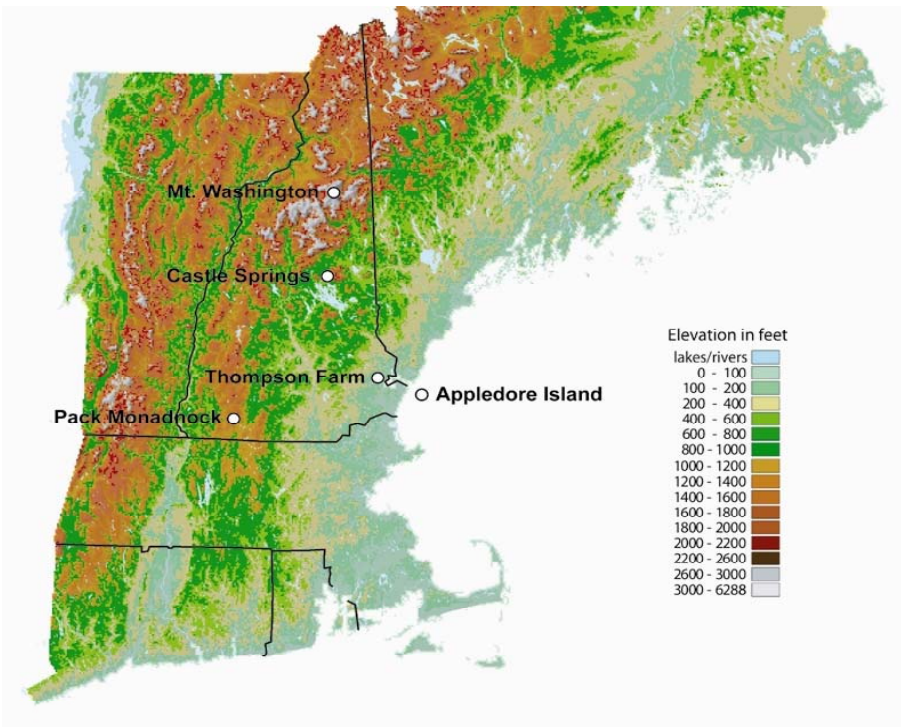
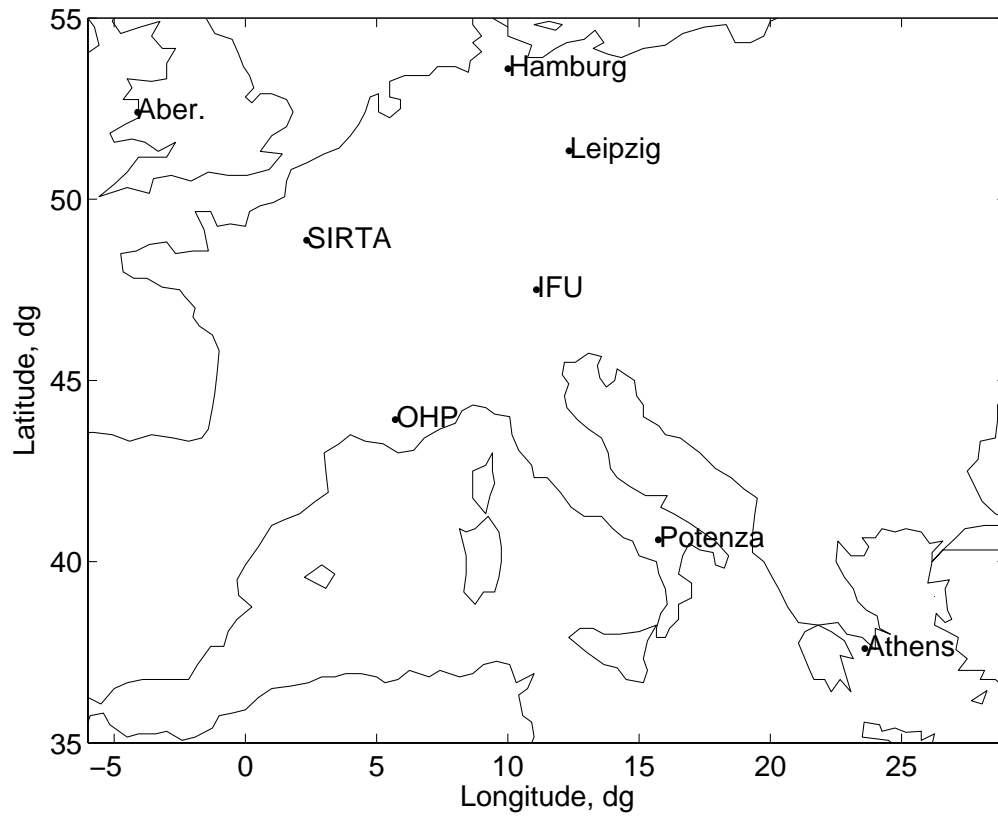


Figure B2. Map of AIRMAP observational network.



1
2
3
4
5

Figure B3. Map of sites in the European Lidar Network.

Tables

Table 1a. Mobile platforms involved in the ICARTT study.

Aircraft	Program, Agency	Emphasis
Douglas DC8	INTEX NA, NASA	Regional distribution of chemically active compounds over North America and their sources (emphasis – free troposphere). Outflow of from North America.
Lockheed WP3	NEAQS/ITCT, NOAA	Emissions and chemical processing downwind from urban areas and industrial point sources in the Northeastern United States (emphasis – boundary layer). Outflow of from North America.
Grumman G-1	DOE	Emissions and chemical processing downwind from urban areas and industrial point sources (emphasis – boundary layer).
Douglas DC-3	NEAQS/ITCT, NOAA	Emissions and chemical processing downwind from urban areas and industrial point sources (emphasis – boundary layer).
BAE 146-301	ITOP, NERC	Observations of chemical processing occurring in air masses transported from the North America to Europe.
Dassault Falcon	ITOP, DLR	Measurements in pollution plumes transported from North America including forest fire plumes originating from Canada and Alaska and quasi Lagrangian studies Measurements of emissions from shipping in the English Channel. Satellite validation and measurement comparisons.
Gulfstream J-31	INTEX NA, NASA	Satellite validation. Regional-scale understanding of anthropogenic aerosol and its direct radiative impact.
Twin Otter	CIRPAS, NSF	The relationship between cloud properties and the properties of the aerosols that are influencing the cloud formation.
Convair 580	MSC	The relationship between cloud properties and the properties of the aerosols that are influencing the cloud formation.
Ship		
Ronald H. Brown	NEAQS/ITCT, NOAA	Chemical composition and aerosol physical and optical properties in the marine boundary layer. Emission from ships. Long-path radiation-aerosol measurements.

Table 1b. Ground sites involved in the ICARTT study.

Location of site(s)	Program, Agency	Emphasis
Five sites located in Northeastern US	AIRMAP, <i>NOAA</i>	Long-term measurement to document and study persistent air pollutants such as O ₃ and fine particles in the region.
Pinnacle State Park in Addison, NY	ASRC, <i>NOAA, NSF</i>	Measurements of aerosol composition, gaseous aerosol precursors, ozone, and solar radiation.
11 Site Radar wind profiler network	NEAQS/ITCT, <i>NOAA, DOE</i>	Regional scale trajectories and transport of air masses.
Chebogue Point Nova Scotia, Canada	NEAQS/ITCT, <i>NOAA, NSF</i>	Determination of the frequency and intensity of pollution events crossing the Canadian maritime provinces; study of aerosol processing.
12 Station Ozonesonde Network	IONS, INTEX NA <i>NASA</i>	Estimation of the North American ozone budget by profiling ozone from sites across the continent.
Pico mountain, Pico Island, Azores, Portugal	PICO-NARE, <i>NOAA, NSF</i>	Determination of the composition of the lower free troposphere in the central North Atlantic region.
European Lidar Networks	ITOP	Identification of atmospheric layers for the surface to 5 km that were influenced by long-range transport not of European origin.

Table A1a. NOAA WP-3D Aircraft Instrumentation for Gas-Phase Measurements

Species/ Parameter	Reference	Technique	Averaging Time	Accuracy	Precision	LOD
NO	[<i>Ryerson, et al., 1999</i>]	NO/O ₃ Chemiluminescence	1s	5%	10 pptv	20 pptv
NO ₂	[<i>Ryerson, et al., 1999</i>]	Photolysis-Chemiluminescence	1s	8%	25 pptv	100 pptv
NO _y	[<i>Ryerson, et al., 1999</i>]	Au converter-Chemiluminescence	1s	10%	20 pptv	50 pptv
O ₃	[<i>Ryerson, et al., 1998</i>]	NO/O ₃ Chemiluminescence	1s	3%	0.1 ppbv	0.2 ppbv
CO	[<i>Holloway, et al., 2000</i>]	VUV Resonance Fluorescence	1s	2.5%	0.5 ppbv	1 ppbv
H ₂ O		Lyman Alpha Absorption	1s	—	—	—
H ₂ O		Thermoelectric hygrometer	3s	±0.2-1.0°C	±0.2-1.0°C	-75°C to +50°C
NMHCs (C ₂ -C ₁₀)	[<i>Schauffler, et al., 1999</i>]	Grab sample/GC	8-30s ¹	5-10%	1-3%	3 pptv
Halocarbons (C ₁ -C ₂)	[<i>Schauffler, et al., 1999</i>]	Grab sample/GC	8-30s ¹	2-20%	1-10%	0.02-50 pptv
Alkyl nitrates (C ₁ -C ₅)	[<i>Schauffler, et al., 1999</i>]	Grab sample/GC	8-30s ¹	10-20%	1-10%	0.02 pptv
VOCs	[<i>de Gouw, et al., 2003</i>]	Proton Transfer Reaction Mass Spectrometer (PTRMS)	1s every 15s	10-20%	5-30%	50-250 pptv
Formaldehyde	[<i>Jimenez, et al., 2005</i>]	Tunable Infrared Diode Laser Absorption Spectroscopy (TIDLAS)	1s	7%	300 pptv	140 pptv
Formic Acid	[<i>Jimenez, et al., 2005</i>]	TIDLAS	1s	33%	400 pptv	180 pptv
PAN, PPN, PiBN, APAN	[<i>Slusher, et al., 2004</i>]	Chemical Ionization Mass Spectrometer (CIMS)	2s 2s	15% 30%	2 % 2 %	1 pptv 5 pptv
MPAN						
NO ₃ , N ₂ O ₅	[<i>Dubé, et al., 2006</i>]	Cavity Ring-Down Spectroscopy (CARDS)	1s	25%	2%	1 pptv
HNO ₃ , NH ₃	[<i>Neuman, et al., 2002</i>]	CIMS	1s	15%	25 pptv	50 pptv
Hydroxyl Radical	[<i>Eisele and Tanner, 1993</i>]	CIMS	30s	35%	1 x 10 ⁶ cm ⁻³	5 x 10 ⁵ cm ⁻³
SO ₂	[<i>Ryerson, et al., 1998</i>]	Pulsed UV Fluorescence	3s	10%	0.35 ppbv	1 ppbv
H ₂ SO ₄	[<i>Eisele and Tanner, 1993</i>]	CIMS	1.1 s	35%	1 x 10 ⁶ cm ⁻³	1 x 10 ⁶ cm ⁻³
SO ₂ , O ₃ , H ₂ O column		Minature Differential Absorption Spectroscopy (MIDAS)				

¹dependent upon altitude

Table A1b. NOAA WP-3D Aircraft Instrumentation for Aerosol and Ancillary Data Measurements

Species/Parameter	Reference	Technique	Averaging Time	LOD
Aerosol Single Particle Composition	[<i>Thomson, et al., 2000</i>]	Particle Analysis by Laser Mass Spec (PALMS)	single particle	<1 cm ⁻³
Aerosol Bulk Ionic Composition	[<i>Weber, et al., 2001</i>] & [<i>Orsini, et al., 2003</i>]	Particle Into Liquid Sampling (PILS) – Ion Chromatography (IC)	3 m	< 0.02 µg/m ³
Aerosol Water Soluble Organic Composition	[<i>Sullivan et al., 2006, this section</i>]	Particle Into Liquid Sampling (PILS) – Total Organic Carbon (TOC)	3 m	0.3 µg/m ³
Aerosol Non-Refractory, Size-Resolved Composition	[<i>Bahreini, et al., 2003</i>]	Aerosol Mass Spectrometer (AMS)	10 m	SO ₄ ⁻² : 0.1 µg/m ³ NO ₃ ⁻ : 0.1 µg/m ³ NH ₄ ⁺ : 0.4 µg/m ³ Organics: 0.6 µg/m ³
Small Aerosol Size Distribution	[<i>Brock, et al., 2000</i>]	Nucleation Mode Aerosol Size Spectrometer (NMASS)	1 s	0.005 – 0.06 µm
Large Aerosol Size Distribution	[<i>Brock, et al., 2003</i>] & [<i>Wilson, et al., 2004</i>]	Light Scattering (white light & laser) with low turbulence inlet	1 s	0.12 – 8.0 µm
Photolytic Flux	[<i>Stark et al., 2006, this section</i>]	280-690 nm spectrally resolved Radiometer, Zenith & Nadir	1 s	2x10 ¹¹ photons cm ⁻² s ⁻¹ @ 500 nm
Broadband Radiation		Pyrgeometer	1 s	3.5 - 50 µm
Broadband Radiation		Pyranometer	1 s	0.28 - 2.8 µm

Table A2. NOAA WP-3D Flights

Flight No.	Flight Description	Date 2004	Takeoff-Landing UT
1	Transit Tampa FL to Pease Tradeport NH	5-Jul	16:10 - 22:11
2	Survey Boston urban plume, Alaskan biomass burning plumes	9-Jul	15:29 - 23:01
3	Boston urban plume at night	11-Jul	22:55 - 03:51
4	North American plume at 60° W, and New York City urban plume	15-Jul	13:10 - 21:13
5	New York City urban plume - Near source	20-Jul	14:11 - 22:13
6	New York City urban plume – Over Gulf of Maine	21-Jul	14:02 - 20:29
7	New York City urban plume – Nova Scotia; DC-8 Intercomparison	22-Jul	13:48 - 21:34
8	Point source and urban plume evolution in Northeast U.S.	25-Jul	14:15 - 22:07
9	Characterize pollution accumulation ahead of cold front	27-Jul	15:03 - 22:27
10	WCB outflow of accumulated pollution; biomass burning plumes	28-Jul	13:54 - 20:33
11	New York City urban plume at night; DC-8 Intercomparison	31-Jul	21:24 - 05:16
12	New York City urban plume at night	3-Aug	01:53 - 08:23
13	Ohio River Valley power plant plumes	6-Aug	14:00 - 22:27
14	NYC, Boston urban plumes at night; DC-8 Intercomparison	7-Aug	20:08 - 04:36
15	Ohio River Valley power plants, NYC urban plumes at night	9-Aug	22:57 - 07:29
16	New York City urban plume – night into day	11-Aug	03:00 - 10:51
17	Cloud investigation	14-Aug	13:55 - 22:10
18	Transit Pease Tradeport NH to Tampa FL, via Atlanta GA	15-Aug	14:34 - 21:29

Table A3. NOAA Research Vessel *Ronald H. Brown* Instrumentation

Species/Parameter	Reference	Technique	Averaging Time	LOD	Uncertainty
JNO ₂ Photolysis rates	[<i>Shetter et al., 2003</i>]	Spectral radiometer	1 min	5e-7 Hz	± 22%
JNO ₃ Photolysis rates	[<i>Stark et al., 2006, this section</i>]	Spectral radiometer	1 min	3e-7 Hz	± 30%
JO(1D) Photolysis rates	[<i>Bohn et al., 2004</i>]	Spectral radiometer	1 min	4e-8 Hz	± 30%
Ozone	[<i>Bates et al., 2005</i>]	UV absorbance	1 min	1.0 ppb	±1.0 ppb or 2%
Ozone	[<i>Williams et al., 2006</i>]	NO chemiluminescence	1 min	0.1 ppbv	±(2%+1.0 ppbv)
NO ₂	[<i>Sinreich et al., 2005</i>]	Passive DOAS	5 min	0.1 ppb	70 ppt
CH ₂ O	[<i>Sinreich et al., 2005</i>]	Passive DOAS	5 min	0.3 ppb	0.2 ppb
BrO	[<i>Sinreich et al., 2005</i>]	Passive DOAS	5 min	1 ppt	0.7 ppt
Ozone vertical profiles	[<i>Thompson et al., 2000</i>]	Ozonesondes	1 sec = 5 m	2 ppbv	3-5%
Ozone vertical profiles	[<i>Zhao et al., 1993</i>]	O ₃ Lidar (OPAL)	10 min	5ppb	<10 ppb
Carbon monoxide	[<i>Gerbig et al., 1999</i>]	UV fluorescence	1 min	1.0 ppb	± 3.0%
Carbon dioxide	LiCor spec	Non-dispersive IR	1 min	0.07 ppm	± 2.5%
Water vapor	LiCor spec	Non-dispersive IR	1 min	1 ppm	± 1%
Sulfur dioxide	[<i>Bates et al., 2005</i>]	Pulsed fluorescence	1 min	100 ppt	<5%
Nitric oxide	[<i>Osthoff et al., 2006</i>]	Chemiluminescence	1 min	18 ppt	± (4% + 7pptv)
Nitrogen dioxide	[<i>Osthoff et al., 2006</i>]	Photolysis cell	1 min	27 ppt	± (6.5% + 93 pptv) @ NO ₂ /NO = 3
Total nitrogen oxides	[<i>Williams et al., 1998</i>]	Au tube reduction	1 min	0.04 ppbv	±(10%+0.08 ppbv)
PANs	[<i>Marchewka et al., 2006, this section</i>]	GC/ECD	1 min	PAN/PPN (5 pptv); PiBN/MPAN (10 pptv)	PAN/PPN ± (5pptv+15%) PiBN/MPAN ± (10 pptv +20%)

Alkyl nitrates	[<i>Goldan et al., 2004</i>]	GC/MS	5 min	≤1 ppt	±20%
NO ₃ /N ₂ O ₅	[<i>Dubé et al., 2006</i>]	Cavity ring-down spect.	1 sec	1 pptv	1 pptv, ±30%
NO ₂	[<i>Osthoff et al., 2006</i>]	Cavity ring-down spect.	1 sec	160 pptv	160 pptv, ±8%
Nitric acid/NH ₃	[<i>Dibb et al., 2004</i>]	Automated mist chamber/IC	5 min	5 pptv	15%
Radon	[<i>Whittlestone & Zahorowski, 1998</i>]	Radon gas decay	13 min		
VOC speciation	[<i>Goldan et al., 2004</i>]	GC/MS	5 min	≤1 ppt	±20%
Seawater and atmospheric pCO ₂	[<i>Sabine et al., 2000</i>]	Non-dispersive IR	30 min		±0.2 ppm
Seawater DMS	[<i>Bates et al., 2000</i>]	S chemiluminescence	30 min	0.2 nM	±8%
Continuous speciation of VOCs	[<i>Warneke et al., 2005</i>]	PTR-MS/CIMS	2 min	50-500 pptv	20%
Aerosol ionic composition	[<i>Quinn et al., 2006, this section</i>]	PILS-IC	5 min		
Aerosol WSOC	[<i>Quinn et al., 2006, this section</i>]	PILS-TOC	1 hr		
Aerosol size and composition	[<i>Quinn et al., 2006, this section</i>]	Aerosol mass spectrometer	5 min	0.1 µg m ⁻³	±20%
Aerosol OC	[<i>Quinn et al., 2006, this section</i>]	On-line thermal/optical	1 hr	0.1 µg m ⁻³	
Aerosol organic functional groups	[<i>Maria & Russell, 2005; Gilardoni et al., 2006, this section</i>]	FTIR	4-12 hours	1 µg m ⁻³	±15%
Aerosol composition, 2 stage (sub/super micron) & 7 stage at 60% RH	[<i>Quinn & Bates, 2005</i>]	Impactors (IC, XRF and thermal optical OC/EC, total gravimetric weight)	4-12 hours		±6-31%
Total and sub-micron aerosol scattering & backscattering (450, 550, 700 nm) at 60% RH	[<i>Quinn & Bates, 2005</i>]	TSI 3563 nephelometers (2)	1 min		±14%

Total and sub-micron aerosol absorption (450, 550, 700 nm) dry	[<i>Sierau et al., 2006, this section</i>]	Radiance Research PSAPs (2)	1 min		±22%
Total and Sub-micron aerosol extinction	[<i>Baynard et al., 2006</i>]	Cavity ring-down spect.	1 min	0.01 Mm ⁻¹	±1%
Aerosol number	[<i>Bates et al., 2001</i>]	CNC (TSI 3010, 3025)	1 sec		±10%
Aerosol size distribution	[<i>Bates et al., 2005</i>]	DMA and APS	5 min		±10%
Total and sub-micron aerosol light scattering hygroscopic growth	[<i>Carrico et al., 2003</i>]	Twin TSI 3563 nephelometers RR M903 nephelometer	20 sec (over each 1% RH)	σ_{spTSI} : 1.85 and 2.78 σ_{bsp} : 1.24 and 2.96 σ_{spRR} : 1.06	σ_{spTSI} : -14 ~ 17 σ_{bsp} : -17 ~ 19
Aerosol optical depth	[<i>Quinn & Bates, 2005</i>]	Microtops	intermittent		± 0.015 AOD
Aerosol backscatter vertical profiles	[<i>Zhao et al., 1993</i>]	O3 Lidar (OPAL)	10 min	1*10 ⁻⁶ m ⁻¹ sr ⁻¹	30% aerosol backscatter
BL wind/aerosol/turbulence	[<i>Grund et al., 2001</i>]	Doppler Lidar (HRDL)	0.5 sec	2-6 km	10-12 cm s ⁻¹
Wind/temp profiles	[<i>Law et al., 2002</i>]	915 MHz wind profiler	5 min	0.5-5 km	±1.4 ms ⁻¹
Temp/RH profiles	[<i>Wolfe et al., 2006, this section</i>]	Sondes	5 sec	0.1 – 18 km	±0.3 C ±4%
LWP	[<i>Zuidema et al., 2005</i>]	Microwave radiometer	5 sec	20 gm ⁻²	±10%
Cloud height	[<i>Fairall et al., 1997</i>]	Ceilometer	15 sec	0.1-7.5 km	±30 m
Cloud drop size, updraft velocity	[<i>Kollias et al., 2001</i>]	3mm doppler radar	5 sec	0.2-12 km	----
Turbulent fluxes	[<i>Fairall et al., 2003</i>] [<i>Fairall et al., 2006, this section</i>]	Bow-mounted EC flux package	20 Hz 10 min, 1 hr	2 Wm ⁻² 0.002 Nm ⁻²	±25% @ 1 hr
Low altitude temperature profiles	[<i>Cimini et al., 2003</i>]	60 GHz scanning microwave radiometer	10 sec	0-0.5 km	±0.3 C
Wind profiles/microturbulence below cloud	[<i>Frisch et al., 1989</i>] [<i>Comstock et al., 2005</i>]	C-Band radar	5 min	0.1-2 km	±1.0 ms ⁻¹

Table A4a. FAAM BAE146 Aircraft Instrumentation for Gas-Phase Measurements

Species/ Parameter	Reference	Technique	Averaging Time	Accuracy	Precision	LOD
NO	[<i>Brough et al, 2003</i>]	NO/O ₃ Chemiluminescence	1 s	10 s	12%	40 ppt
NO ₂	[<i>Brough et al, 2003</i>]	Photolysis-Chemiluminescence	1 s	10 s	35%	350 ppt
NO _y	[<i>Brough et al, 2003</i>]	Au converter-Chemiluminescence	1 s	10 s	21%	70 ppt
O ₃		UV absorption	3 s	5 %	1 ppbv	2 ppbv
CO	[<i>Gerbig et al, 1999</i>]	VUV Resonance Fluorescence	1 s		1 ppbv	2 ppbv
H ₂ O	----	Lyman Alpha Absorption and dewpoint	1 s	±1°	-----	-----
NMHCs (C ₂ -C ₈), DMS, acetone.	[<i>Schauffler, et al., 1999</i>]	Grab sample/ GC	60 s	5-10%	1-3%	10 - 1 pptv
Halocarbons (C ₁ -C ₂)	[<i>Schauffler, et al., 1999</i>]	Grab sample/ GC	60 s	5-10%	1-5 %	0.1 ppt
Alkyl nitrates (C ₁ -C ₅)	[<i>Schauffler, et al., 1999</i>]	Grab sample/ GC	60 s	5-20%	1-5 %	0.005 ppt
VOCs	----	Proton Transfer Reaction Mass Spectrometer	1-2 s	10-50%	10 %	20-80 ppt
PAN	[<i>Roberts, et al., 2004</i>]	Dual GC/ECD	≈ 90 s	10%	3 %	10 pptv
HCHO	[<i>Cárdenas et al, 2000</i>]	Hantzsch Fluorometric	10 s	30%	12%	50 pptv
Peroxides (inorganic and organic)	[<i>Penkett et al, 1995</i>]	Fluorometric	10 s			5 pptv
Peroxy radicals (RO ₂ + HO ₂)	[<i>Green, et al., 2006</i> ; <i>Monks, et al., 1998</i>]	Chemical Amplifier	30-60 s	±40%	6%	2 pptv

Table A4b. FAAM BAE146 Aircraft Instrumentation for Aerosol and Ancillary Data Measurements

Species/ Parameter	Reference	Technique	Averaging Time	LOD
Position, winds, u,v,w	----	INS, GPS, 5 port turbulence probe	0.1 s	$\sim 0.01 \Delta p / P_s$
Black Carbon CCN	<i>[Stolzenburg and McMurry, 1991]</i>	Particle Soot Absorption Photometer Condensation particle counter	1 s	0 cm^{-3}
Aerosol Bulk Composition	<i>[Jayne et al, 2000]</i>	Aerosol Mass Spectrometer (AMS)	30 s	$15 - 150 \text{ ng m}^{-3}$ (species dependant)
NO ₂ photolysis $j(\text{NO}_2)$	<i>[Junkerman, et al., 1989; Volz-Thomas, et al., 1996]</i>	Fixed bandwidth radiometry	1 s	----
O ₃ photolysis $j(\text{O}^1\text{D})$	<i>[Junkerman, et al., 1989; Volz-Thomas, et al., 1996]</i>	Fixed bandwidth radiometry,	1 s	----

Table A5. FAAM BAE146 Flights

Flight No.	Flight Description	Date 2004	Takeoff-Landing UT
B028	Transit Cranfield U.K. to Faial, Azores (refuel Oporto) Fire Plumes encountered in UK SW approaches	12-Jul	09:30 – 21:30
B029	North West of Azores, low-level US outflow (P3) and Alaskan fires	15-Jul	08:42 – 13:26
B030	S and W of Azores, low/mid level polluted features from US, Lagrangian opportunity	17-Jul	12:56 – 17:37
B031	North of Azores to aircraft range limit into NY plume.	19-Jul	09:04 – 14:05
B032	Major mid troposphere interception of biomass plumes	20-Jul	08:37 – 13:15
B033	To West of Azores for ENVISAT underpass and low-level pollution	22-Jul	09:20 – 13:49
B034	Re interception of NY plume and outflow from Africa, refuel Santa Maria	25-Jul	09:28 – 16:24
B035	DC8 intercomparison to West of the Azores mainly in clean marine air	28-Jul	11:57 – 16:32
B036	Upper level export in wcb from US + Alaskan fires at higher T	29-Jul	08:30 – 13:00
B037	Low level wcb sampled by P3, + fires + stratosphere filament	31-Jul	08:30 – 13:15
B038	North of Azores into polluted low level WCB	1-Aug	07:44 – 12:44
B039	Transit Faial, Azores to Cranfield U.K (refuel Oporto) with DLR Falcon intercomparison	3-Aug	07:22 – 15:14

Table A6a DLR Falcon Gas-Phase and Ancillary Measurements

Species/ Parameter	Reference	Technique	Averaging Time	Accuracy	Precision	LOD
NO	[Schlager et al., 1997]	NO/O3 Chemiluminescence	1 s	7%	3%	2 pptv
NO _y	[Ziereis <i>et al.</i> , 2000]	Au converter-Chemiluminescence	1 s	12%	5%	15 pptv
O ₃	[Schlager et al, 1997]	UV absorption	5 s	5%	2%	0.5 ppbv
CO	[Gerbig <i>et al.</i> , 1996]	VUV Resonance Fluorescence	5 s	5%	2%	1 ppbv
CO	[Wienhold et al., 1998 & Fischer et al., 2002]	TD-LAS	5 s	7%	3%	2 ppbv
NMHCs(C ₂ -C ₁₀)	[Rappenglück <i>et al.</i> , 1998]	Grab sample/GC	60 s	5-10%	1-5%	3 pptv
CH ₄	[Wienhold et al., 1998]	TD-LAS	5 s	7%	5%	0.03 ppmv
CO ₂	[Fischer et al., 2002]	IR - absorption	1 s	2%	0.1%	0.3 ppbv
SO ₂	[Speidel et al., 2006, in preparation]	Ion trap mass spectrometry	2 s	10%	3%	10 pptv
J(NO ₂)	[Volz-Thomas et al., 1996]	Filter radiometry	1 s	5E-4 s ⁻¹	1E-4 s ⁻¹	-
humidity	[Schumann et al., 1995]	Lyman Alpha Absorption	1 s	0.3 g m ⁻³	0.01 g m ⁻³	-
Temperature	[Schumann et al., 1995]	Pt 100, Pt 500	1 s	0.5 °	0.1°	-
Wind (horiz., vert.)	[Schumann et al., 1995]	INS, GPS, five hole probe	1 s	1 m s ⁻¹ (horiz.) 0.3 m s ⁻¹ (vertical)	0.1 m s ⁻¹ (horiz.) 0.05 m s ⁻¹ (vertical)	-

Table A6b. DLR Falcon Aircraft Instrumentation for Aerosol Measurements

Species/ Parameter	Reference	Technique	Averaging Time	LOD
Ultrafine particle size distribution	[Schröder & Ström, 1997] & [Feldpausch et al., 2006]	Condensation particle counters operated at different lower cut-off diameters & Diffusion Screen Separator	5 s	1 cm ⁻³
Aitken mode size distribution	[Petzold et al., 2006, this section]	Differential Mobility Analyser (DMA)	70 s	1 cm ⁻³
Accumulation mode size distribution (dry state)	[Petzold et al., 2002]	Passive Cavity Aerosol Spectrometer Probe (PCASP 100X)	5 s	0.1 cm ^{-3?}
Volume fraction of volatile/refractory particles	[Clarke, 1991]	Thermodenuder connected to condensation particle counters	5 s	
Volume absorption coefficient	[Bond et al., 1999]	Particle Soot Absorption Photometer (PSAP)	20 s	0.1 Mm ⁻¹ at STP

Table A7. DLR Falcon Flights

Flight No.	Flight Description	Date 2004	Takeoff-Landing UT
1	Oberpfaffenofen (near Munich) – Po valley: NA FF & urban plume	02-Jul.	13.14 – 15.19
2	Cranfield - Northsee: intercomparison with BAe146	07 Jul	11.50 – 14.11
3	Oberpfaffenhofen – Po valley: urban plume	13-Jul	08.05 – 10.50
4	Transfer Oberpfaffenhofen – Creil (near Paris)	19-Jul	09.23 – 10.47
5	Creil – San Sebastian (Sp): New York/Boston plume, NA FF plume	22-Jul	09.40 – 10.57
6	San Sebastian – Creil: New York / Boston plume, NA FF plume	22-Jul	15.05 – 17.03
7	Creil – Brest – English Channel: NA FF plume, ship emissions	23-Jul	12.11 – 16.02
8	Creil – Shannon (Ireland): New York / Boston plume, NA FF plume	25-Jul	13.37 – 16.40
9	Shannon – Creil: New York Boston plume, NA FF plume	25-Jul	17.42 – 19.53
10	Creil – English Channel: New York/Boston plume, London plume	26-Jul	15.07 – 18.50
11	Creil – Gulf of Biscay: NA FF plume, ship emissions	30-Jul	15.00 – 18.35
12	Creil – Northern France: upper level outflow from USA	31-Jul	12.07 – 13.55
13	Creil – Northwest France: intercomparison Falcon with BAe146	03-Aug	14.24 – 17.25

(FF : forest fire, NA: North America)

Table A8. J31 Aircraft Instrumentation

Species/Parameter	Reference	Technique	Averaging Time	LOD
Optical depth, water vapor column	[<i>Thomson, et al., 2000</i>] & [<i>Thomson, et al., 2000</i>]	Tracking Sun photometer, 354-2138 nm	3 s	
Solar spectral flux	[<i>Weber, et al., 2001</i>]	Spectrometer (x-y nm) with nadir and zenith hemispheric collectors	?	
Pressure, temperature, dew point		[Rosemount, Vaisala]	?	
Aircraft position and orientation		[Applanix]		

Table A9. Twin Otter Aircraft Instrumentation for Aerosol and Ancillary Data Measurements

Parameter	Reference	Technique	Averaging Time	Detection Limit	Size Range Detected
Particle number concentration	Mertes et al. [1995] Buzorius [2001]	Condensation Particle Counter (TSI CPC 3010)	1 s	0-10,000 particles/cm ⁻³	D _p > 10 nm
Cloud condensation nuclei concentration	Rissman et al. [2006]	Linear temperature gradient growth chamber with optical detection (Caltech 3-column CCN counter)	1 s	0-10,000 particles/cm ⁻³	N/A
Aerosol size distributions at dry and humid condition	Wang and Flagan [1990], Wang et al. [2003]	Scanning differential mobility analyzer (Dual Automated Classified Aerosol Detector - DACAD)	73 s	N/A	10-700 nm
Aerosol size distribution		Passive Cavity Aerosol Spectrometer Probe (PCASP)	1 s	N/A	0.1-2.6 μm
Aerosol bulk ionic composition & soluble organic composition	Weber et al. [2001] Sorooshian et al. [2006]	Particle-into-Liquid Sampler (PILS)	5 m	0.02-0.28 μg/m ³ (depending on species)	< 1 μm
Aerosol bulk composition (non-refractory species)	Jayne et al. [2000] Bahreini et al. [2003]	Aerodyne Quadrupole Aerosol Mass Spectrometer (AMS)	30 s or 1 m	0.2-2.3 μg/m ³ (depending on species)	D _{va} ~ 40 nm - 1 μm
Bulk aerosol functional group	Maria et al. [2002]	FTIR spectroscopy of samples extracted from Teflon filter	~ 1 h	N/A	N/A
Soot absorption	Arnott et al. [1999; 2006]	Photoacoustic Absorption Spectrometer	1 s	1 Mm ⁻¹	10 nm - 5 μm
Soot absorption	Bond et al. [1999]	Particle Soot Absorption Photometer (PSAP)	1 s or higher	N/A	N/A
Soot absorption	Baumgardner et al. [2004]	Single Particle Soot Photometer (SP2)	N/A	N/A	150 nm - 1.5 μm
Separation of cloud droplets from interstitial aerosol	Noone et al. [1988]	Counterflow Virtual Impactor	N/A	N/A	N/A
Cloud droplet size distribution	Baumgardner et al. [2001]	Cloud, Aerosol, and Precipitation Spectrometer (CAPS)	1 s	0-1,000 particles/cm ⁻³	0.4 μm - 1.6 mm
Cloud droplet size distribution	Cerni [1983]	Forward Scattering Spectrometer Probe (FSSP)	1 s	N/A	1-46 μm
Cloud droplet liquid water content	Gerber et al. [1994]	Light diffraction (Gerber PVM-100 probe)	1 s	N/A	~ 5-50 μm

Table A10. CIRPAS Twin Otter Flights

Flight Number	Date (2004)	Flight Description	Take-off / Landing UTC
1	Aug 2	Aerosol characterization over NW Ohio and Indiana, Convair coordination	15:07-20:32
2	Aug 3	Clouds S of Cleveland	16:57-21:52
3	Aug 6	Conesville power plant plume & cloud, Convair coordination	16:17-20:41
4	Aug 8	Conesville power plant plume in clear air	18:18-21:45
5	Aug 9	Conesville power plant plume & cloud	17:09-22:16
6	Aug 10	Monroe power plant plume & cloud	18:04-23:00
7	Aug 11	Cloud physics at SE shore of Lake Erie	17:54-22:46
8	Aug 13	Pollution from Detroit, Monroe power plant plume, Convair coordination	18:31-23:03
9	Aug 16	Cloud physics SW of Cleveland, Convair coordination	18:16-22:37
10	Aug 17	Cloud physics SW of Cleveland, Convair coordination	18:13-21:24
11	Aug 18	Clouds, SW of Ontario, Convair coordination	15:37-19:10
12	Aug 21	Conesville power plant plume & cloud	17:40-22:52

Table A11 Canadian Convair 580 Flights

Flight No.	Flight Description	Date	Takeoff-Landing UT
1	Out of Cleveland to 20,000' over Lake Erie and in BL southeast of Cleveland	21-Jul	17:54 - 20:13
2	Transit, Cleveland to Bangor, MA for TIMs	21-Jul	22:13 - 00:53
3	TIMs flight from Bangor with profiles over Fundy and at Chebogue Point	22-Jul	15:24 - 19:13
4	TIMs flight from Bangor with profiles north of Saint John, Fundy and Kejimikujik	22-Jul	20:35 - 00:07
5	Transit, Bangor to Cleveland	23-Jul	15:24 - 18:45
6	Out of Cleveland, profile to 10000' over L Erie, cloud sampling south of L Erie	23-Jul	20:40 - 23:54
7	Evening flight to Terra Haute for aerosol nitrate, engine problem at Terra Haute	27-Jul	00:14 - 03:27
8	Cloud sampling south of Cleveland	31-Jul	18:01 - 22:32
9	Cleveland to Indianapolis for forecasted aerosol nitrate	2-Aug	12:01 - 17:02
10	Indianapolis to Cleveland for nitrate, coordinated with CIRPAS Twin Otter	2-Aug	18:25 - 20:20
11	BL cloud sampling over SW Ontario	3-Aug	14:57 - 18:29
12	Towering Cu sampling south of Cleveland over Ohio	3-Aug	20:26 - 00:10
13	Towering Cu sampling south of Cleveland over Ohio	5-Aug	16:24 - 21:02
14	Towering Cu sampling over Conesville with CIRPAS Twin Otter	6-Aug	16:18 - 20:38
15	Sampling over eastern Ohio in polluted air with little cloud	9-Aug	
16	Sampling aerosol and boundary layer cloud to the east and	10-Aug	16:24 - 20:15

	downwind of Chicago		
17	Sampling aerosol and cloud further east and downwind of Chicago	10-Aug	21:22 - 00:54
18	Sampling boundary layer cloud over SW Ontario downwind of Detroit-Windsor	11-Aug	18:29 - 21:44
19	Sampling Cumulus in boundary layer along south shore of Lake Erie	12-Aug	17:40 – 21:20
20	Sampling towering Cu over Toledo and south of Akron	13-Aug	19:16 – 23:24
21	Sampling moderately polluted air and clouds over Ohio	16-Aug	18:46 – 21:56
22	Sampling polluted air over Ohio with little cloud	17-Aug	18:02 – 20:48
23	Sampling BL cloud over SW Ontario downwind of Detroit-Windsor, coordinated with Twin Otter	18-Aug	15:04 – 18:47

TableB1a. Chebogue Point Instrumentation for Gas-Phase Measurements

Species/ Parameter	Reference	Technique	Averaging Time	Accuracy	Precision	LOD
O ₃	Goldstein et al 2004	UV Absorption, Dasibi 1008-RS	1 m	2%	1 ppbv	1 ppbv
CO	Goldstein et al 2004	Infra-red Absorption, Gas Filter Corrleation, TEI 48CTL	1 m	2%	1%	20 ppbv
H ₂ O	Goldstein et al 2004	Infra-red Absorption, Licor 6262	1 m	5 %	1 %	NA
CO ₂	Goldstein et al 2004	Infra-red Absorption, Licor 6262	1 m	1 ppm	0.2 ppm	NA
NMHCs (C ₃ -C ₁₀)	Millet et al., 2005; 2006, this section	In-situ GC/MS/FID	30 m	10%	2-8%	1 -25 pptv
Halocarbons (C ₁ -C ₂)	Millet et al., 2005; 2006, this section	In-situ GC/MS/FID	30 m	10%	2-7%	<1-2 pptv
Alkyl nitrates (C ₁ -C ₅)	Millet et al., 2005; 2006, this section	In-situ GC/MS/FID	30 m	10-25%	9-25%	0.4-1 pptv
Oxygenated VOC (C ₁ -C ₅)	Millet et al., 2005; 2006, this section	In-situ GC/MS/FID	30 m	10-15%	4-15%	2-100 pptv
VOCs	Holzinger et al., 2006, this section	PTRMS, Ionicon Analytik	1 min	10-30%	5-30%	10-250 pptv
PAN, PPN, MPAN, PiBN, APAN	<i>Marchewka et al.</i> , 2006, this section	Dir. Injection., GC/ECD	1 min, at 5 min intervals	5pptv+15% 5pptv+20%	2 % 2 %	5 pptv 5 pptv
NO ₂ , ΣPNs, ΣANs, HNO ₃ , NO _y *	Day et al., 2002	TD-LIF	1 min	10-20 %	10 %	50-150 pptv
Radon	[<i>Whittlestone &</i>	dual-flow loop, two-filter Rn	30 m	20%	8%	100 mBq m ⁻³

	<i>Zahorowski, 1998]</i>	detector, ANSTO Inc.				
Total gaseous mercury	Kellerhals et al, 2003	CVAFS, Tekran 2537A	5 min	2 %	2 %	<0.1 ng/m ³
SO ₂	Aerodyne	Thermo Electron 43S SO ₂ monitor	1 min		0.1 ppbv	0.1 ppbv

Table B1b. Chebogue Point Instrumentation for Aerosol and Ancillary Data Measurements

Species/ Parameter	Reference	Technique	Averaging Time	LOD
Aerosol mass and elemental composition	VanCuren et al. 2005	8-RDI Sampler and s-XRF analysis	3 hour	<ng/m ³ for elements 0.5 µg/m ³ for mass
Aerosol Bulk Ionic Composition and Total Mass	Quinn et al., 2000	Impactors, sub-1 µm and sub-10 µm size fractions	12 hours	1 ng/m ³
Non-refractory aerosol composition with aerodynamic sizing	Jayne et al., 2000	Aerodyne Aerosol Mass Spectrometer (AMS)	1 min (30 min reported)	30 < D _{va} < 1000 nm; 20 ng m ⁻³ (SO ₄ ²⁻); 7 ng m ⁻³ (NO ₃ ⁻); 0.17 µg m ⁻³ (NH ₄ ⁺); 0.12 µg m ⁻³ (OM)
Chemically-resolved volatility	Huffman et al., 2006	Inlet thermal denuder system for AMS	20 min	As AMS
Particle optical size and density	Cross et al., 2006	Light scattering module for AMS	Real-time	D _o > 180 nm; D _{va} < 1 µm
Aerosol Size Distribution	Williams et al., 2000	Differential Mobility Particle Sizer (DMPS)	10 min	3 < D _{mob} < 800 nm
Particle hygroscopic growth (D _{mob} = 40, 89 & 217 nm)	Cubison et al., 2005	Hygroscopicity Tandem Differential Mobility Analyzer (HTDMA)	1 hour	0.85 < g(RH) < 2.25
Particle volatility (D _{mob} = 130 nm)	Burtscher et al., 2001	Volatility Tandem Differential Mobility Analyzer (VTDMA)	15 min	N/A
Aerosol absorbance and equivalent black carbon		Thermo Electron 5012 Multi-Angle Absorption Photometer (MAAP)	1 min	0.66 Mm ⁻¹ (B _{abs}); 0.1 µg m ⁻³ (BC)
Particle number concentrations		TSI 3022a Condensation Particle Counter (CPC)	1 min	D > 7 nm
Particle number concentration	Hering et al., 2005	Water Condensation Particle Counter (Quant 400, prototype for TSI 3785)	1 min	5 nm
Aerosol organic functional groups	Maria and Russell, 2005	FTIR	4-12 hours	1 µg/m ³ accuracy 15%
Speciated Organic Composition	Williams et al, 2006	Thermal Desorption Aerosol GC/MS/FID (TAG)	30 min	typically 0.05–0.7 ng/cm ³

wind profiles	White et al, 2006, this section	915-MHz radar wind profiler	60 min	
temperature profiles	White et al, 2006, this section	radio acoustic sounding system	5 min	
cloud and aerosol backscatter	Duck et al., 2006 this section	lidar	1 min	
aerosol optical depth and size distribution	Duck et al., 2006 this section	sun photometer	1 min	
Aerosol number concentration	Sinclair and Hoopes, 1975; Delene and Ogren, 2002	TSI 3010 Condensation Particle Counter (CPC)	1 min	0 /cm ³
Aerosol light absorption	Bond et al., 1999; Delene and Ogren, 2002	Radiance Research particle soot absorption photometer (PSAP)	1 min	0.9 Mm ⁻¹ noise
Aerosol total and back light scattering at 3 wavelengths	Ahlquist and Charlson, 1967; Delene and Ogren, 2002	TSI 3563 integrating nephelometer	1 min	1.8 Mm ⁻¹ noise at 20 Mm ⁻¹ scattering
Hygroscopic Growth (f(RH))	Rood et al., 1989	Humidograph (humidity conditioner plus second TSI 3563 nephelometer)	30 min	
Cloud condensation nuclei (CCN) at 5 supersaturations	Roberts and Nenes, 2005	Droplet Measurement Technologies CCN counter	30 min	~0.75 um lowest size bin
Aerosol size distribution (0.02-0.5 μm)	Buzorius et al., 2004	Scanning electrical mobility sizer, Brechtel Manufacturing Inc	1.2 min	0.01μm-20 cm ⁻³ μm ⁻¹ 0.5 μm→4 cm ⁻³ μm ⁻¹
Wind speed and direction	Goldstein et al., 2004	Propeller anemometer, R.M. Young	30 min	
RH, Tair	Goldstein et al., 2004	Vaisala Inc., model HMP45C	30 min	
Photosynthetically active radiation	Goldstein et al., 2004	Quantum Sensor, LiCor Inc., 190SZ	30 min	

Table B2. Locations of NOAA and cooperative agency boundary-layer wind profilers available for the ICARTT study.

Location	Desig.	Latitude	Longitude	Elevation	RASS	Sponsor
Appledore Island, ME	ADI	42.99	-70.62	5 m	Yes	NOAA
Bar Harbor, ME	BHB	44.44	-68.36	4 m	Yes	NOAA
Chebogue Pt., Nova Scotia	CHE	43.70	-66.10	15 m	Yes	NOAA
Concord, NH	CCD	43.21	-71.52	104 m	Yes	NOAA
Lunenburg Bay, Nova Scotia	LUN	44.40	-64.30	30 m	Yes	Environment Canada
New Brunswick, NJ	RUT	40.50	-74.45	10 m	Yes	Rutgers University and NJ Dept. of Environ. Protection
Pease Int'l. Tradeport, NH	PSE	43.09	-70.83	30 m	Yes	NOAA
Pittsburgh, PA	PIT	40.48	-80.26	335 m	Yes	NOAA
Plymouth, MA	PYM	41.91	-70.73	46 m	Yes	NOAA
R/V Ronald H. Brown	RHB	Variable	Variable	5 m	No	NOAA
Storrs, CT	STS	41.80	-72.23	198 m	No	NOAA

Table B3a. CHAiOS Instrumentation for Gas-Phase Measurements

Species/ Parameter	Reference	Technique	Averaging Time	Accuracy	Precision	LOD
NO ₂	[<i>Alicke et al., 2002; Stutz et al., 2002</i>]	Long-Path DOAS	5 to 15 m	0.15 or 0.05 ppbv	Greater of 3% or accuracy	Accuracy x 2
HCHO	[<i>Alicke et al., 2002; Stutz et al., 2002</i>]	Long-Path DOAS	5 to 15 m	0.3 ppbv	Greater of 3% or accuracy	Accuracy x 2
O ₃	[<i>Alicke et al., 2002; Stutz et al., 2002</i>]	Long-Path DOAS	5 to 15 m	2 ppbv	Greater of 3% or accuracy	Accuracy x 2
HONO	[<i>Alicke et al., 2002; Stutz et al., 2002</i>]	Long-Path DOAS	5 to 15 m	0.05 ppbv	Greater of 3% or accuracy	Accuracy x 2
NO ₃	[<i>Alicke et al., 2002; Stutz et al., 2002</i>]	Long-Path DOAS	5 to 15 m	1.7 ppbv	Greater of 3% or accuracy	Accuracy x 2
SO ₂	[<i>Alicke et al., 2002; Stutz et al., 2002</i>]	Long-Path DOAS	5 to 15 m	0.07 ppbv	Greater of 3% or accuracy	Accuracy x 2
BrO	[<i>Alicke et al., 2002; Stutz et al., 2002</i>]	Long-Path DOAS	5 to 15 m	~0.6 pptv	Greater of 3% or accuracy	Accuracy x 2
OIO	[<i>Alicke et al., 2002; Stutz et al., 2002</i>]	Long-Path DOAS	5 to 15 m	1 to 5 pptv	Greater of 3% or accuracy	Accuracy x 2
IO	[<i>Alicke et al., 2002; Stutz et al., 2002</i>]	Long-Path DOAS	5 to 15 m	0.6 pptv	Greater of 3% or accuracy	Accuracy x 2
I ₂	[<i>Alicke et al., 2002; Stutz et al., 2002</i>]	Long-Path DOAS	5 to 15 m	4 to 25 pptv	Greater of 3% or accuracy	Accuracy x 2
NO ₂	[<i>Pikelnaya et al., 2006,</i>	MAX-DOAS	5 to 15 m	5.0x10 ¹⁴	Greater of 3% or accuracy	Accuracy x 2

	this section]			molec cm ⁻²	accuracy	
HCHO	[Pikelnaya et al., 2006, this section]	MAX-DOAS	5 to 15 m	1.1 x 10 ¹⁶	Greater of 3% or accuracy	Accuracy x 2
BrO	[Pikelnaya et al., 2006, this section]	MAX-DOAS	5 to 15 m	1 x 10 ¹³	Greater of 3% or accuracy	Accuracy x 2
OIO	[Pikelnaya et al., 2006, this section]	MAX-DOAS	5 to 15 m	1.5 x 10 ¹³	Greater of 3% or accuracy	Accuracy x 2
IO	[Pikelnaya et al., 2006, this section]	MAX-DOAS	5 to 15 m	5 x 10 ¹²	Greater of 3% or accuracy	Accuracy x 2
I ₂	[Pikelnaya et al., 2006, this section]	MAX-DOAS	5 to 15 m	5 x 10 ¹³	Greater of 3% or accuracy	Accuracy x 2
HCOOH	[Pszenny et al., 2004]	Tandem mist chamber	2 h	~15%	Greater of 10-15% or 0.5 x DL	5 pptv
CH ₃ COOH	[Pszenny et al., 2004]	Tandem mist chamber	2 h	~15%	Greater of 10-15% or 0.5 x DL	3 pptv
HCl	[Pszenny et al., 2004]	Tandem mist chamber	2 h	~15%	Greater of 10-15% or 0.5 x DL	10 pptv
HNO ₃	[Pszenny et al., 2004]	Tandem mist chamber	2 h	~15%	Greater of 10-15% or 0.5 x DL	11 pptv
NH ₃	[Pszenny et al., 2004]	Tandem mist chamber	2 h	~15%	Greater of 10-15% or 0.5 x DL	8 pptv
Cl* (see footnote)	[Pszenny et al., 2004]	Tandem mist chamber	2 h	~15%	Greater of 15% or	5 pptv

					10 pptv	
Total inorganic Br	<i>Rahn et al., 1976</i>	Filter pack	15 h (daytime) or 9 h (nighttime)	~15%	22%	0.06 pptv
Total inorganic I	<i>Rahn et al., 1976</i>	Filter pack	15 h (daytime) or 9 h (nighttime)	~15%	10%	0.25 pptv
C ₂ -C ₁₀ NMHCs	[<i>Zhou et al., 2005</i>]	Canisters	5 m (hourly)	5%	0.1-3% (C ₂ -C ₅) 5% (C ₆ -C ₁₀)	2 pptv (C ₂ -C ₅) 3 pptv (C ₆ -C ₁₀)
C ₂ -C ₁₀ NMHCs	[<i>Talbot et al., 2005</i>]	PTR-MS	10 m	10%	15%	10-100 pptv
C ₂ -C ₁₀ NMHCs	[<i>Sive et al., 2005</i>]	GC-FID/ECD/MS	7.5 m every 40 m	5%	0.3-3% (C ₂ -C ₅) 5-7% (C ₆ -C ₁₀)	2 pptv (C ₂ -C ₅) 3 pptv (C ₆ -C ₁₀)
Halocarbons	[<i>Zhou et al., 2005</i>]	Canisters	5 m (hourly)	5-20%	1-13%	CH ₃ Cl: 50 pptv; CH ₃ Br, CH ₃ I: 1 pptv; C ₂ H ₅ I: 0.001 pptv; others: 0.01 pptv
Halocarbons	[<i>Sive et al., 2005</i>]	GC-FID/ECD/MS	7.5 m every 40 m	5-20%	1-13%	CH ₃ Cl: 25 pptv; CH ₃ Br, CH ₂ Cl ₂ : 1 pptv; C ₂ H ₅ I: 0.001 pptv; others: 0.01 pptv
C ₁ -C ₅ Alkyl nitrates	[<i>Zhou et al., 2005</i>]	Canisters	5 m (hourly)	10%	5%	0.01 pptv

Alkyl nitrates	[Sive <i>et al.</i> , 2005]	GC-FID/ECD/MS				
OCS	[Zhou <i>et al.</i> , 2005]	Canisters	5 m (hourly)	10%	4%	50 pptv
OCS	[Sive <i>et al.</i> , 2005]	GC-FID/ECD/MS	7.5 m every 40 m	5-20%	1-13%	25 pptv
OVOCs	[Talbot <i>et al.</i> , 2005]	PTR-MS	10 m	10%	15%	10-100 pptv
OVOCs	[Sive <i>et al.</i> , 2005]	GC-FID/ECD/MS	7.5 m every 40 m	10%	5-10%	10-100 pptv

Table B3b. CHAiOS Instrumentation for Aerosol and Ancillary Data Measurements

Species/Parameter	Reference	Technique	Averaging Time	LOD
Aerosol Bulk & Size-segregated Ionic Composition	[<i>Pszenny et al.</i> , 2004]	Bulk filters & Cascade Impactors/Ion Chromatography	15 h (daytime) or 9 h (nighttime)	~0.2 to ~50 ng m ⁻³ for individual species
Aerosol Total Br and I	[<i>Pszenny et al.</i> , 2004; <i>Rahn et al.</i> , 1976]	Bulk filters & Cascade Impactors/Neutron Activation	15 h (daytime) or 9 h (nighttime)	Br ~0.2 ng m ⁻³ I ~1.5 ng m ⁻³
Aerosol Organic Functional Groups	[<i>Gilardoni et al.</i> , 2006, this section]	Bulk filters/FTIR	8-16 h	1 µg m ⁻³
Aerosol Number	[<i>Russell et al.</i> , 2006, this section]	CNC (TSI 3025)	1 s	~5 cm ⁻³
Aerosol Size Distribution	[<i>Russell et al.</i> , 2006, this section]]	DMA and APS	3 m	---
Photolytic Flux		Bentham spectroradiometer, Model No. DMc 150 FC	5 m	unknown

Table B4. PICO-NARE instrumentation

Species/Parameter	Reference	Technique	Averaging Time	Accuracy (2-sigma)	Precision (2-sigma)	LOD	Measurement period
NO	[<i>Ryerson, et al., 1999</i>]	NO/O ₃ Chemiluminescence	30 s	4%+4 pptv	7 pptv	4 pptv (1-hr average)	2003-2005
NO ₂	[<i>Ryerson, et al., 1999</i>]	Photolysis- Chemiluminescence	30 s	4% + 7 pptv	18 pptv	7 pptv (1-hr average)	2003-2005
NO _y	[<i>Ryerson, et al., 1999</i>]	Au converter- Chemiluminescence	20 s	15% + 4 pptv	17 pptv	4 pptv (1-hr average)	2003-2005
O ₃	[<i>Ryerson, et al., 1998</i>] [<i>Honrath et al., 2004</i> ; <i>Owen et al., 2006, this section</i>]	NO/O ₃ Chemiluminescence	60 s	3%	< 1 ppbv	1 ppbv	2001-2005
CO	[<i>Honrath et al., 2004</i> ; <i>Owen et al., 2006, this section</i>]	Non-dispersive infrared absorption	30 min	7%	4 to 9 ppbv	2 ppbv	2001-2005
Black carbon	[<i>Fialho et al., 2005</i>]	Multi-wavelength Aethalometer	1 hr	Not characterized	25 ng/m ³	25 ng/m ³	2001-2005
NMHCs (C ₂ -C ₆)	[<i>Tanner et al., 2006</i>]	Continuous GC	12 min and 60 min	5-10%	5-10%	<10 pptv	2004-2005

Table B5. Timetable of measurements by European Lidar Network.

Date	5/7	19/7	20/7	21/7	22/7	23/7	24/7	25/7	26/7	27/7	28/7	29/7	30/7	31/7	1/8	2/8	3/8
OHP O3, Aerosol		15-21 UT	15-20 UT	7-17 UT	8 UT, 19 UT	19 UT	7-20 UT	18-20 UT	6-24 UT	0-20 UT	8 UT, 20 UT	5-22 UT	5-22 UT	5-22 UT	18-21 UT	6 UT 20 UT	6 UT
SIRTA Aerosol	6-18 UT	6-17 UT	7 UT		7 UT	5-12 UT			6-15 UT	6-18 UT	6-18 UT	6-18 UT	6-16 UT			7-18 UT	6 UT
Athens O3				8 UT, 15 UT							13 UT						6-12 UT
Athens Aerosol	12 UT	8-21 UT		11 UT					8-21 UT							21 UT	
IFU Aerosol			x	x		x					x	x					
Leipzig Aerosol	x	x			x							x					x
Hamburg Aerosol		x			13-21 UT											x	
Potenza Aerosol		13-21 UT	9- 21 UT		17- 21 Ut				20- 22 UT			16- 21 UT				8- 24 UT	12- 22 UT